INFORMATION TO USERS

This manuscript has been reproduced from the microfilm master. UMI films the text directly from the original or copy submitted. Thus, some thesis and dissertation copies are in typewriter face, while others may be from any type of computer printer.

The quality of this reproduction is dependent upon the quality of the copy submitted. Broken or indistinct print, colored or poor quality illustrations and photographs, print bleedthrough, substandard margins, and improper alignment can adversely affect reproduction.

In the unlikely event that the author did not send UMI a complete manuscript and there are missing pages, these will be noted. Also, if unauthorized copyright material had to be removed, a note will indicate the deletion.

Oversize materials (e.g., maps, drawings, charts) are reproduced by sectioning the original, beginning at the upper left-hand corner and continuing from left to right in equal sections with small overlaps.

Photographs included in the original manuscript have been reproduced xerographically in this copy. Higher quality 6" x 9" black and white photographic prints are available for any photographs or illustrations appearing in this copy for an additional charge. Contact UMI directly to order.

ProQuest Information and Learning
300 North Zeeb Road, Ann Arbor, MI 48106-1346 USA
800-521-0600

New Multiuser Detection Schemes for Direct-Sequence Code-Division Multiple Access Systems

by

XIAOFENG WANG
M.Eng., Beijing University of Posts and Telecommunications, 1994
B.Sci., Wuhan University, 1991

A Thesis Submitted in Partial Fulfillment of the
Requirements for the Degree of

DOCTOR OF PHILOSOPHY

in the Department of Electrical and Computer Engineering

We accept this thesis as conforming
to the required standard

Dr. A. Antoniou, Co-Supervisor (Department of Electrical and Computer Engineering)

Dr. W.-S. Lu, Co-Supervisor (Department of Electrical and Computer Engineering)

Dr. V. K. Bhargava, Member (Department of Electrical and Computer Engineering)

Dr. D. Olesky, Outside Member (Department of Computer Science)

Dr. W.-P. Zhu, External Examiner (Concordia University)

Supervisors: Dr. A. Antoniou & Dr. W.-S. Lu

ABSTRACT

In this dissertation, three multiuser detectors are developed for different application scenarios in direct-sequence code-division multiple access systems. The first detector is an overlapping widow decorrelating detector aimed at asynchronous reverse links. In companion with the design of this detector, a study on the decay property of the ideal decorrelating impulse response is presented, resulting in a quantitative description of the decay rate as a function of the Cholesky factors of the cross-correlation matrix of user signature signals. This result can serve as a guide for determining window length of decorrelating or minimum mean-squared error multiuser detection in asynchronous multiuser systems. Based on this result, a signal-adapted window-length determination algorithm is developed for the proposed detector. Several supporting utilities for efficient implementation of the proposed detector are also described.

The second detector is a linear multiuser detector that is also aimed at the reverse links. Particularly, it is desirable for cases where the number of users is small and, thus, significant performance gain over the existing linear multiuser detectors is possible. Unlike in the decorrelating and MMSE detectors, minimizing the bit-error rate is taken as the optimization objective in the proposed detector. To avoid undesired local minima of the highly nonlinear BER cost function, a set of convex constraints is proposed for the optimization problem. It is shown that this constrained optimization problem has a unique solution once the decorrelating detector exists. It is also shown that the proposed detector achieves the best performance among linear detectors for most realistic situations. In addition, a Newton barrier method is developed for efficiently calculating the coefficient vector of the proposed detector (i.e., the solution of the constrained optimization problem).

The third detector is an adaptive detector that is aimed at the forward link where information about interfering users is often unavailable. The proposed detector con-

sists of a bank of blind adaptive filters, one for each resolvable path, followed by a channel estimator and a coherent diversity combiner. To allow blind adaptation, the impulse response of each filter is decomposed into two orthogonal parts: one part is fixed as the decorrelating coefficient vector for the path in the absence of interfering users and the other is free to be adapted according to the mean-squared error criterion. Assuming perfect adaptation, the performance of the proposed detector is shown to be between those of the decorrelating detector and the minimum mean-squared error detector. Other studies conducted include the effects of fading on the performance of the proposed detector and the behavior of the proposed blind adaptation algorithm.

Examiners:

Dr. A. Antoniou, Co-Supervisor (Department of Electrical and Computer Engineering)

Dr. W.-S. Lu, Co-Supervisor (Department of Electrical and Computer Engineering)

Dr. V. K. Bhargava, Member (Department of Electrical and Computer Engineering)

Dr. D. Olesky, Outside Member (Department of Computer Science)

Dr. W.-P. Zhu, External Examiner (Concordia University)

Table of Contents

List of Tables

List of Figures

LIST OF ACRONYMS

AME	Asymptotic multiuser efficiency
AWGN	additive white Gaussian noise
BER	Bit-error rate
BPSK	Binary phase-shift keying
CDMA	code-division multiple access
CMBER	Constrained minimum BER
CMMSE	Constrained minimum mean-squared error
DPSK	Differential phase shift keying
DS-CDMA	Direct-sequence code-division multiple access
FDMA	Frequency-division multiple access
FIR	Finite-duration impulse response
IIR	Infinite-duration impulse response
IMT-2000	International Mobile Telecommunications-2000
IR	Impulse response
ISI	Inter-symbol interference
LMS	Least-mean square
LOS	Line of sight
LTI	Linear time-invariant
MDD	Multipath decorrelating detector
MFR	Matched-filter receiver
MIMO	Multiple-input multiple-output
MMSE	Minimum mean-squared error
MOE	Mean output energy

MRC	Maximum-ratio combining
MSE	Mean-squared error
MUI	Multiuser interference
NF	Near-far
OAMMSE	Orthogonally anchored MMSE
OWD	Overlapping window decorrelating
RDD	RAKE decorrelating detector
SINR	Signal-to-interference-plus-noise ratio
SNR	Signal-to-noise ratio
TDMA	Time-division multiple access
WSUS	Widesense stationary uncorrelated scattering

Acknowledgement

I would like to express my profound sense of gratitude to my supervisors, Professors. A. Antoniou and W.-S. Lu. I am grateful to them for having provided me the opportunity of study in Victoria. I am indebted to them for their valuable guidance, encouragement, financial support, and many more.

I would like to thank the members of my dissertation committee. I am obliged to thank Professor V. K. Bhargava for providing me the access to the library of Digital Communications Laboratory, and for having organized many interesting seminars from which I greatly benefited. I am deeply indebted to Professor D. Olesky for his excellent teaching in Numerical Analysis II and careful review of this dissertation. I am grateful to Dr. Wei-Ping Zhu at Concordia University for his kind acceptance to be the external examiner of this dissertation and for his valuable suggestions.

Special thanks to my wife, Ping Yu, for her continuous support and encouragement. Without her support and encouragement, I would not have come to Victoria pursuing Ph.D. degree and would not have finished this dissertation.

I would like to extend my sincere thanks to all professors, office stuff, and fellow graduate students at the department for the wonderful studying and research environment and for their assistance in various ways.

To

my parents Fayuan Wang and Caixia Li

and to my wife Ping Yu

Chapter 1

Introduction

Over the last decade, the demand of wireless communication services has experienced an unprecedented growth. With this growth, radio spectrum has been recognized as one of the very precious resources of nature and, as such, is required to be more efficiently utilized. Because of its bandwidth (spectrum) efficiency and some other attractive properties, direct-sequence code-division multiple access (DS-CDMA) has recently become the most popular technique for multiplexing wireless users [1]-[4]. It was adopted in the recent air interface standards IS-95 and IS-665 and is also the choice of the third-generation wideband wireless systems called International Mobile Telecommunications-2000 (IMT-2000).

In a CDMA system, users are multiplexed by distinct spreading codes and share the entire transmission bandwidth simultaneously. When the spreading codes are not orthogonal to each other or when the user signals arrive at the receiver asynchronously, multiuser interference (MUI) exists and is the major limiting factor to system capacity.

MUI in the form of the so-called co-channel interference or adjacent-channel interference has been of concern in frequency-division multiple access (FDMA) and time-division multiple access (TDMA) systems in the past. It is only recently that multiuser detection as a scheme for suppressing MUI has received great interest with the growing popularity of DS-CDMA in wireless communications. This dissertation presents several new multiuser detection schemes for DS-CDMA systems.

1.1 Previous Work

In conventional DS-CDMA systems, a matched-filter receiver (MFR) is used to demodulate user information bits. The MFR is only optimal for single-user transmission over additive white Gaussian noise (AWGN) channels. Its performance drastically degrades in the presence of high-power interferers. This phenomenon is often referred to as near-far (NF) problem [5] and has motivated considerable effort to develop NF-resistant multiuser detectors. In his pioneering work, Verdú developed the optimal multiuser detector which maximizes the *joint a posteriori probability* with a computational complexity that grows exponentially with the number of users [5]. Following the optimal multiuser detector, various suboptimal multiuser detectors with much reduced computational complexity have been proposed.

For the reverse link (e.g., from mobile stations to the base station) where information about the signature signals, timing, and sometimes received amplitudes of all active users is available, two classes of centralized, suboptimal, multiuser detectors, namely, linear and nonlinear multiuser detectors, have emerged [6][7]. Linear multiuser detectors are characterized by linear mappings that are applied to the soft output of the conventional MFR in order to reduce the amount of MUI received by each user. Since linear mappings are determined by spreading codes, linear multiuser detectors are particularly suitable for systems using periodic spreading codes, i.e., a short spreading code is periodically used for each symbol of a user. Two well known linear multiuser detectors are the decorrelating detector for synchronous systems [8] and for asynchronous systems [9], and the minimum mean-squared-error (MMSE) detector [10]. The decorrelating detector minimizes the MUI regardless of the presence of background noise and, hence, is analogous to the zero-forcing equalizer for single-user dispersive channels [11]. In comparison, the MMSE multiuser detector minimizes the mean-squared error (MSE) and is analogous to the MMSE [11] equalizer for single-user dispersive channels. The linear mappings of the decorrelating and MMSE detectors are the inverses of the cross-correlation matrix of the user spread-

ing codes and their modified version, respectively. The decorrelating detector is of particular importance because it not only achieves the optimal NF resistance without knowledge of the received signal energies but also lays the ground for the development of other more sophisticated multiuser detectors.

Nonlinear multiuser detectors include the successive cancellation detector [12][13], multistage detector [14][15], and decision-feedback multiuser detectors [16]-[18]. A notable advantage of the successive cancellation and multistage multiuser detectors is that, unlike the linear detectors, they do not need to compute the inverse of the cross-correlation matrix of the spreading codes and, hence, are particularly useful for systems with aperiodic spreading codes. Since these nonlinear multiuser detectors use previous decision outputs to help the current decision, their performance largely depends on the reliability of initial estimates. In addition, they all need to estimate the received signal amplitudes and generally have more complex structure than that of the linear multiuser detectors.

For the forward link, often the information of interfering users is *not* available at mobile units, which precludes the use of centralized multiuser detectors. Recently, attempts have been made to develop adaptive multiuser detectors that eliminate the need for information about interfering users. An adaptive decorrelating detector was developed and studied in [19][20] and an adaptive MMSE multiuser detector was introduced in [21] and [22]. As in the case of adaptive channel equalization for single-user dispersive channels, the mean-squared-error criterion is advantageous over the zero-forcing criterion on which the decorrelating detector is based. Consequently, the adaptive MMSE multiuser detector has received more attention.

In [23], it was shown that minimizing the output energy of a linear multiuser detector under the constraint that the energy of the desired user is maintained is equivalent to minimizing the MSE. Based on this observation, a blind adaptive detector called the minimum mean-output-energy (MOE) detector was derived to further eliminate the need for training sequences. This blind adaptation mechanism is of particular

importance for fading channels where frequent re-training is required by an adaptive detector. Another interesting approach for designing blind multiuser detectors is the subspace approach proposed in [24]. However, subspace-based multiuser detectors are computationally much more complex and their performance is sensitive to the degree of accuracy in the estimates of noise or signal subspaces.

In addition to the above mentioned work, there has also been great interest in combining multiuser detectors with diversity reception techniques to eliminate MUI and achieve frequency diversity and/or space diversity gain simultaneously [25]-[27]. A very recent attempt along this line is to combine multiuser detection techniques and coding techniques [28][29].

1.2 Scope of the Dissertation

This dissertation consists of six chapters. Chapter 2 presents preliminary knowledge about DS-CDMA systems as well as multiuser detection. Chapters 3, 4, and 5 make up the main body of the dissertation. They describe three new multiuser detectors for different communication scenarios. Chapter 6 presents concluding remarks and suggestions for further research.

The major concern of Chapter 3 is the design of an efficient centralized multiuser detector for DS-CDMA systems. Since the detector is targeted for the reverse link, where user synchronization is difficult, asynchronous transmission must be considered. In this case, the ideal decorrelating and MMSE multiuser detectors are both noncausal and of infinite length. A new multiuser detector that combines the advantages of linear multiuser detectors and the decision feedback detector is proposed. The proposed detector divides the successive received symbols into overlapped windows and performs detection window by window. Efficient algorithms are also developed for updating the detector by exploiting the three-band tridiagonal structure of the system cross-correlation matrix. One of the major contribution of Chapter 3 is the

study of the convergence and decay properties of the ideal decorrelating impulse response (IR). Based on the results obtained, a signal-adapted criterion for window-length determination is developed. The proposed detector is then further extended to frequency-selective multipath fading channels and its combination with diversity receivers is examined. It is important to note that the proposed detection scheme and the results on the properties of the ideal decorrelating IR can be readily extended to the case of MMSE multiuser detectors for asynchronous channels.

Chapter 4 is also focused on centralized multiuser detection. Since the bit-error rate (BER) is the ultimate performance index, we study the error probability function in a multiuser communication scenario. It is shown that the existence of local minima of the error probability function can be eliminated by imposing a set of appropriate convex constraints. It is also shown that once the decorrelating detector exists (i.e., the spreading codes are linear independent to each other), the proposed minimization problem has a unique solution. The uniqueness of the solution enables us to convert the constrained optimization problem to an equivalent convex programming problem. A Newton barrier method is then developed for solving the convex problem. Simulations are given to demonstrate that the resulting linear mulituser detector that takes the solution as its coefficient vector always outperforms the decorrelating detector. For most realistic cases, the proposed detector achieves the best performance among all linear multiuser detectors. Note that a single-user communication over a dispersive channel can be deemed to be special case of a multiuser communication, as will be explained later. The proposed detector also applies to the equalization for single-user channels. As in the case of multiuser communications, better performance than that of the conventional zero-forcing and MMSE equalizers can be achieved.

Chapter 5 is devoted to adaptive multiuser detection for the forward link. A blind multiuser detector is proposed for frequency-selective fading channels. The proposed detector consists of a bank of blind adaptive filters, where the IR of each filter consists of two orthogonal parts: one part is fixed as the decorrelating coefficient

vector for a resolvable path in the absence of other users while the other is free to be adapted according to the MSE criterion. Under the proposed settings, minimizing the MSE is shown to be equivalent to minimizing the output energy. Consequently, the detector can be adapted without the need of training. In fact, to make the proposed detector work, the only information needed is the timing and spreading code of the desired user. In addition, we propose to add a channel estimator following the adaptive filter bank. Since the MUI is largely suppressed by the adaptive filters, channel estimation techniques for single-user communications can be used. With the estimated channel parameters, coherent diversity combining can be performed to best achieve multipath diversity gain. The proposed structure also applies to systems with multiple antennas to achieve space diversity gain. Another contribution of this chapter is the examination of the behavior of the blind adaptation algorithm. Conditions for convergence and the steady-state MSE of the algorithm are studied.

1.3 Contributions

The main contribution of Chapter 3 is a study on the convergence and decaying properties of the ideal decorrelating IR. Although linear multiuser detection has been subjected to intensive study in the past, the study that will be presented in Chapter 3 is, to our knowledge, the first attempt to quantify the decay rate of the decorrelating IR. The results provide guidelines on the implementations of linear multiuser detection in asynchronous systems, regardless of the schemes used to truncate the processing window. For instance, the results allow one to analytically determine the appropriate observation window length for a given set of user signatures and the degree of power imbalance, whereas extensive simulations are needed otherwise. Another important new result is that although an exact decorrelating solution exists for a finite observation window, its performance is always worse than that of the ideal decorrelating detector and increases as the window length increases. This new

result clears the misconception: The detection of asynchronous users is trivial since their mutual interference can be completely removed for a finite observation window. Other contributions include the proposed detection scheme, efficient algorithms for updating the proposed detector, and a method for window-length determination.

The main contribution of Chapter 4 is the design of a constrained minimum-BER linear detector, which yields optimal BER performance among linear detectors for most of practical situations. The crucial and novel ideal in this design is the introduction of a set of convex constraints to the highly nonlinear BER cost function. The resultant constrained optimization problem has a unique minimizer, which is also, for most realistic situations, the global minimizer of the unconstrained BER cost function. As an associated product, a Newton barrier method is also developed to search the detector coefficients.

In Chapter 5, the design of a blind adaptive detector for frequency-selective channels is among the first attempts to attack adaptive multiuser detection problem in frequency-selective channels. The novelty here is to employ a bank of adaptive filters, each being aimed at a path and being anchored on the coefficient vector of the decorrelctaing filter associated with the path as if there were no other interferers. This novel setting allows a blind adaptation. In addition, interesting new results are obtained from a study on the effects of channel fading on the convergence of the proposed detector and an examination on the behavior of the proposed blind adaptation algorithm.

Chapter 2

DS-CDMA and Multiuser Detection Preliminaries

2.1 Introduction

As described earlier, different multiuser detectors are used depending on the type of user information available. In addition, a successful detector design must consider many other factors such as channel characteristics, type of spreading codes used, timing among users, etc. In this chapter, some background knowledge, concepts, and terminology pertaining to wireless channels and direct-sequence code-division multiple access (DS-CDMA) models are presented to provide the basis on which the subsequent chapters are developed. Several multiuser detectors that were developed in the late 80's and early 90's are also briefly introduced.

2.2 Mobile Radio Channels

2.2.1 Channel Characteristics

A wireless channel can be described by two characteristics: *time dispersion* and *time variation*. Time dispersion arises when the multiple replicas of the transmitted signal that propagate over different transmission paths arrive at the receiver with different time delays. Time variation is caused by the changes of transmission media or

movement of the transmitter and receiver.

Let us first examine the effects of the channel on signal transmission. In wireless communications, transmit signals are usually bandlimited around the carrier frequency and can be represented in general as

$$s(t) = \mathrm{Re}[s_l(t)e^{j2\pi f_c t}] \tag{2.1}$$

where $s_l(t)$ is a baseband signal and f_c is the carrier frequency. When the above signal is transmitted over a time-varying channel with multiple paths, the received signal is given by

$$r(t) = \sum_n \alpha_n(t)s[t - \tau_n(t)] \tag{2.2}$$

where $\alpha_n(t)$ and $\tau_n(t)$ are the attenuation factor and delay associated with path n, respectively. Substituting (2.1) into (2.2), we can find that the equivalent baseband signal is

$$r_l(t) = \sum_n \alpha_n(t)e^{-j2\pi f_c \tau_n(t)} s_l[t - \tau_n(t)] \tag{2.3}$$

From (2.3), we see that the impulse response (IR) of the equivalent lowpass channel is given by

$$c(\tau, t) = \sum_n \alpha_n(t)e^{-j2\pi f_c \tau_n(t)} \delta[\tau - \tau_n(t)] \tag{2.4}$$

where $\delta(t)$ is the Dirac delta function and $c(\tau, t)$ represents the response of the channel at time t to an impulse applied at time $t - \tau$. Hence the equivalent lowpass channel also has an equivalent number of paths with a complex path gain $\alpha_n(t)e^{-j2\pi f_c \tau_n(t)}$ associated with delay τ_n.

Since f_c is usually large, a small change in $\tau_n(t)$ will cause a significant change in phase shift of $2\pi f_c \tau_n(t)$. At times, the phase shifts associated with different paths result in the signal replicas adding constructively, which leads to a large signal envelope at the receiver. At other times, the signal replicas add destructively and the

received envelope is very small or essentially zero. This amplitude variation in the received signal is called *signal fading.*

When the number of paths is large, which is often the case, the IR $c(\tau, t)$ can be modeled as a complex-valued Gaussian random process and so does the received baseband signal $s_l(t)$. In the absence of a line-of-sight (LOS) or specular path, the envelopes of the IR $|c(\tau, t)|$ and the received signal are zero-mean and Rayleigh distributed at any time t [11]. In such a case the channel is said to be a *Rayleigh fading* channel. If there exists a LOS or specular path, the envelopes of the IR and the received signal have nonzero means and are Rice distributed. This type of fading is called *Ricean fading* [11]. In addition, a Nakagami-m distribution is also often used to model the fading signal envelopes which becomes the Rayleigh distribution when $m = 1$ [30].

When there is only one path with a constant gain and the only impairment in the channel is AWGN, the channel is called an AWGN channel. Because of its simplicity, an AWGN channel is often a convenient starting point for subsequent analysis. When there exists one LOS path with a strong gain compared to the gains of other paths, and the mobile units are relatively stationary and free from local scattering, the channel can be well approximated in terms of an AWGN channel.

2.2.2 Classification of Multipath Fading Channels

Multipath fading channels are classified according to their time spread and time variation rate. A strict definition of these two characteristics involves the channel correlation functions and power spectra, which will be described below.

We first examine the time dispersion of the channel. When the gains of different paths are uncorrelated with each other, which is often the case [30], the autocorrelation function of the IR can be defined as

$$\phi(\tau; t) = \frac{1}{2} E[c^*(\tau_1; t_1) c(\tau_2; t_1 + t)] \tag{2.5}$$

where E stands for the expectation and c^* is the complex-conjugate of c. If $t = 0$, the resulting correlation function $\phi(\tau) \equiv \phi(\tau; 0)$ is called the *multipath intensity profile* or the *delay power spectrum* of the channel. Typically, the value of $\phi(\tau)$ decreases with increasing τ and a typical $\phi(\tau)$ is plotted in Fig. 2.1. The range of values of τ over which $\phi(\tau)$ is essentially nonzero is called the *multipath spread* of the channel and is denoted by T_m. If the Fourier transform of $\phi(\tau; \Delta t)$ with respect to τ is denoted by $\Phi(f; t)$ and $\Phi(f) \equiv \Phi(f; 0)$, then the range of values of Δf over which $|\Phi(f)|$ is essentially nonzero is called the *coherence bandwidth* of the channel. As a result of the relationship between $\phi(\tau)$ and $\Phi(f)$, we have

$$\Delta f \approx \frac{1}{T_m} \tag{2.6}$$

If the bandwidth of a transmitted signal is large compared to the coherence bandwidth Δf of the channel, the channel is said to be *frequency selective* and is sometimes referred to as a *wideband channel.* In this case, the different components in the signal that are separate in frequency larger than Δf are affected differently by the channel and, as a consequence, the signal is severely distorted. On the other hand, if the signal bandwidth is small relative to Δf, then the channel is said to be *frequency nonselective* (or flat) in that all frequency components in the signal are passed with approximately equal gain and linear phase. Flat channels are also known as *narrowband channels.*

We now discuss the time varying nature of the channel. If the Fourier transform of $\Phi(f; t)$ with respect to t is denoted by $S(f; \lambda)$ and $S(\lambda) \equiv S(0; \lambda)$, then the range of values of λ over which $S(\lambda)$ is essentially nonzero is called the *Doppler spread* of the channel and is denoted by B_d. Using the Fourier transform relationship between $S(\lambda)$ and $\Phi(t) \equiv \Phi(0; t)$, we conclude that the reciprocal of B_d is a measure of the time duration over which the channel IR is essentially invariant, that is,

$$\Delta t \approx \frac{1}{B_d} \tag{2.7}$$

Since Δt represents the time duration over which two received signals have a large amplitude correlation, it is called the *coherence time* of the channel. The coherence

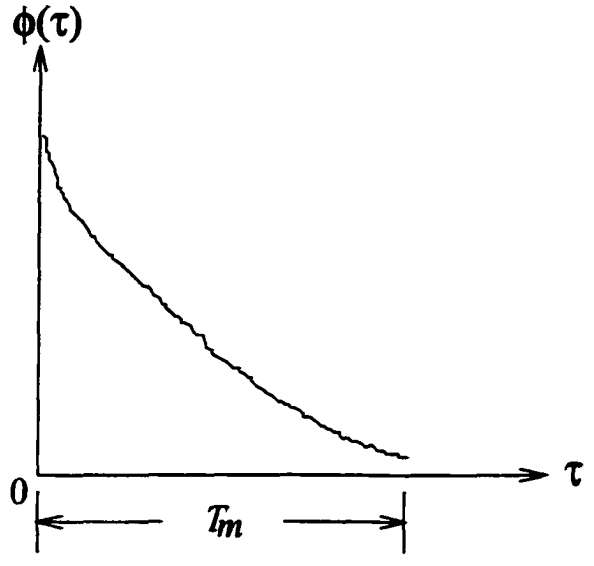

Figure 2.1. *The delay power spectrum of a typical mobile channel.*

time and the Doppler spread are largely determined by the velocity of the mobile station. If Δt is defined as the time duration over which $\Phi(t)$ is greater than 0.5, then the coherence time is approximately given by

$$\Delta t \approx \frac{9}{16\pi f_m} \tag{2.8}$$

where f_m is the maximum Doppler shift, v is the velocity of the mobile station, and λ is the carrier wave length [32]. A channel is said to be *fast fading* if its coherence time is smaller than the symbol period of the transmitted signal. In this case, the Doppler spread is significant relative to the signal bandwidth. On the other hand, if the coherence time is much larger than the symbol period of the transmitted signal or, equivalently, the Doppler spread is much less than the signal bandwidth, the channel is said to be *slowly fading.*

In summary, depending on the time dispersion of a channel relative to the symbol interval T of the transmitted signal, the channel is said to be frequency selective or nonselective; and depending on its time varying rate relative to T, the channels is said to be fast or slowly fading. It should be noted that time dispersion and the

time varying rate are two uncorrelated aspects of a channel. Consequently, multipath fading channels can be classified into 4 classes as illustrated in Fig. 2.2.

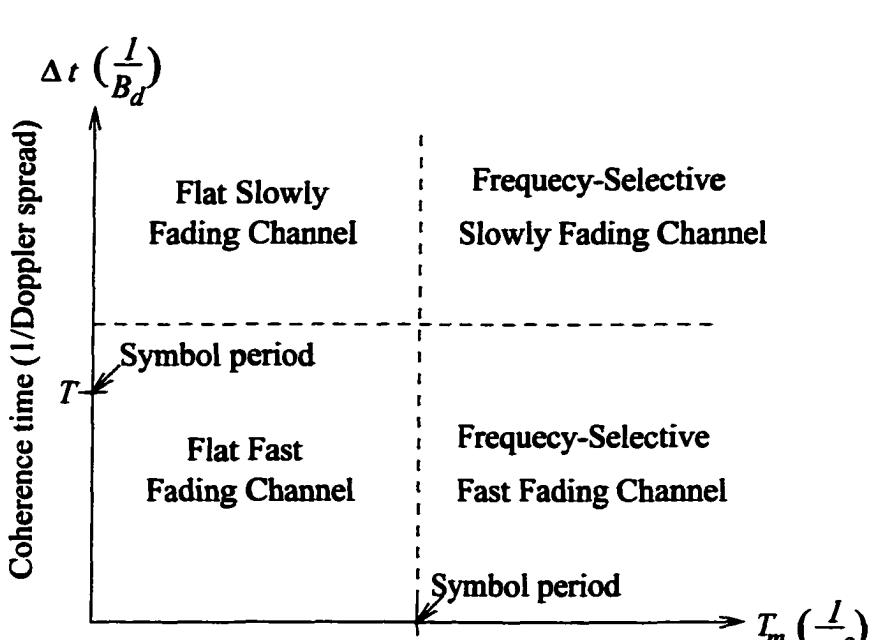

Figure 2.2. *Classification of multipath fading channels.*

2.2.3 A Tapped-Delay-Line Model for Frequency-Selective Channels

When a bandlimited signal is transmitted over a frequency-selective fading channel, the received signal includes multiple copies of the signal which are attenuated and delayed in time. These copies are affected differently by the channel with respect to amplitude and phase angle. For this reason, frequency-selective fading channels are much more difficult to model than flat fading channels and must be considered as linear filters. Using the IR formula given by (2.4) directly is inconvenient because the delays $\{\tau_n(t)\}$ can take arbitrary values and vary in time.

Denote the bandwidth occupied by the bandlimited signal by W. Since the channel

is frequency selective, we have $1/W < T_m$ and assume that the channel is slowly fading such that the channel IR is virtually constant over one symbol period. By applying the sampling theorem, we can express the IR of the equivalent lowpass channel as [11]

$$c(\tau, t) = \sum_n c_n(t)\delta(\tau - n/W) \tag{2.9}$$

Compared to (2.4), the above formula for the channel IR has a number of advantages:

- The delays are fixed to be multiples of $1/W$.
- The number of paths that must be considered is fixed and can be reduced. For a channel with multipath spread T_m, the number of resolvable paths is $L = \lceil T_m/W \rceil$, where $\lceil x \rceil$ rounds x to the nearest integer towards positive infinity.

Based on (2.9), a tapped-delay-line model truncated according to the multipath spread can be derived as shown in Fig. 2.3. In the special case of Rayleigh fading, the magnitudes $|c_n(t)|$ are Rayleigh distributed and the phase angles are uniformly distributed in the range 0 to 2π. With the assumption of uncorrelated scattering, $c_n(t)$ are mutually uncorrelated. As will be shown later, the above tapped-delay-line model enables us to design a receiver that can achieve the frequency diversity inherent in the wideband DS-CDMA signals.

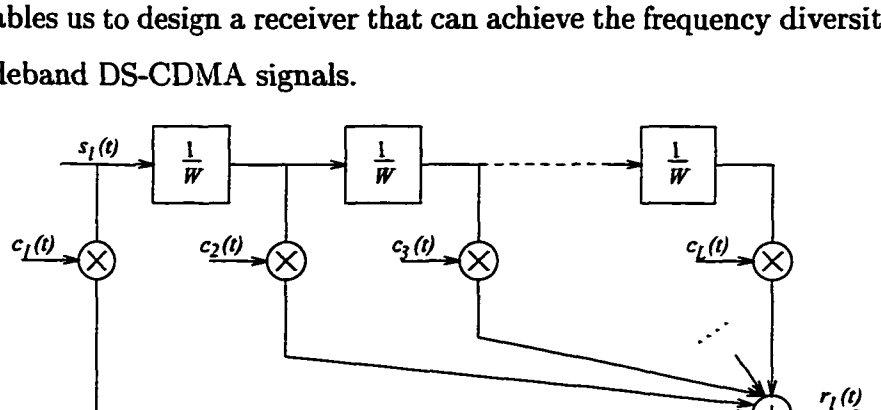

Figure 2.3. *A tapped-delay-line model for frequency-selective channels.*

2.3 DS-CDMA

2.3.1 User Multiplexing

DS-CDMA is a user multiplexing technique by which users can transmit signals at the same time, occupying the same frequency band, and are distinguished by their distinct spreading codes. Before transmission, the information signal is multiplied by a signature signal whose bandwidth is orders of magnitude larger than the bandwidth of the information signal. Here, we only consider short signature signals that are applied periodically to each information symbol, which can be expressed as

$$s_k(t) = \sum_{n=0}^{G-1} g_k(n)p(t - nT_c) \tag{2.10}$$

where $g_k(n), 0 \leq n \leq G-1$ is the spreading code assigned to the kth user, $p(t)$ is a pulse of duration T_c, and $T_c = T/G$ is the chip interval. Without loss of generality, we can always assume that the signature signals have unit energy, i.e.,

$$\int_0^T s_k(t)s_k^*(t)dt = 1 \quad \text{for } k = 1, 2, \ldots, K \tag{2.11}$$

Since there are G chips per symbol, the signal bandwidth is increased by G times. For this reason, the multiplication process at the transmitter is often called spreading and G is called the *spreading gain.*

If all the signature signals are nearly orthogonal to each other, the user information symbol can be recovered at the receiver by simply multiplying the received signal by the signature signal of the desired user. This multiplication process at the receiver is called despreading. Compared with FDMA and TDMA, DS-CDMA provides a number of advantages. These include soft capacity limit, easier handoff, anti-jamming, and frequency diversity, etc., [32]. One of the main disadvantages of DS-CDMA systems is the near-far (NF) problem that occurs when user powers are largely unbalanced at a receiver. If the signature signals are not perfectly orthogonal to each other, the amount of multiuser interference (MUI) to a signal with low power

becomes significant. As will be described shortly, this problem is especially severe in conventional DS-CDMA systems where a matched-filter receiver (MFR) is used.

2.3.2 Conventional Receiver

Throughout the thesis, antipodal signaling is assumed, hence each information symbol carries one information bit and takes values of $+1$ or -1 with equal probabilities. Another consequence of this assumption is that the spreading codes are real-valued. This assumption is not critical but simplifies notation. With minor modifications, the results obtained in this dissertation can be readily extended to the cases of other modulation schemes by assuming complex-valued symbols and spreading codes.

To investigate the NF problem, we now examine signal transmission and receiving in a conventional DS-CDMA system that is shared by K users. Without loss of generality, frequency-selective fading channels will be assumed so that flat fading and AWGN channels can be viewed as special cases. That is, a frequency-selective fading channel becomes a flat fading channel if there is only one path and is further simplified to an AWGN channel if the path gain of the only path is time invariant. Let the message length be N and denote by $b_k(n)$, e_k, $s_k(t)$ the nth information bit, the energy per bit, and the signature signal of the kth user, respectively. Thus the baseband signal at a receiver can be expressed as

$$y(t) = \sum_{k=1}^{K} \sum_{n=0}^{N-1} \sum_{l=1}^{L} \sqrt{e_k} c_{k,l}(t) b_k(n) s_k[t - nT - \tau_k - (l-1)/W] + z(t) \qquad (2.12)$$

where $z(t)$ is a complex-valued white Gaussian noise process with power spectral density $N_0/2$, L is the largest resolvable path among all channels between transmitters and the receiver, and $c_{k,l}(t)$ and τ_k are the lth path gain and the delay associated with the kth user, respectively. Without loss of generality, we assume that users are numbered by their relative delays, i.e., $0 = \tau_1 \leq \tau_2 \cdots \leq \tau_k \leq T$.

In conventional DS-CDMA systems, MUI is treated as AWGN on the grounds that its statistical properties are similar to that of AWGN if the number of users is large.

Thus a single-user matched filter should be nearly optimal for signal detection. Since the symbol interval is usually selected such that $T \gg T_m$, the inter-symbol interference (ISI) due to the cross correlations between $s_k[t-(l-1)/W]$ and $s_k[t-T-(m-1)/W]$ for $m < l$ can be neglected. Consequently, the MFR for frequency-selective channels can be implemented as illustrated in Fig. 2.4. As can be seen from the figure, the L delayed copies of the signature signal of the desired user are first multiplied by the path gains associated with the corresponding delays and then summed to form a composite signature signal. The time-reversed version of the composite signature signal is taken as the IR of a filter through which the received signal is passed. Finally, the output of the filter is sampled at appropriate times to obtain decision statistics. Looking at it in another way, the receiver consists of L matched filters and each filter is matched to one delayed replica of the signature signal. The L outputs are then weighted by corresponding delays and summed to form decision statistics. Since this receiver acts like an ordinary garden rake, it is called the *RAKE* receiver.

Note that the L replicas of the signal are mutually independent. The probability that all the signal components are in a deep fade simultaneously is largely reduced compared to the cases where only one replica of the signal is available. Hence the RAKE receiver has the potential to achieve an Lth-order diversity gain which is inherent in wideband DS-CDMA signals.

Now assume that the channel fading is sufficiently slow such that $c_{m,l}(t)$ can be treated as constants during one symbol interval and define $c_{m,l}(n) \equiv c_{m,l}(t)$ for $nT+\tau_k \le t \le (n+1)T+\tau_k$, where k is the number associated with the desired user. Hence the decision statistics can be expressed as

$$u_k(n) = \sum_{l=1}^{L} |c_{k,l}(n)|^2 \sqrt{e_k} b_k(n) + \mathrm{Re}\left\{ \sum_{l=1}^{L} \int_0^T z(t-nT-\tau_k) c_{k,l}^* s[t-(l-1)/W]\, dt \right\} + I_1 + I_2 \quad (2.13)$$

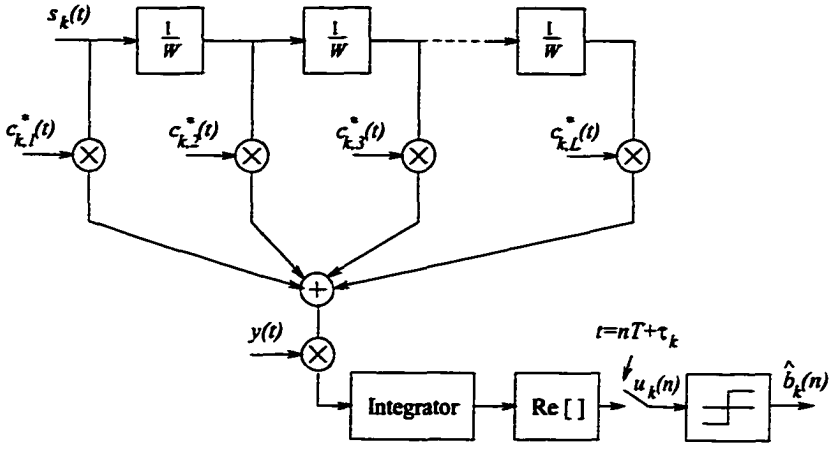

Figure 2.4. *RAKE receiver for frequency-selective fading channels.*

where

$$I_1 = \sqrt{e_k} b_k(n) \operatorname{Re}\left\{ \sum_{l=1}^{L} \sum_{i=1, i\neq l}^{L} c^*_{k,l}(n) c_{k,i}(n) \right\} \cdot \int_0^T s_k[t-(l-1)/W] s_k[t-(i-1)/W]\, dt \tag{2.14}$$

$$\begin{aligned} I_2 = \operatorname{Re}\Bigg\{ & \sum_{j=k+1}^{K} \sum_{m=-1}^{0} \sum_{l=1}^{L} \sum_{i=1}^{L} b_j(n+m) \sqrt{e_j} c_{j,i}(n+m) c^*_{k,l}(n) \\ & \cdot \int_0^T s_k[t-(l-1)/W] s_j[t-mT-\tau_j+\tau_k-(i-1)/W]\, dt \\ & + \sum_{j=1}^{k-1} \sum_{m=0}^{1} \sum_{l=1}^{L} \sum_{i=1}^{L} b_j(m+n) \sqrt{e_j} c_{j,i}(m+n) c^*_{k,l}(n) \\ & \cdot \int_0^T s_k[t-(l-1)/W] s_j[t-mT-\tau_j+\tau_k-(i-1)/W]\, dt \Bigg\} \end{aligned} \tag{2.15}$$

It is evident from (2.13) that the decision statistics consist of four components: the information bit to be detected, a noise component due to AWGN, a self-interference component denoted by I_1, and an MUI component denoted by I_2. Because of the uncertainty inherent in user delays and the existence of multiple paths, orthogonality among all signature signals and their delayed versions is impossible. In order to control the interference and hence the cross-correlations among signature signals and

their delayed versions, pseudo-random sequences can be used. In such a case, all cross-correlations are relatively small. However, the power imbalance at the receiver can be very severe given the dynamics of mobile channels. Whenever there is an interferer with large power relative to e_k, the performance of the RAKE receiver for user k will be unacceptable.

Note that if there exist a large number of users with equal powers, then the central limit theorem applies and the output of the RAKE receiver (or the MFR for AWGN channels) is approximately Gaussian. For such a case, one might think the RAKE receiver is at least nearly optimal. However, the reality is that the performance of the RAKE receiver can still be far from optimal. This is because the output of the single-user matched filter does not provide sufficient statistics unless all the signature signals and their delayed versions are mutually orthogonal to each other.

2.4 Optimal Mutiuser Detection

The optimal multiuser detector selects the most probable sequence of bits given the received signal observed during the whole transmission period. Since it maximizes the a joint posteriori probability, it is also often called the *maximum-likelihood sequence* receiver. Let $\mathbf{b}$ is a vector collecting all user bits sequentially, i.e.,

$$\mathbf{b} = [\mathbf{b}^T(0)\ \mathbf{b}^T(1)\ \cdots\ \mathbf{b}^T(N-1)]^T \tag{2.16}$$

where

$$\mathbf{b}(n) = [\mathbf{b}_1(n)\ \mathbf{b}_2(n)\ \cdots\ \mathbf{b}_K(n)]^T \tag{2.17}$$

The joint a posteriori probability can be denoted as $P(\hat{\mathbf{b}}/y(t))$, where $\hat{\mathbf{b}}$ is a possible estimate of $\mathbf{b}$ and $y(t)$ is the received signal.

For the sake of notational simplicity, we assume an AWGN channel. Hence the received signal can be obtained by letting $c_{k,1}(n) = 1$ and $c_{k,l}(n) = 0$ for $l > 1, k =$

$1, 2, \ldots, K$ in (2.12) as

$$y(t) = \sum_{k=1}^{K} \sum_{n=0}^{N-1} \sqrt{e_k} b_k(n) s_k(t - nT - \tau_k) + z(t) \tag{2.18}$$

It can then be shown that maximizing $P[\hat{\mathbf{b}}/y(t)]$ is equivalent to maximizing the log-likelihood function

$$\begin{aligned}\Lambda(\hat{\mathbf{b}}) &= \int_0^{NT+T} [y(t) - \sum_{k=1}^{K} \sum_{n=0}^{N-1} \sqrt{e_k} \hat{b}_k(n) s_k(t - nT - \tau_k)]^2 \, dt \\ &= \int_0^{T+NT} y^2(t) dt - 2 \sum_{k=1}^{K} \sum_{n=0}^{N-1} \sqrt{e_k} \hat{b}_k(n) \int_0^{NT+T} y(t) s_k(t - nT - \tau_k) \, dt \\ &\quad + \sum_{k=1}^{K} \sum_{l=1}^{K} \sum_{n=0}^{N-1} \sum_{m=0}^{N-1} \sqrt{e_k e_l} \hat{b}_k(n) \hat{b}_l(m) \int_0^{NT+T} s_k(t - nT - \tau_k) s_l(t - mT - \tau_l) \, dt\end{aligned} \tag{2.19}$$

where $\hat{b}_k(n)$ is the $(nK + k)$th entry of $\hat{\mathbf{b}}$.

The nth output of the matched filter for the kth user can be expressed as

$$r_k(n) \equiv \int_0^{T+NT} y(t) s_k(t - nT - \tau_k) \, dt \tag{2.20}$$

Thus the second term on the right-hand side of (2.19) can be expressed as $2\hat{\mathbf{b}}^T \mathbf{E} \mathbf{r}$, where

$$\mathbf{r} = [\mathbf{r}^T(0) \; \mathbf{r}^T(1) \; \cdots \; \mathbf{r}^T(N-1)]^T \tag{2.21}$$

$$\mathbf{r}(n) = [r_1(n) \; r_2(n) \; \cdots r_K(n)]^T \tag{2.22}$$

and $\mathbf{E}$ is an $NK \times NK$ matrix whose $(Kn + k)$th entries for $n = 0, 1, \ldots, N-1$ are $\sqrt{e_k}$. Let

$$h_0(k, l) = \int_{-\infty}^{+\infty} s_k(t - \tau_k) s_l(t - \tau_l) \, dt \tag{2.23}$$

$$h_1(k, l) = \int_{-\infty}^{+\infty} s_k(t - \tau_k) s_l(t - \tau_l + T) \, dt \tag{2.24}$$

$$\tag{2.25}$$

and denote $\mathbf{H}_0$ and $\mathbf{H}_1$ as the $K \times K$ matrices whose (k,l)th entries are $h_0(k,l)$ and $h_1(k,l)$, respectively. It can be verified that the third term on the right-hand side of (2.19) can be expressed as $\hat{\mathbf{b}}^T\mathbf{E}\mathbf{R}_N\mathbf{E}\hat{\mathbf{b}}$, where

$$\mathbf{R}_N = \begin{bmatrix} \mathbf{H}_0 & \mathbf{H}_1^T & 0 & \dots & \dots & 0 \\ \mathbf{H}_1 & \mathbf{H}_0 & \mathbf{H}_1^T & 0 & \dots & 0 \\ \vdots & \vdots & \vdots & \vdots & \vdots & \vdots \\ 0 & 0 & 0 & \mathbf{H}_1 & \mathbf{H}_0 & \mathbf{H}_1^T \\ 0 & 0 & 0 & 0 & \mathbf{H}_1 & \mathbf{H}_0 \end{bmatrix} \tag{2.26}$$

is an $(N \times N)$-block tridiagonal matrix.

Since the first term at the right-hand side of (2.19) is a constant, maximizing $\Lambda(\hat{\mathbf{b}})$ is equivalent to maximizing the metric given by

$$C(\hat{\mathbf{b}}) = \hat{\mathbf{b}}^T\mathbf{E}\mathbf{R}_N\mathbf{E}\hat{\mathbf{b}} - 2\hat{\mathbf{b}}^T\mathbf{E}\mathbf{r} \tag{2.27}$$

From the above equation, it is clear that the optimal maximum-likelihood sequence detector requires the signal amplitudes, which can be estimated, in practice, by using the method described in [33]. As can also be observed, the optimal multiuser detection is a combinatorial optimization problem. This optimization problem has been shown to belong to a class of NP-complete problems [34]. If a block processing approach is taken, the maximum-likelihood sequence detector must compute 2^{NK} metrics and select the $\hat{\mathbf{b}}$ that gives the largest metric $C(\hat{\mathbf{b}})$ by the fact that there exist 2^{NK} possible bit sequences. Evidently, this approach involves too much computation to implement in practice. Furthermore, the long decision delay also limits its practical application. A much better way is to detect the information bits sequentially by using the Viterbi algorithm [5]. Since each information bit is only previously overlapped by the other $K-1$ information bits, the prior information, on which the decision of each information bit depends, can be sufficiently described by its previous $K-1$ information bits. In other words, the system has 2^{K-1} states and the computational complexity of the sequential maximum-likelihood sequence detector is $\mathcal{O}(2^{K-1})$ per

bit and irrelevant to N. This is a great reduction in the amount of computation as compared to that of the block processing approach. However, the computational complexity is still exponential with respect to the number of users.

Another important observation from (2.27) is that the output vector $\mathbf{r}$, which collects the outputs of the matched filters for all users, provides sufficient statistics for the detection of all the transmitted information bits. This is in contrast to the fact that the outputs from one matched filter alone do not provide sufficient statistics for the detection of bits of the corresponding user alone. Consequently, a detector can directly work on $\mathbf{r}$ without losing any information.

2.5 Linear Multiuser Detection

Linear multiuser detectors are detectors that apply a linear operation to the received signal to obtain decision statistics. Once the linear mapping is computed, it can be used for all the detection of all incoming bits until the system parameters changes. Hence linear detectors are especially efficient for DS-CDMA systems with periodic spreading codes systems where key parameters change only occasionally. Another important advantage of linear detectors is that efficient adaptation mechanisms can be developed so as to adaptively search for linear mappings without the need of information about interferers. For this reason, research on multiuser receivers for the forward link has been almost exclusively focused on linear receiving techniques.

There are basically two approaches to derive a linear multiuser detector. One approach is the bit-rate approach whereby the front-end matched filters are always assumed to be present and linear mapping is applied to the outputs of the matched filters. The other one is the chip-rate approach where linear mappings are directly applied to the received signal $y(t)$. Although in a certain situation, one approach can be more convenient than the other, the two approaches are equivalent from an information perspective. In the sequel, we take the bit-rate approach to describe the

two most popular linear multiuser detectors, namely, the decorrelating and minimum mean-squared error (MMSE) multiuser detectors.

2.5.1 Decorrelating Multiuser Detection

Let us consider an AWGN channel. It follows from (2.18) and (2.20) that

$$\mathbf{r} = \mathbf{R}_N \mathbf{E} \mathbf{b} + \mathbf{n} \tag{2.28}$$

where $\mathbf{n}$ is an AWGN vector with zero mean and a covariance matrix $N_0 \mathbf{R}_N/2$.

The decorrelating detector seeks to minimize the amount of MUI regardless of the existence of AWGN. This minimization criterion is called zero-forcing criterion. Since $\mathbf{R}_N$ is almost always positive definite in practice, the MUI can be completely eliminated by using a linear mapping given by

$$\mathbf{L}_d = \mathbf{R}_N^{-1} \tag{2.29}$$

Hence the soft output of the decorrelating detector is given by

$$\begin{aligned} \hat{\mathbf{b}} &= \mathbf{L}_d \mathbf{r} \\ &= \mathbf{E}\mathbf{b} + \mathbf{R}_N^{-1}\mathbf{n} \end{aligned} \tag{2.30}$$

It is clear from (2.29) and (2.30) that the decorrelating detector does not need information about user amplitudes.

An interesting observation can be made by interpreting asynchronous transmission as an equivalent synchronous transmission, where NK synchronous users transmit one information bit each and the signature signals are of duration $NT + T$. For example, the $(nK + k)$th user in the equivalent synchronous system transmits bit $b_k(n)$ and its signature signal is given by

$$\hat{s}_{nK+k}(t) = \begin{cases} s_k(t - nT - \tau_k) & nT + \tau_k < t < nT + T + \tau_k \\ 0 & \text{otherwise} \end{cases} \tag{2.31}$$

Let $\hat{\mathbf{s}}_k$ be a column vector representing the critically sampled version of $\hat{s}_k(t)$ and denote the matrix whose kth column is $\hat{\mathbf{s}}_k$ as $\hat{\mathbf{S}}$. We can write

$$\mathbf{R}_N = \hat{\mathbf{S}}^T\hat{\mathbf{S}} \tag{2.32}$$

$$\mathbf{r} = \hat{\mathbf{S}}^T\mathbf{y} \tag{2.33}$$

where $\mathbf{y}$ is a column vector representing the critically sampled version of $y(t)$. From (2.29) and (2.33), the linear mapping applied to the received signal $\mathbf{y}$ for the kth synchronous user is given by

$$\mathbf{w}_k = \hat{\mathbf{S}}\mathbf{L}_d\mathbf{e}_k \tag{2.34}$$

where $\mathbf{e}_k$ is the kth coordinate column vector. Hence, we have

$$\mathbf{w}_k^T\hat{\mathbf{S}} = \mathbf{e}_k^T\mathbf{R}_N^{-1}\hat{\mathbf{S}}^T\hat{\mathbf{S}} = \mathbf{e}_k^T \tag{2.35}$$

In effect, the decorrelating mapping applied to the received signal $y(t)$ for the kth user is orthogonal to the signature signals of all the other users, as illustrated in Fig. 2.5. Hence, as the Gaussian noise vanishes, the decorrelating detection is free of error regardless of the power of interferers. In fact, it has been shown that the decorrelating detector achieves optimal NF resistance [9].

An undesirable feature of the decorrelating detector is that noise is always enhanced. From (2.30), the covariance matrix of the AWGN at the output of the decorrelating detector is

$$E[\mathbf{R}_N^{-1}\mathbf{n}\mathbf{n}^T\mathbf{R}_N^{-1}] = \frac{N_0}{2}\mathbf{R}_N^{-1} \tag{2.36}$$

Since the signature signals have unit energy, the diagonal entries of $\mathbf{R}_N$ are equal to 1. Since the difference between the inverse of a principle submatrix of a matrix and the corresponding principal submatrix of the inverse of the matrix is positive semidefinite or positive definite [35], the diagonal entries of $\mathbf{R}_N^{-1}$ are greater or equal to 1. Hence the variance of the AWGN at the soft output of the decorrelating detector is greater than or equal to $N_0/2$, which is the noise variance at the output of the matched filter.

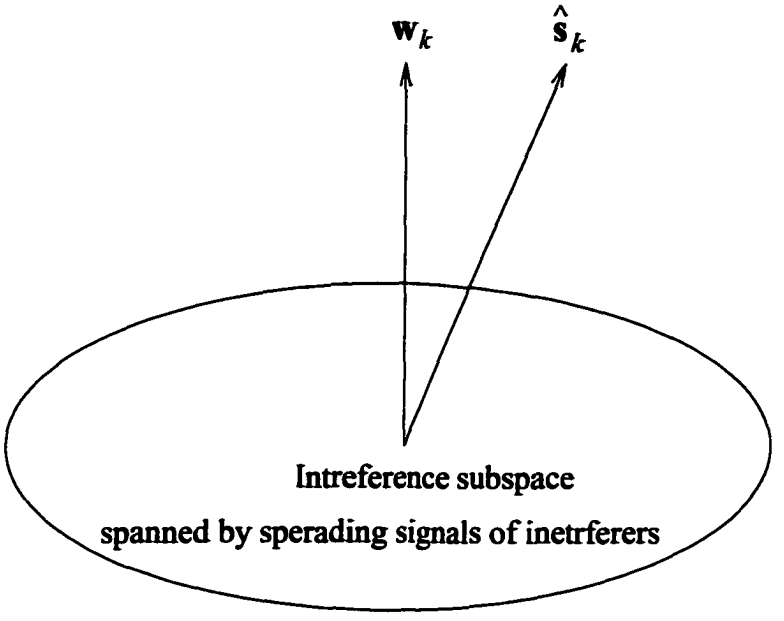

Figure 2.5. *An interpretation of decorrelating filtering.*

2.5.2 MMSE Multiuser Detection

In contrast to the decorrelating detector, the MMSE multiuser detector seeks to maximize the signal-to-interference-plus-noise ratio (SINR) or, equivalently, to minimize the output mean-squared error (MSE) given by

$$M = E[\|\mathbf{Lr} - \mathbf{Eb}\|^2] \tag{2.37}$$

The solution of the above minimization problem with respect to $\mathbf{L}$ is the MMSE linear mapping $\mathbf{L}_m$ given by

$$\mathbf{L}_m = \left[\mathbf{R}_N + \frac{N_0}{2}\mathbf{E}^{-2}\right]^{-1} \tag{2.38}$$

The above solution for synchronous transmission was deduced in [21] and [23]. Here we describe a simple way to obtain the solution.

Proof Since information bits are mutually independent, it is sufficient to consider the detection of any one information bit. Denote the kth row of a linear mapping $\mathbf{L}$ by $\mathbf{w}_k^T$. Minimizing the MSE given by (2.37) is equivalent to minimizing

$$M_k = E[(\mathbf{w}_k^T\mathbf{r} - \mathbf{e}_k^T\mathbf{Eb})^2]$$

$$= E[\mathbf{w}_k^T \mathbf{r}\mathbf{r}^T \mathbf{w}_k - 2\mathbf{e}_k^T \mathbf{E}\mathbf{b}\mathbf{r}^T \mathbf{w}] + 1 \tag{2.39}$$

Substituting (2.28) into the above equation, we have

$$M_k = \mathbf{w}_k^T \mathbf{R}_N^2 \mathbf{E}^2 \mathbf{w}_k + \frac{N_0}{2} \mathbf{w}_k^T \mathbf{R}_N \mathbf{w}_k - 2\mathbf{e}_k \mathbf{E}^2 \mathbf{R}_N \mathbf{w}_k + 1 \tag{2.40}$$

It follows that the vector $\mathbf{w}_k$ that minimizes M_k is given by

$$\mathbf{w}_k = \left[\mathbf{R}_N + \frac{N_0}{2}\mathbf{E}^{-2}\right]^{-1} \mathbf{e}_k \tag{2.41}$$

Comparing the above equation with (2.38), we can see that $\mathbf{w}_k^T$ is the kth row of $\mathbf{L}_m$.

Since the MMSE detector takes the background noise into account, it usually outperforms the decorrelating detector. A more important advantage of the MMSE detector is that it can be readily implemented adaptively. For mobile stations where only one user is of interest and the signature signals of interferers are unknown, an adaptive implementation is desirable. Hence, in this case, the MMSE detector is the preferred choice. On the other hand, for base stations where all the users need to be detected and their signature signals are known, a nonadaptive, more efficient implementation of joint detection is possible. Consequently, in this case the advantages of the MMSE detector may be offset by its need of information about user amplitudes in nonadaptive implementation.

2.6 Conclusions

We have briefly introduced the characteristics, classifications, and modeling of mobile radio channels. We have also introduced the conventional CDMA receiver, i.e., the RAKE receiver (or the MFR for frequency-nonselective channels), and three early multiuser detectors, namely, the optimal multiuser detector, the decorrelating detector, and the MMSE detector. Through this introduction, we have provided background knowledge, concepts, and terminology that are necessary for the development of new multiuser detectors in the following chapters.

Chapter 3

An Overlapping Window Decorrelating Multiuser Detector for Mobile Base Stations

3.1 Introduction

The decorrelating detector is perhaps the most popular detector owing to its many advantages. Specifically, it achieves the optimal near-far (NF) resistance without the need for information about the received signal energies. This makes the decorrelating detector an attractive base-station solution for DS-CDMA mobile radio systems. In addition, the structural simplicity of the decorrelating detector allows one to combine it easily with diversity receivers, such as the RAKE and antenna array receivers, to eliminate multiuser interference (MUI) and achieve diversity gain simultaneously [25]-[27]. Furthermore, the development of the decorrelating detector lays the ground for the development of several more sophisticated multiuser detectors, and many results about the decorrelating detector can often be directly extended to other detectors. For instance, the decorrelating detector can play a key role in the well-known multistage multiuser detector [14].

Despite tremendous progress made on decorrelating detection, problems pertaining to its practical implementation still exist. For a synchronous system with K

users, successive information bits are not overlapped. Consequently, decorrelating detection can be performed bit by bit. In this case, the system cross-correlation is of size $K \times K$ and the decorrelating detector can be readily implemented. However, for asynchronous systems, which are very popular, ideal decorrelating detection can only be performed after the entire message has been received, where the term 'message' is taken to mean that no data are transmitted immediately before and after the transmitted data packet. Hence, the cross-correlation matrix is of size $NK \times NK$, where N is the the message length. Evidently, the implementation of the ideal decorrelating detector for asynchronous systems is not trivial. Since the message length N is usually very large, computing and updating the inverse of the cross-correlation matrix is computationally too complex and the detection delay is unacceptable. Hence, modifications must be made in practical implementations. In order to differentiate it from its modified versions, the standard decorrelating detector based on the received signal observed during the entire message transmission will be referred to as the *ideal decorrelating detector.*

To achieve an acceptable detection delay, a window approach for implementing the ideal decorrelating detector was first suggested in [10], and a number of window-based decorrelating detectors have been developed recently [36]-[38]. A problem related to these detectors is the edge effect caused by the MUI from the transmitted signals outside the working window, where the working window is the window that is currently being processed. In [36], the edge effect is avoided by periodically leaving a regular symbol interval without transmission. Clearly, this approach leads to reduced bandwidth efficiency. In [37], the redundancy inherent in the convolutional code was exploited and the right-edge effect is eliminated by using prediction of the future bits based on the decoded bits. However, this approach only applies to systems using convolutional codes and requires extra coordination among users, which can be cumbersome for system management. In [38], an interesting observation relating to the decay of the impulse response of the ideal decorrelating detector was made, which led

to the so-called truncated decorrelating detector whose performance can be arbitrarily close to that of the ideal decorrelating detector if the window length is sufficiently large. However, the actual decay rate as well as the method by which the window length is determined were not addressed.

Another method to obtain a finite-length decorrelating detector is based on the chip-rate approach. This approach leads to an exact finite-duration impulse response (FIR) solution and avoids the edge effects [39]. However, the bit-rate approach has been widely adopted in the past for problems where user codes are known. This is because an exact decorrelating solution does not necessarily imply a satisfactory performance and issues concerning practical implementation are easier to handle in the bit-rate approach. No matter which approach is adopted, similar problems concerning practical implementation exist. These include (a) a matrix of large size needs to be inverted, and (b) an appropriate window (or filter) length needs to be determined to assure a satisfactory performance with moderate computational complexity.

In this chapter, we first compare the ideal decorrelating detector with the exact FIR decorrelating detector proposed in [39] in terms of performance. We show that the ideal decorrelating detector consistently achieves better performance. We then discuss issues on the implementation of the two detectors. It is shown that problems pertaining to the ideal decorrelating detector also exist for the exact FIR decorrelating detector.

In order to solve the aforementioned problems, we propose a new window-based detector, which will be referred to as the *overlapping window decorrelating* (OWD) detector. In the proposed detector, the left-edge effect is eliminated by using the previously detected information bits and the right-edge effect is treated as additive white Gaussian noise (AWGN). The right-edge effect is controlled by selecting a sufficiently large window length. A great deal of attention is given to the convergence and decay properties of the ideal decorrelating impulse response (IR). Although some of our analysis results have been noted in the past [10][38], our results give more insight to

the problem at hand and lead to an interesting quantitative description of the decay rate. Two supporting utilities are also developed to make the OWD detector practically useful. These are a block-recursive algorithm for efficiently updating the OWD detector and a signal-adapted criterion that determines the minimum window length for satisfactory performance under the NF situation of a given system. Furthermore, the use of the OWD detector in conjunction with the conventional RAKE receiver for multipath fading channels is addressed. An analysis and extensive computer simulations are carried out which show that a performance very close to that of the ideal decorrelating detector can be achieved by the OWD detector with a small to moderate window length. In fact, in some cases the OWD detector can even outperform the ideal decorrelating detector.

3.2 Exact FIR Decorrelating Detection

In [39], an exact FIR decorrelating detector was developed by taking a chip-rate approach. This detector achieves a zero-forcing solution regardless of the message length N. One may conclude that it is advantageous to take a chip-rate approach and, therefore, problems related to the ideal decorrelating detector are avoided. This conclusion is unfortunately incorrect. In this section, we compare the exact FIR decorrelating detector with the ideal decorrelating detector in terms of performance and implemetation complexity.

3.2.1 Existence of Zero-Forcing Solution

For the sake of simplicity, we consider a DS-CDMA system with periodic spreading codes over an AWGN channel. In this case, the ideal decorrelating detector comprises a bank of matched filters followed by the linear mapping $\mathbf{R}_N^{-1}$ given by (2.26). To achieve an exact zero-forcing solution with a moderate detection delay, we only observe a window of the asynchronous transmission that covers the information bits

of interest. Within a window, each information bit is deemed to originate from a different synchronous user. In doing so, an asynchronous system is interpreted as an equivalent synchronous system. Assuming that the working window covers exactly M bits of asynchronous user 1 and none of the other users is synchronous with user 1, then there are $MK+K-1$ virtual synchronous users. Without loss of generality, we number the equivalent synchronous users according to the starting times of their transmissions, as illustrated in Fig. 3.1. If all the user signature signals are linearly independent of each other, an exact decorrelating solution exists. Let us collect all the user codes (critically sampled signature signals) of the virtual synchronous users within a processing window in matrix $\mathbf{S}_s$. Then the FIR decorrelating coefficient vector for the bit at the center of the window of the jth user is the $(Kp+j-1)$th column of matrix $\mathbf{S}_s\mathbf{R}^{-1}$. The cross-correlation matrix $\mathbf{R}$ is of dimension $MK+K-1$ and is given by

$$\begin{aligned}\mathbf{R} &= \mathbf{S}_s^T\mathbf{S}_s \\ &= \begin{bmatrix} \mathbf{X}_1 & \mathbf{Y}^T & 0 & \dots & \dots & \dots & 0 \\ \mathbf{Y} & \mathbf{H}_0 & \mathbf{H}_1^T & 0 & \dots & \dots & 0 \\ 0 & \mathbf{H}_1 & \mathbf{H}_0 & \mathbf{H}_1^T & \dots & \dots & 0 \\ \vdots & \vdots & \vdots & \vdots & \vdots & \vdots & \vdots \\ 0 & 0 & 0 & 0 & \mathbf{H}_1 & \mathbf{H}_0 & \mathbf{H}_1^T \\ 0 & 0 & 0 & 0 & 0 & \mathbf{H}_1 & \mathbf{X}_2 \end{bmatrix}\end{aligned} \tag{3.1}$$

where $\mathbf{H}_0$ and $\mathbf{H}_1$ are defined in (2.24) and (2.25), respectively, $\mathbf{Y} \in \mathcal{R}^{K\times(K-1)}$ consists of the second to the Kth columns of $\mathbf{H}_1$, and $\mathbf{X}_1 = \{x_1(i,j)\}$ and $\mathbf{X}_2 = \{x_2(i,j)\}$ are $(K-1)\times(K-1)$ and $K\times K$ matrices, respectively. If $s_k(t)$ represents the signature signal of the kth asynchronous user, we then have

$$x_1(i,j) = \int_T^\infty s_{i+1}(t-\tau_{i+1})s_{j+1}(t-\tau_{j+1})\,dt \tag{3.2}$$

$$x_2(i,j) = \int_0^T s_i(t-\tau_i)s_j(t-\tau_j)\,dt \tag{3.3}$$

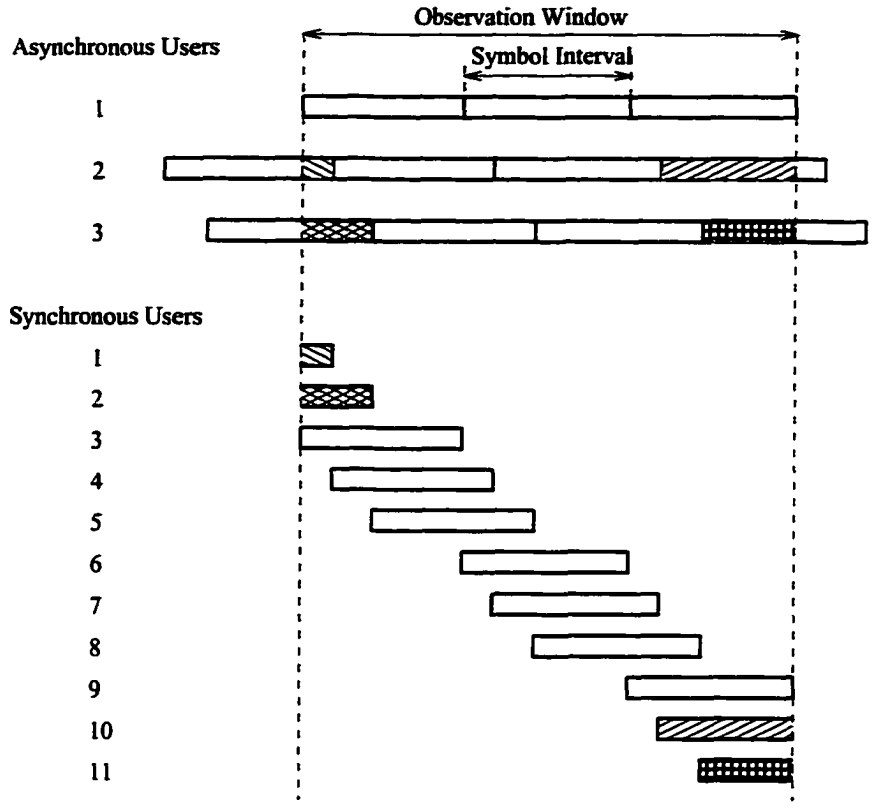

Figure 3.1. *Arrangement of virtual synchronous users in an asynchronous transmission.*

It follows from the above two equations and (2.24) that

$$\tilde{\mathbf{X}}_1 + \mathbf{X}_2 = \mathbf{H}_0 \tag{3.4}$$

where

$$\tilde{\mathbf{X}}_1 = \begin{bmatrix} 0 & \mathbf{0} \\ \mathbf{0} & \mathbf{X}_1 \end{bmatrix} \tag{3.5}$$

In the above analysis, we have assumed that $\mathbf{R}$ is positive definite to ensure that an exact zero-forcing solution exists. However, it is difficult to verify the positive definiteness of $\mathbf{R}$ by checking if all the spreading codes of virtual synchronous users are linearly independent of each other. For this reason, we now provide a sufficient

condition on the existence of the exact FIR decorrelator.

Proposition 3.1: For an arbitrary window length $M \leq N$, an exact zero-forcing solution exists if it exists for a window length 1, or, equivalently,

$$\mathbf{R}_1 = \begin{bmatrix} \mathbf{X}_1 & \mathbf{Y}^T \\ \mathbf{Y} & \mathbf{X}_2 \end{bmatrix} \tag{3.6}$$

is positive definite.

The proof of this proposition can be found in Appendix A.

It is also shown in Appendix A that if an exact FIR zero-forcing solution exists for a window length M, then it exists for any other window length larger than M. Having said that, however, an exact FIR decorrelator does not necessarily yield satisfactory performance as shown below.

3.2.2 Performance and Implementation Issues

Since the exact FIR decorrelator achieves a zero-forcing solution, the MUI is completely eliminated. The only impairment in the outputs of the detector is AWGN. Denoting the output AWGN as $\mathbf{n}_s$, its covariance matrix can be found as

$$E[\mathbf{n}_s \mathbf{n}_s^T] = \frac{N_0}{2}\mathbf{R}^{-1} \tag{3.7}$$

Comparing the exact decorrelating detector with the ideal decorrelating detector in terms of performance, we have the following proposition.

Proposition 3.2: For a time-invariant system, the ideal decorrelating detector consistently achieves better performance than an exact FIR decorrelating detector with a window length M less than the message length N.

Proof Note that both of the two detectors completely eliminate MUI at the outputs of the detectors. Hence, it is sufficient to only consider the variance of the

output noise. Comparing (3.7) with (2.36), we need only to show that the diagonal entries of $\mathbf{R}^{-1}$ are larger than or equal to the corresponding diagonal entries of $[\mathbf{R}_N^{-1}]_{Kn+2:K(n+M+1)}$ for any integer n, where $\mathbf{A}_{a:b}$ denotes the square matrix consisting of columns and rows of a to b of $\mathbf{A}$ and $\mathbf{R}_N$ is given by (2.26). For a given n, replacing $[\mathbf{R}_N]_{Kn+2:K(n+M+1)}$ by $[\mathbf{R}_N]_{Kn+2:K(n+M+1)} - \mathbf{R}$ in $\mathbf{R}_N$, we have

$$\hat{\mathbf{R}}_N = \text{diag}\{\mathbf{V}_1\ \mathbf{0}\ \mathbf{V}_2\} \tag{3.8}$$

where $\mathbf{V}_1$ consists of the last nK columns and rows of $\mathbf{V}$, $\mathbf{V}_2$ consists of the first $(N-M-1-n)K-1$ columns and rows of $\mathbf{V}$, and $\mathbf{V}$ is defined by (3.1) with a sufficiently large window length. Since there exists an exact FIR decorrelating solution for a window of length greater than or equal to M, there exists a positive definite $\mathbf{V}$. As a result, $\mathbf{V}_1$ and $\mathbf{V}_2$ must be positive definite. It then follows from (3.8) that $\hat{\mathbf{R}}_N$ is positive semidefinite. In Appendix B, it is shown that if the matrix obtained by replacing a principle matrix of a positive matrix $\mathbf{A}$ by the difference between the principle matrix and another positive definite matrix $\mathbf{B}$ is positive (semi)definite, then the difference between $\mathbf{B}^{-1}$ and the corresponding principle matrix of $\mathbf{A}^{-1}$ is positive (semi)definite. By this fact, we can conclude that $\mathbf{R}^{-1} - [\mathbf{R}_N^{-1}]_{Kn+1:K(n+M+1)}$ is positive semidefinite, i.e., the diagonal entries of $\mathbf{R}^{-1}$ are greater than or equal to the corresponding diagonal entries of $[\mathbf{R}_N^{-1}]_{Kn+1:K(n+M+1)}$. ■

In the proof of Proposition 3.2, it is shown that if the window length used is less than the message length N, then the exact FIR decorrelating detector increases the noise variance more than the ideal decorrelating detector does. Similarly, it can be proved that the larger the window length, the less the noise enhancement and the better the performance. On the other hand, a larger window length implies higher computational complexity and longer detection delay. Therefore, the window length needs to be carefully selected in practice. Interestingly, the problem of window-length determination also exists in the bit-rate approach.

It is also clear that directly updating the coefficient vector is computationally

not feasible. For instance, for a typical mobile system with 20 users, a moderate window length 5, and a processing gain 64, a matrix of size 119×119 needs to be first computed and updated. For one user, the 64×5 coefficients of the exact-decorrelating filter can then be obtained by multiplying $\mathbf{S}_s$ with the corresponding column of the updated matrix. This certainly requires too much computation and memory. From (3.1), $\mathbf{R}$ has the same structure as $\mathbf{R}_N$ except the size. This suggests an efficient implementation as follows. Instead of using one long FIR filter that spans the entire working window, we can employ three short-length matched filters for each user at the front end, which are matched to the entire user spreading code, the earlier portion and the latter portion of the user code, respectively. An immediate advantage of this approach is that updating the receiver due to changes of the system profile becomes easier. If the changes are due to user activation/deactivation, the matched filters do not need to be updated. Collecting the outputs of the matched filters in a column vector $\mathbf{r}_s$, the soft output of the detector can then be written as $\mathbf{R}^{-1}\mathbf{r}_s$. The remaining processing is the linear mapping defined by $\mathbf{R}^{-1}$. This operation is similar to the ideal decorrelating linear mapping. Hence if an efficient algorithm exists for the ideal decorrelating detection, it will also apply to the exact decorrelating detector.

In summary, the chip-rate approach provides an alternative solution to the problem at hand and leads to an exact FIR decorrelator. However, this decorrelator does not necessarily yield satisfactory performance. Problems that exist in the bit-rate approach, such as window-length determination and inverting and updating of a large size matrix, also exist in the chip-rate approach. One advantage that the bit-rate approach can provide is the potential of a simple implementation. That is, one matched filter is needed for each user if the bit-rate approach is taken whereas three matched filters must be used for each user in the chip-rate approach.

In the rest of the chapter, we will take a chip-rate approach and develop algorithms for matrix updating, user detection, and window-length determination. Because of the similarity of the two approaches, it will become clear that the algorithms described can

be readily applied to solve the corresponding problems in the exact FIR decorrelator. It will also become apparent that with the same window length, the proposed detector outperforms the exact FIR decorrelator.

3.3 An Overlapping Window Decorrelating Detector

3.3.1 Detection Scheme

We consider multiuser transmission through an AWGN channel shared by K asynchronous users in a DS-CDMA system. To be practical, the system is assumed to be *time dependent* in that user signature signals may vary with time. In this case, the output of the matched filters is still given by (2.28) with redefined $\mathbf{R}_N$ and $\mathbf{E}$. For the sake of clarity, we rewrite (2.28) as

$$\mathbf{r} = \mathbf{R}_N \mathbf{E} \mathbf{b} + \mathbf{n} \tag{3.9}$$

where

$$\mathbf{E} = \text{diag}\{\mathbf{E}(1) \cdots \mathbf{E}(N)\} \tag{3.10}$$

$$\mathbf{E}(k) = \text{diag}\{\sqrt{e_1(k)}\ \sqrt{e_2(k)} \cdots \sqrt{e_K(k)}\} \tag{3.11}$$

$$\mathbf{R}_N = \begin{bmatrix} \mathbf{H}_0(1) & \mathbf{H}_1^T(1) & 0 & \dots & \dots & 0 \\ \mathbf{H}_1(1) & \mathbf{H}_0(2) & \mathbf{H}_1^T(2) & 0 & \dots & 0 \\ \vdots & \vdots & \vdots & \vdots & \vdots & \vdots \\ 0 & 0 & 0 & \mathbf{H}_1(N-2) & \mathbf{H}_0(N-1) & \mathbf{H}_1^T(N-1) \\ 0 & 0 & 0 & 0 & \mathbf{H}_1(N-1) & \mathbf{H}_0(N) \end{bmatrix} \tag{3.12}$$

and $\mathbf{H}_m(k)$ for $m = 0, 1$ is a $K \times K$ matrix whose (i, j)th entry is given by

$$h_{m,ij}(k) = \int_{-\infty}^{\infty} s_i^k(t - \tau_i) s_j^{k-1}(t + mT - \tau_j)\, dt \quad \text{for} \quad m = 0, 1 \tag{3.13}$$

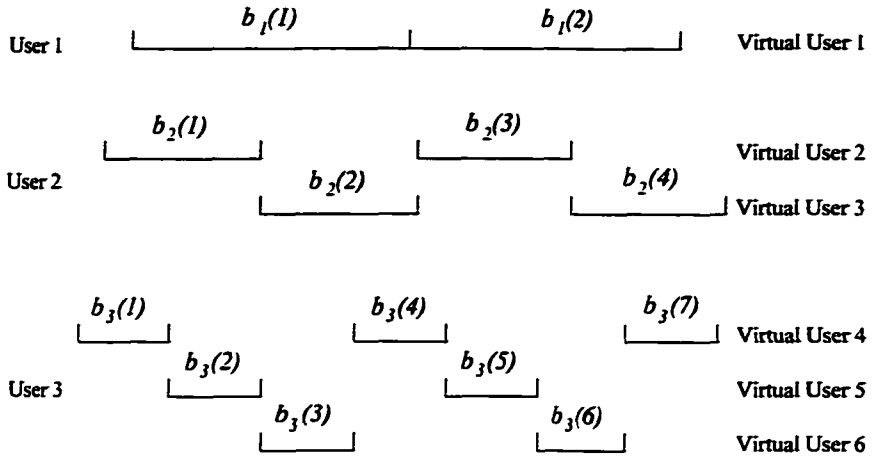

Figure 3.2. *An interpretation of a multirate system.*

where $s_i^k(t)$ denotes the normalized signature signal associated with the kth bit of the ith user. Since the user delays are arranged in ascending order, $\mathbf{H}_1(k)$ is an upper triangular matrix.

Note that the above model also applies to a multirate system where the largest permissible spreading gain is a multiple of all other allowable spreading gains. In this case, a user with a smaller spreading gain can be viewed as a number of virtual users. The virtual users associated with a real user have identical signature signals but occupying different time slots in one symbol interval. This interpretation is illustrated in Fig. 3.2.

Within a window of length $M = 2p + 1$ centered at time index i, (3.9) can be written as

$$\mathbf{r}_i - \mathbf{r}_b - \mathbf{r}_e = \mathbf{R}_M \mathbf{E}_i \mathbf{b}_i + \mathbf{n}_i \tag{3.14}$$

where

$$\begin{aligned}
\mathbf{b}_i &= [\mathbf{b}^T(i-p) \ \cdots \ \mathbf{b}^T(i) \ \cdots \ \mathbf{b}^T(i+p)]^T \\
\mathbf{r}_i &= [\mathbf{r}^T(i-p) \ \cdots \ \mathbf{r}^T(i) \ \cdots \ \mathbf{r}^T(i+p)]^T \\
\mathbf{r}_b &= \{[\mathbf{H}_1(i-p-1)\mathbf{E}(i-p-1)\mathbf{b}(i-p-1)]^T \ 0 \ \cdots \ 0\}^T \\
\mathbf{r}_e &= [0 \ \cdots \ 0 \ \mathbf{b}^T(i+p+1)\mathbf{E}(i+p+1)\mathbf{H}_1(i+p)]^T
\end{aligned}$$

$$\mathbf{E}_i = \text{diag}\{\mathbf{E}(i-p) \cdots \mathbf{E}(i) \cdots \mathbf{E}(i+p)\}$$

In (3.14), $\mathbf{n}_i$ represents Gaussian noise and $\mathbf{R}_M \in \mathcal{R}^{MK \times MK}$ is a submatrix of $\mathbf{R}_N$, which is also given by (3.12) except that index k in $\mathbf{H}_m(k)$ assumes values from $i-p$ to $i+p$ instead of from 1 to N. It follows that within the window, $\mathbf{b}_i$ can be estimated as

$$\tilde{\mathbf{b}}_i = \mathbf{R}_M^{-1}(\mathbf{r}_i - \mathbf{r}_b - \mathbf{r}_e) \tag{3.15}$$

which requires knowledge of $\mathbf{r}_b$ and $\mathbf{r}_e$. The MUI at the beginning of the window, $\mathbf{r}_b$, can be approximated by using the soft outputs $\tilde{\mathbf{b}}(i-p-1)$ whereas the MUI at the end of the window, $\mathbf{r}_e$, is *not* available within the window. The OWD detector is deduced from (3.14) by neglecting term $\mathbf{r}_e$ and estimating the user information bits as

$$\hat{\mathbf{b}}_i = \mathbf{R}_M^{-1}\tilde{\mathbf{r}}_i \tag{3.16}$$

where

$$\tilde{\mathbf{r}}_i = \mathbf{r}_i - \mathbf{r}_b \tag{3.17}$$

In order to avoid an inaccurate estimate caused by neglecting $\mathbf{r}_e$, we take an overlapping-window approach whereby a window is overlapped by the next window in p transmission intervals. Consequently, only the first $p+1$ bits in a working window need to be detected. This scheme is illustrated in Fig. 3.3. As will be shown latter, the IR of the ideal decorrelating detector usually decays very quickly. Hence if the window length M is sufficiently large, the effect from the MUI term $\mathbf{r}_e$ on the detection of the user information bits at the first $p+1$ transmission intervals is negligible. Moreover, if an incorrect estimate of $\mathbf{r}_b$ is used in (3.17), the effect of the resulting left-edge correction on the detection of $\mathbf{b}(i)$ is also negligible. Since only $\tilde{\mathbf{b}}(i)$ is used for the left-edge correction in the next working window, the error caused by an incorrect left-edge correction will not propagate.

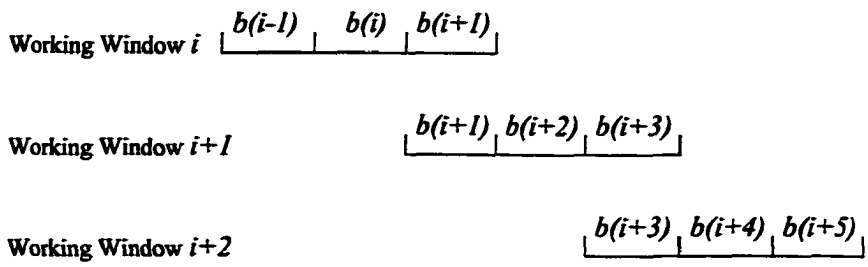

Figure 3.3. *OWD detection scheme with* $p = 1$.

3.3.2 Detector Updating

For efficient implementation of the proposed detector as well as to facilitate later analysis, the following Cholesky decomposition

$$\mathbf{R}_N = \mathbf{L}\mathbf{L}^T \tag{3.18}$$

will be used, where $\mathbf{L}$ is a lower-triangular matrix. From (3.12) and (3.18), it can be verified that $\mathbf{L}$ has the form

$$\mathbf{L} = \begin{bmatrix} \mathbf{C}_1 & & & & \\ \mathbf{D}_1 & \mathbf{C}_2 & & \mathbf{0} & \\ & \mathbf{D}_2 & \mathbf{C}_3 & & \\ & & \ddots & \ddots & \\ \mathbf{0} & & & \mathbf{D}_{N-1} & \mathbf{C}_N \end{bmatrix} \tag{3.19}$$

where $\mathbf{C}_i$ is a $K \times K$ lower-triangular matrix and $\mathbf{D}_i$ is a $K \times K$ upper-triangular matrix. From (3.18) and (3.19), the following recursive relations can be deduced:

$$\mathbf{C}_1\mathbf{C}_1^T = \mathbf{H}_0(1) \tag{3.20a}$$

$$\mathbf{C}_i\mathbf{D}_i^T = \mathbf{H}_1^T(i) \qquad \text{for } 1 \le i \le N-1 \tag{3.20b}$$

$$\mathbf{C}_{i+1}\mathbf{C}_{i+1}^T = \mathbf{H}_0(i+1) - \mathbf{D}_i\mathbf{D}_i^T \quad \text{for } 1 \le i \le N-1 \tag{3.20c}$$

As for $\mathbf{R}_N$, the Cholesky decomposition $\mathbf{R}_M = \mathbf{L}_M\mathbf{L}_M^T$ exists, where $\mathbf{L}_M$ has the same structure as matrix $\mathbf{L}$ in (3.19) except for the size and has $\hat{\mathbf{C}}_j$ and $\hat{\mathbf{D}}_j$

$(1 \leq j \leq M-1)$ as the jth blocks on its main diagonal and the first lower subdiagonal, respectively. Consequently, recursive relations similar to those in (3.20) hold for $\hat{\mathbf{C}}_j$, $\hat{\mathbf{D}}_j$ and the corresponding blocks in $\mathbf{R}_M$. For the working window with the central transmission interval represented by i, these recursive formulas lead to the following efficient updating algorithm:

Algorithm 3.1: Updating the Cholesky factors of $\mathbf{R}_M$

Step 1 Initialize $\hat{\mathbf{K}}_1 = \mathbf{H}_0(i-p)$ and set $j = 1$.

Step 2 Perform the Cholesky decomposition $\hat{\mathbf{K}}_j = \hat{\mathbf{C}}_j \hat{\mathbf{C}}_j^T$.

Step 3 If $j \geq M$, stop; otherwise solve $\hat{\mathbf{C}}_j \hat{\mathbf{D}}_j^T = \mathbf{H}_1^T(i-p-1+j)$ for $\hat{\mathbf{D}}_j$.

Step 4 Set $j := j+1$, compute $\hat{\mathbf{K}}_j = \mathbf{H}_0(i-p-1+j) - \hat{\mathbf{D}}_{j-1}\hat{\mathbf{D}}_{j-1}^T$, and repeat from Step 2.

■

Two remarks on Algorithm 3.1 are in order. (a) By exploiting the tridiagonal structure of $\hat{\mathbf{C}}_i$ and $\hat{\mathbf{D}}_i$, the updating can be accomplished by using $O[5M(K-1)^3/6]$ flops.[1] (b) For systems where the correlations change only occasionally, such as those that employ periodic signature signals over AWGN channels, the Cholesky factors converge very fast. Consequently, updating the Cholesky factors can be accomplished within several successive windows rather than within one window. In each of these working windows, the Cholesky factors are updated up to a certain level, say level i, with the rest of the $\hat{\mathbf{C}}_j$ and $\hat{\mathbf{D}}_j$ for $j > i$ approximated by $\hat{\mathbf{C}}_i$ and $\hat{\mathbf{D}}_i$, respectively. This updating scheme will be referred to as *decentralized updating.*

Once the proposed detector is updated, users are detected using the following algorithm:

Algorithm 3.2: User detection

[1]One floating-point multiplication plus one floating-point addition are counted as one flop.

Solve $\hat{\mathbf{C}}_1\mathbf{y}(1) = \tilde{\mathbf{r}}(1)$ for $\mathbf{y}(i-p)$

for $j = 2$ to $2p+1$

Solve $\hat{\mathbf{C}}_j\mathbf{y}(j) = \tilde{\mathbf{r}}(j+i-p-1) - \hat{\mathbf{D}}_{j-1}\mathbf{y}(j-1)$ for $\mathbf{y}(j)$

end

Solve $\hat{\mathbf{C}}_{2p+1}^T\hat{\mathbf{b}}(i+p) = \mathbf{y}(2p+1)$ for $\hat{\mathbf{b}}(i+p)$

for $j = 2p, 2p-1, \ldots, 1$

Solve $\hat{\mathbf{C}}_j^T\hat{\mathbf{b}}(j+i-1-p) = \mathbf{y}(j) - \hat{\mathbf{D}}_{j+1}^T\mathbf{y}(j+1)$ for $\hat{\mathbf{b}}(j+i-1-p)$

end ■

Algorithm 3.2 can be implemented in terms of the structure illustrated in Fig. 3.4. The algorithm requires $O[(6p+1)K^2]$ flops for detecting $p+1$ bits within one working window. Therefore, about $6K$ flops per user bit are required, which is *linear* with respect to the number of users, given that the Cholesky factors are known.

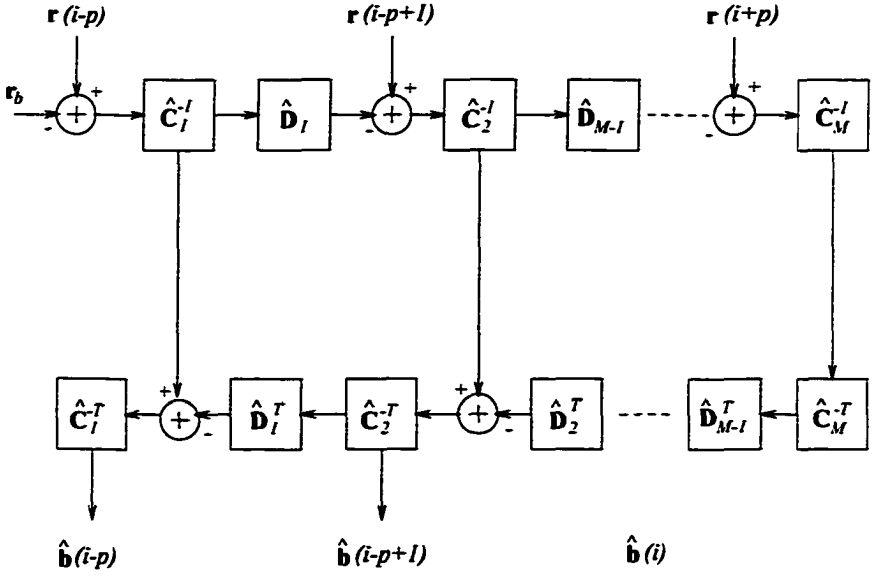

Figure 3.4. *Architechture for the OWD detector.*

3.4 Decay Rate of Impulse Response

We now provide an analysis on the decay rate of the IR of the ideal decorrelating detector. This analysis facilitates the determination of the required window length for the OWD detector.

Consider the ideal decorrelating detector as a multiple-input multiple-output (MIMO) discrete-time system with impulse response $\mathbf{F}(m,n) \in \mathcal{R}^{K\times K}$. The (i,j)th entry of $\mathbf{F}(m,n)$ represents the response of user i at time m due to an impulse applied at time n from user j [41]. Evidently, $\mathbf{F}(m,n)$ is the (m,n)th block of the linear mapping $\mathbf{R}_N^{-1}$. Since $\mathbf{L}$ is lower triangular, $\mathbf{L}^{-1} = \{\mathbf{P}_{ij} \in \mathcal{R}^{K\times K}, 1 \le i,j \le N\}$ is also lower triangular. From (3.12) and the fact that $\mathbf{L}^{-1}\mathbf{L} = \mathbf{I}$, the (i,j)th block $\mathbf{P}_{ij}$ with $i \ge j$ can be recursively found and is given by

$$\mathbf{P}_{ij} = (-1)^{i-j}\mathbf{C}_i^{-1}\prod_{k=1}^{i-j}\mathbf{M}_{i-k} \qquad \text{for } i \ge j \tag{3.21}$$

where $\mathbf{M}_i = \mathbf{D}_i\mathbf{C}_i^{-1}$. Equation (3.21) in conjunction with $\mathbf{R}_N^{-1} = \mathbf{L}^{-T}\mathbf{L}^{-1}$ leads to

$$\mathbf{F}(m,n) = \begin{cases} \sum_{j=m}^{N}\mathbf{P}_{jm}^T\mathbf{P}_{jn} & \text{for } m = n \\ (-1)^{m-n}\mathbf{F}(m,m)\prod_{k=1}^{m-n}\mathbf{M}_{m-k} & \text{for } m > n \\ (-1)^{n-m}\prod_{k=m}^{n-1}\mathbf{M}_k^T\mathbf{F}(n,n) & \text{for } n > m \end{cases} \tag{3.22}$$

Note that $\mathbf{M}_i = \mathbf{H}_1(i)\mathbf{K}_i^{-1}$ and $\mathbf{H}_1(i)$ may vary randomly with i, where $\mathbf{K}_i = \mathbf{C}_i\mathbf{C}_i^T$. Although the exact decay rate of the impulse response of the ideal decorrelating detector for time-dependent systems is rather difficult, it was shown in [38] that the impulse response in a time-dependent system on the average decays faster than in a time-invariant system, given that the two systems have similar cross-correlation properties among the signature signals. Similar observation was also made on the impulse response of the noise whitening filter for a CDMA system [40]. Consequently, one can obtain an approximate upper bound of the decay rate of the impulse response

in a time-dependent system by analyzing a time-invariant system. In what follows, we analyze the decay behavior of a time-invariant system.

For a time-invariant system, it was shown in [9] that as $N \to \infty$ the ideal decorrelating detector tends to assume the form of a K-input K-output linear time-invariant (LTI) infinite-duration impulse response (IIR) filter with transfer function

$$\mathbf{G}(z) = [\mathbf{H}_1^T z + \mathbf{H}_0 + \mathbf{H}_1 z^{-1}]^{-1} \tag{3.23}$$

where $\mathbf{H}_0 \equiv \mathbf{H}_0(k)$ and $\mathbf{H}_1 \equiv \mathbf{H}_1(k)$ for all k. Therefore, as $i \to \infty$, $\mathbf{C}_i$, $\mathbf{D}_i$, and $\mathbf{K}_i = \mathbf{C}_i\mathbf{C}_i^T$ converge to their limits $\mathbf{C}$, $\mathbf{D}$, and $\mathbf{K}$, respectively. A necessary and sufficient condition for the stability of the LTI IIR filter was obtained via the frequency-domain approach in [9]. That is, there is a stable, noncausal realization of the ideal decorrelating detector as $N \to \infty$, if and only if the signals' cross-correlations are such that

$$\det[\mathbf{H}_1^T e^{j\omega} + \mathbf{H}_0 + \mathbf{H}_0 e^{-j\omega}] \neq 0, \ \forall \omega \in [0, 2\pi] \tag{3.24}$$

The above condition is equivalent to require that no matter what the received signal energies are, the received signal does not vanish if at least one information bit has been transmitted. In other words, the signature signals in the equivalent synchronous system of the asynchronous system must be linearly independent to each other (see Sec. 2.5.1). This condition is conceptually easy to understand but difficult to verify in practice. For the purpose of our analysis, we give a necessary and sufficient condition for the stability in terms of the Cholesky factors of $\mathbf{R}_N$ as follows.

Proposition 3.3: The ideal LTI decorrelating filter is stable if and only if the limiting $\mathbf{C}$ is nonsingular and the spectral radius of $\mathbf{M} = \mathbf{D}\mathbf{C}^{-1}$, denoted by $\rho(\mathbf{M})$, is strictly less than 1.

Proof Assuming that $\mathbf{C}$ is nonsingular, then $\mathbf{C}^{-1}$ exists and the impulse response of the LTI decorrelating filter can be written as

$$\mathcal{A}_k = (\mathcal{A}_{-k})^T = \lim_{\substack{n\to\infty \\ N\to\infty}} \mathbf{F}(n+k, n)$$

$$= (-1)^k \mathcal{A}_0 \mathbf{M}^k \qquad \text{for } k \geq 0 \tag{3.25}$$

where

$$\mathcal{A}_0 = \sum_{i=0}^{\infty} [(\mathbf{C}^{-1}\mathbf{M}^i)^T (\mathbf{C}^{-1}\mathbf{M}^i)] \tag{3.26}$$

Since $\|\mathbf{C}^{-1}\|$ is bounded, there exist positive constants c_1 and c_2 such that

$$c_1 \max_{1 \leq i,j \leq K} (\mathbf{M}^k)_{ij} \leq \max_{1 \leq i,j \leq K} (\mathbf{C}^{-1}\mathbf{M}^k)_{ij} \leq c_2 \max_{1 \leq i,j \leq K} (\mathbf{M}^k)_{ij} \tag{3.27}$$

where $(\cdot)_{ij}$ stands for the (i,j)th entry of the matrix inside the bracket. For a given $\epsilon > 0$, there is a constant c such that

$$|(\mathbf{M}^k)_{ij}| \leq c(\rho(\mathbf{M}) + \epsilon)^k \tag{3.28}$$

for all $k > 0$ and $i, j = 1, 2, ..., K$ [35]. From (3.27) and (3.28), it can be shown that $\mathcal{A}_0$ is finite if and only if $\rho(\mathbf{M}) < 1$. Assuming that $\rho(\mathbf{M}) < 1$, by (3.28) we have

$$c_3 \rho^k(\mathbf{M}) \leq |\max_{1 \leq i,j \leq K} (\mathcal{A}_k)_{ij}| \leq c_4(\rho(\mathbf{M}) + \epsilon)^k \tag{3.29}$$

for any $k > 0$, where c_3 and c_4 are positive constants. Since $\rho(\mathbf{M}) < 1$, (3.29) implies that the impulse response $(\mathcal{A}_k)_{ij}$ of the (i,j)th subsystem is absolutely summable. The sufficiency now follows from the fact that a MIMO system is stable if and only if every subsystem is stable. To prove the necessity, we assume that the LTI filter is stable. Then matrix $\mathbf{C}$ must be nonsingular and (3.27) holds. Since $\mathcal{A}_0$ is finite for a stable filter, $\rho(\mathbf{M})$ must be less than 1. ■

As an immediate consequence of (3.29), we can state the following proposition:

Proposition 3.4: If the LTI decorrelating filter is stable, its impulse response decays with an asymptotic decay rate $\rho(\mathbf{M})$. ■

It follows that if $\rho(\mathbf{M}) < 1$ is small, then the impulse response of the LTI decorrelating filter decays rapidly. Indeed, as will be demonstrated by our numerical examples in Sec 3.8, $\rho(\mathbf{M})$ is usually much smaller than 1 for systems with moderate

cross-correlation properties among the signature signals. It is also interesting to note that the convergence rate of $\mathbf{K}_i$ to $\mathbf{K}$ is linear with respect to $\rho^2(\mathbf{M})$ as shown in Appendix C. By (3.20), fast convergence of $\mathbf{K}_i$ implies fast convergence of $\mathbf{M}_i$. Therefore, the decay rate of the impulse response of the OWD detector is approximately equal to $\rho(\mathbf{M})$ for a sufficiently large window length M.

3.5 Window-Length Determination

We now turn our attention to the determination of the window length. Denoting the first k elements of vector $\mathbf{y}$ as $[\mathbf{y}]_{1:k}$, then $[\tilde{\mathbf{b}}_i]_{1:kK}$ contains the estimates of the user information bits within the first k transmission intervals in $\tilde{\mathbf{b}}_i$. The difference between $[\hat{\mathbf{b}}_i]_{1:(p+1)K}$ in (3.16) and $[\tilde{\mathbf{b}}_i]_{1:(p+1)K}$ in (3.15) can be written as

$$[\mathbf{R}_M^{-1}\mathbf{r}_e]_{1:(p+1)K} = \{[\hat{\mathbf{F}}(1,M)\mathbf{x}]^T \ [\hat{\mathbf{F}}(2,M)\mathbf{x})]^T \ \cdots \ [\hat{\mathbf{F}}(p+1,M)\mathbf{x}]^T\}^T \quad (3.30)$$

where $\mathbf{x} = \mathbf{H}_1(i+p+1)^T\mathbf{E}(i+p+1)\mathbf{b}(i+p+1)$ and $\hat{\mathbf{F}}(n,M) \in \mathcal{R}^{K\times K}$ is the (n,M)th block of $\mathbf{R}_M^{-1}$, and can be interpreted as the impulse response of the OWD detector. Replacing N in (3.22) with M, we have

$$\hat{\mathbf{F}}(n,M) = (-1)^{M-n}(\prod_{k=n}^{M-1}\hat{\mathbf{M}}_k^T)\hat{\mathbf{K}}_M^{-1} \quad (3.31)$$

where $\hat{\mathbf{M}}_k = \hat{\mathbf{D}}_k\hat{\mathbf{C}}_k^{-1}$ and $\hat{\mathbf{K}}_k = \hat{\mathbf{C}}_k\hat{\mathbf{C}}_k^T$. Denoting $\hat{\mathbf{F}}(n,M)\mathbf{H}_1^T(i+p+1)$ as $\tilde{\mathbf{F}}_n$, then (3.31) in conjunction with $\hat{\mathbf{M}}_M = \mathbf{H}_1(i+p+1)\hat{\mathbf{K}}_M^{-1}$ leads to

$$\tilde{\mathbf{F}}_n = (-1)^{M-n}(\prod_{k=n}^{M}\hat{\mathbf{M}}_k^T) \quad (3.32)$$

The right-edge effect $\mathbf{r}_e$ can be neglected if $\|\tilde{\mathbf{F}}_n\|_\infty$ for $n \le p+1$ is sufficiently small, where $\|\cdot\|_\infty$ denotes the infinity norm [35]. Since the IR of the detector decays, $\|\tilde{\mathbf{F}}_{p+1}\|_\infty$ is in general larger than $\|\tilde{\mathbf{F}}_n\|_\infty$ for $p+1 > n$; hence the window length can be determined as the smallest M such that

$$\|\tilde{\mathbf{F}}_{p+1}\|_\infty < \epsilon \quad (3.33)$$

where $\epsilon > 0$ is a prescribed tolerance. In the next section, it will be shown that in a practical system ϵ can be selected such that $\epsilon\sqrt{\kappa} \ll 1$, where κ is the received power imbalance at the receiver.

For systems with constant correlations within the working window and for sufficiently large p, the fast convergence of $\hat{\mathbf{M}}_k$ implies that $\hat{\mathbf{M}}_k \approx \hat{\mathbf{M}}_{p+1}$ if $k > p+1$. Hence, (3.32) leads to

$$\|\tilde{\mathbf{F}}_{p+1}\|_\infty < c[\rho(\hat{\mathbf{M}}_{p+1})]^{p+1} \tag{3.34}$$

In a practical implementation, constant c in (3.34) can be simply taken as $\|\hat{\mathbf{M}}_{p+1}\|_\infty / \rho(\hat{\mathbf{M}}_{p+1})$, and $\rho(\hat{\mathbf{M}}_{p+1})$ can be estimated using various numerical methods such as the power method [35]. For slowly varying systems where correlations remain approximately unchanged within a working window, the criterion in (3.33) in conjunction with (3.34) can be used to determine the window length when the OWD detector needs to be updated.

3.6 OWD Detection For Frequency-Selective Fading Channels

An important feature of DS-CDMA is its inherent capability in combating multipath fading. For mobile radio and indoor wireless channels, for example, the signal bandwidth is larger than the coherent bandwidth of the channels, and the RAKE receiver can be employed to achieve frequency diversity. However, like the conventional matched-filter receiver for AWGN channels, the RAKE receiver suffers from NF effects in the presence of MUI. This problem has motivated researchers to develop multiuser receivers that can eliminate the MUI and achieve diversity gain simultaneously. Two methods for extending the capability of the ideal decorrelating detector were proposed in [25] and [26], respectively. In this section, we will show that these two methods can also be used in the OWD detector. We will also compare the re-

sulting combined receivers in terms of performance and issues relating to practical implementation.

Consider a system similar to that discussed in Sec. 3.3 for the case of a frequency-selective multipath fading channel. As in Sec. 2.3, we assume that the channel fading is sufficiently slow such that the channel coefficients are constant during one transmission interval. Then a channel coefficient vector for the kth user at the ith transmission interval can be defined as $\mathbf{c}_k(i) = [c_{k,1}(i)\ c_{k,2}(i)\ \cdots\ c_{k,L}(i)]^T$. In order to achieve multipath diversity, the received signal is first passed through a bank of KL filters matched to the delayed, normalized, user signature signals, and the outputs are then sampled at the symbol interval T. As in (3.9), the concatenation of N successive sampled vectors can be written as

$$\hat{\mathbf{r}} = \tilde{\mathbf{R}}_N \mathbf{W}\mathbf{E}\mathbf{b} + \mathbf{n} \tag{3.35}$$

where $\tilde{\mathbf{R}}_N$ is of size $NKL \times NKL$ and has the same structure as that of $\mathbf{R}_N$ in (1) except that in the present case there are KL virtual users and

$$\mathbf{W} = \text{diag}\{\mathbf{W}(0)\ \ \mathbf{W}(1)\ \ \cdots\ \ \mathbf{W}(N)\} \tag{3.36}$$

$$\mathbf{W}(i) = \text{diag}\{\mathbf{c}_1(i)\ \ \mathbf{c}_1(i)\ \ \cdots\ \ \mathbf{c}_K(i)\} \tag{3.37}$$

There are two methods to design multiuser receivers for multipath fading channels as illustrated in Figs. 3.5 and 3.6, respectively. In the first method, the outputs of the corresponding L matched filters for each user are first combined, and then a decorrelation operation is applied to the combined signals [25]. In the second method, a decorrelation operation is first applied to the output signals of the KL matched filters as if there were KL users, and then the L demodulated signals for each user are combined to form the estimated user information bits [26]. We refer the first method to as the RAKE decorrelating detector (RDD) and the second one as the multipath decorrelating detector (MDD).

In the RDD, the output of the maximum-ratio combiner is $\mathbf{r} = \mathbf{W}^H\hat{\mathbf{r}}$, where $\mathbf{W}^H$ denotes the Hermitian transpose of $\mathbf{W}$. Following the maximal-ratio combiner, the

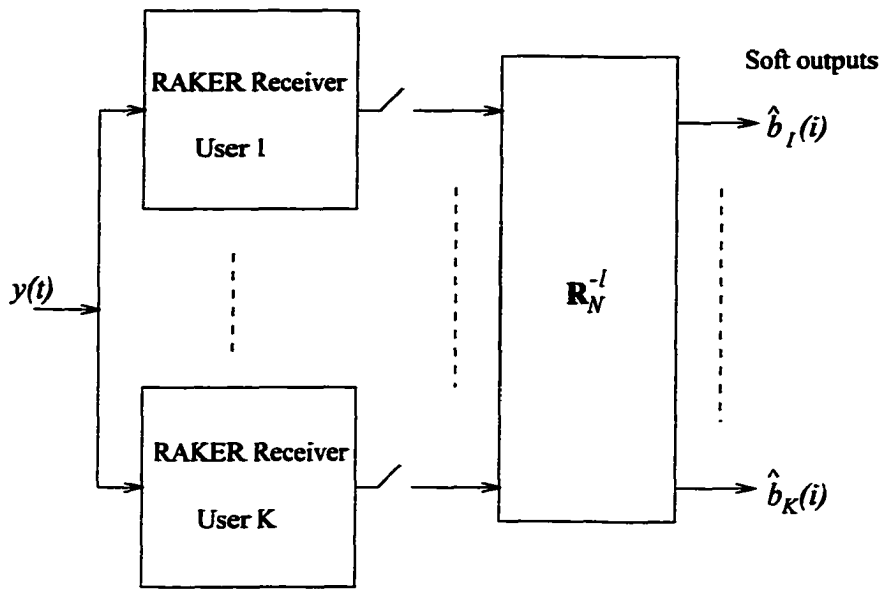

Figure 3.5. *A block diagram of RDD*

decorrelating detector with linear mapping $\mathbf{R}_N^{-1} = (\mathbf{W}^H \tilde{\mathbf{R}}_N \mathbf{W})^{-1}$ is employed. It is clear that $\mathbf{R}_N$ is still defined by (3.12) with the (i,j)th entry of the correlation $\mathbf{H}_m(k)$ in $\mathbf{R}_N$ given by

$$h_{m,ij}(k) = \int_{-\infty}^{\infty} \hat{s}_i^k(t-\tau_i)\hat{s}_j^{k-1}(t+mT-\tau_j)\,dt \quad \text{for } m=0,1 \tag{3.38}$$

where

$$\hat{s}_i^k = \sum_{n=0}^{L-1} c_{i,n}(k) s_i^k(t-n/W) \tag{3.39}$$

is the composite signature signal of the kth bit of user i. The soft output of the RDD is given by

$$\hat{\mathbf{b}}^{\text{RDD}} = \mathbf{R}_N^{-1}\mathbf{r} + \hat{\mathbf{n}} = \mathbf{E}\mathbf{b} + \hat{\mathbf{n}} \tag{3.40}$$

where the noise term $\hat{\mathbf{n}}$ has the covariance matrix $N_0\mathbf{R}_N^{-1}/2$. Note that $\mathbf{R}_N$ in (3.40) is a block tridiagonal matrix. Therefore, the methods described in Sec. 3.3 can also be used for the RDD to perform detection and updating.

In the MDD, the linear mapping for the ideal decorrelating detector is $\tilde{\mathbf{R}}_N^{-1}$. For the ith information bit of a user, a noise whitening function, $[\mathbf{T}_k(i)^H]^{-1}$, is applied

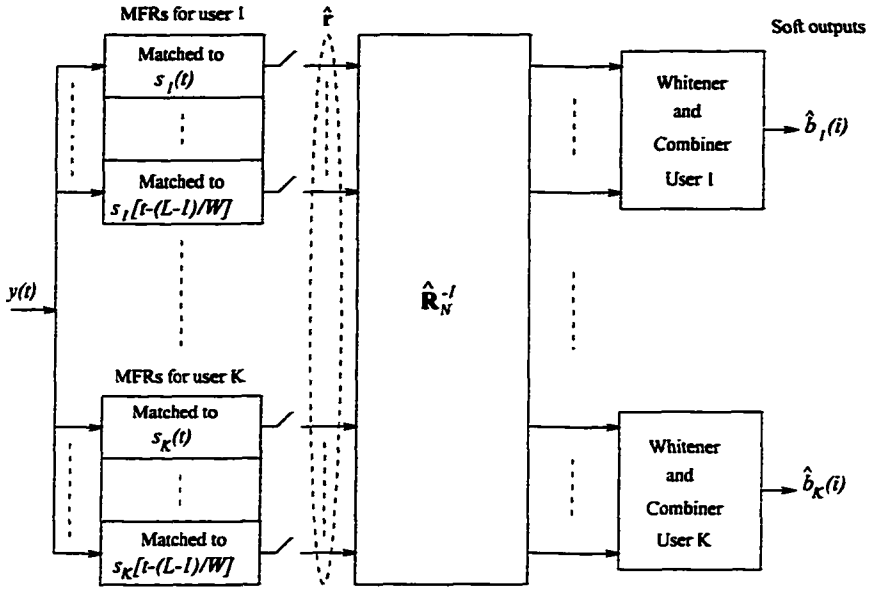

Figure 3.6. *A block diagram of MDD*

to the corresponding L soft outputs of the decorrelating detector. The function is obtained by performing the Cholesky decomposition $\mathbf{A}(l,l) = \mathbf{T}_k(i)^H \mathbf{T}_k(i)$, where $l = (i-1)K + k$ and $\mathbf{A}(l,l) \in \mathcal{R}^{L \times L}$ is the (l,l)th block of $\tilde{\mathbf{R}}_N^{-1}$. The L outputs are then fed to the maximal-ratio combiner and the resulting decision statistic for the ith bit of the kth user is given by

$$\hat{b}_k^{\mathrm{MDD}}(i) = \mathbf{c}_k(i)^H \mathbf{A}(l,l)^{-1} \mathbf{c}_k(i) \sqrt{e_k(i)} b_k(i) + \tilde{n} \tag{3.41}$$

where $\tilde{n}$ has a variance $N_0/2\mathbf{c}_k(i)^H \mathbf{A}(l,l)^{-1} \mathbf{c}_k(i)$.

For synchronous systems, it was shown that the RDD consistently achieves better performance than the MDD [27]. As proved in Appendix D, this is also true for asynchronous systems. As a matter of fact, the performance degradation of the MDD with respect to the RDD increases with the number of users and resolvable paths. This degradation becomes more significant in asynchronous systems. However, $\mathbf{R}_N$ in the RDD depends on the channel coefficient vectors $\mathbf{c}_k(i)$ which are difficult to estimate in the presence of MUI, particularly for fast fading channels. On the other hand, the channel coefficients in the MDD are needed only after decorrelating and,

hence, can be estimated in the absence of MUI. Therefore, the RDD is desirable for slowly fading channels and the MDD is suitable for fast fading channels. The OWD detector can be easily used to replace the ideal decorrelating detector in either the RDD or the MDD. If the RDD is adopted, the correlations in $\mathbf{R}_N$ change frequently and the system seen by the OWD detector is fast time varying; on the other hand, if the MDD is adopted, the correlations in $\tilde{\mathbf{R}}_N$ change only occasionally and $\tilde{\mathbf{R}}_N^{-1}$ can be updated using the decentralized implementation of Algorithm 3.1.

3.7 Performance Analysis

Since the OWD detector uses the reconstructed information bits to correct the left-edge effect (i.e., the MUI at the beginning of the window), an exact bit-error rate (BER) formula is difficult to obtain. In order to analyze the performance degradation due to neglecting the right-edge effect, we assume a perfect left-edge correction. This assumption leads to an accurate estimation for the exact BER of the OWD detector since the error due to an incorrect left-edge correction does not accumulate, as discussed in Sec. 3.3. Since the most inaccurate estimate of user bits usually occurs in the central transmission interval of a working window, we only discuss the BER of the user bits in this interval as a worst case study. Let $P_k(i)$ be the BER of the ith bit of the kth user and assume that i is the index for the central transmission interval of a working window. If the probabilities of transmitting a $+1$ or a -1 are equal, then (3.16) implies that

$$P_k(i) = P\{[\mathbf{R}_M^{-1}\tilde{\mathbf{r}}_i]_{pK+k} < 0 \mid b_k(i) = 1\} \tag{3.42}$$

where $[\mathbf{y}]_k$ represents the kth entry of vector $\mathbf{y}$. From (3.15) and (3.17), we have

$$P_k(i) = \mathbf{Q}\left\{\frac{\sqrt{e_k(i)} + \nu[\mathbf{b}(i+p+1)]}{\sqrt{d_{pK+k}N_0/2}}\right\} \tag{3.43}$$

where

$$Q(x) = \int_x^\infty (1/\sqrt{2\pi}) e^{-v^2/2}\, dv$$

d_{pK+k} is the $(pK+k, pK+k)$th entry of $\mathbf{R}_M^{-1}$, and $\nu[\mathbf{b}(i+p+1)] = [\mathbf{R}_M^{-1}\mathbf{r}_e]_{pK+k}$ describes the right-edge effect to the detection of $b_k(i)$.

In order to determine the window length, or equivalently the tolerance ϵ described in Sec. 3.5, we need two more performance measures, namely, the *asymptotic multiuser efficiency* (AME) and the *NF resistance*. The AME characterizes the performance degradation due to the MUI in a vanishing noise case [9]. For the OWD detector, the AME of the ith bit of the kth user can be deduced as

$$\eta_k(i) = \max^2 \left\{ 0,\ \frac{1}{\sqrt{e_k(i)}} \min_{\substack{\mathbf{b}(i+p+1)\in\{-1,1\}^K \\ b_k(i)=1}} \frac{\sqrt{e_k(i)} + \nu[\mathbf{b}(i+p+1)]}{\sqrt{d_{pK+k}}} \right\} \tag{3.44}$$

The NF resistance of the ith bit of kth user is defined as its worst case AME over all possible energies of the other information bits. According to this definition, the OWD is not NF resistant. However, given that the received power is finite in practice, the concept of the *power-limited NF resistance* introduced in [38] applies, and the power-limited NF resistance of the ith bit of the kth user is given by

$$\bar{\eta}_k(i) = \inf_{\substack{0\le e_l(j)\le e_{\max}(j) \\ (l,j)\neq(k,i)}} \eta_k(i) \tag{3.45}$$

where $e_{\max}(j) = \max_{1\le l\le K} e_l(j)$. It follows that

$$\bar{\eta}_k(i) = \max^2 \left\{ 0,\ \frac{1 - \mu\sqrt{e_{\max}(i+p+1)/e_k(i)}}{\sqrt{d_{pK+k}}} \right\} \tag{3.46}$$

where μ is the l_1 norm [35] of the kth row of $\mathbf{F}(p+1, M)\mathbf{H}_1(i+p+1)^T$. In mobile CDMA communications, the received power imbalance serves as a performance measure of power control and is defined as

$$\kappa = \max_{1\le j\le N} \frac{e_{\max}(j)}{e_{\min}(j)} \tag{3.47}$$

where $e_{\min}(j) = \min_{1 \le l \le K} e_l(j)$. If $\|\mathbf{F}(p+1, M)\mathbf{H}_1(i+p+1)^T\|_\infty < \epsilon$, a lower bound for $\bar{\eta} = \min_{k,i} \bar{\eta}_k(i)$ can be deduced as

$$\bar{\eta} \ge \max^2 \left\{ 0, \frac{1 - \epsilon\sqrt{\kappa}}{\sqrt{d_{pK+k}}} \right\} \tag{3.48}$$

This can serve as a guide for the selection of tolerance ϵ for the determination of the window length.

We conclude this section with an observation concerning the performance of the OWD detector relative to that of the ideal decorrelating detector. It can be seen from (3.44) and (3.48) that if ϵ is selected such that $\epsilon\sqrt{\kappa} \ll 1$, the AME and the power-limited NF resistance of the proposed detector is approximately equal to $1/d_{pK+k}$. In [9], the AME of the ideal decorrelating detector was derived as $1/d^{\text{ideal}}_{(i-1)K+k}$, where $1/d^{\text{ideal}}_k$ denotes the (k,k)th entry of $\mathbf{R}_N^{-1}$. Since $\mathbf{R}_M$ is a principal submatrix of $\mathbf{R}_N$, we have $1/d_{pK+k} \ge 1/d^{\text{ideal}}_{(i-1)K+k}$ [35]. This shows that in some cases the performance of the OWD detector can even be better than that of the ideal detector. This feature is a consequence of the fact that the OWD detector neglects the MUI from outside the working window and hence causes a smaller noise enhancement.

3.8 Numerical Examples

The performance of the proposed detector was examined for the cases of two and multiple users.

3.8.1 Two-User System

We first consider a two-user time-invariant system. The simplicity of the system allows us to carry out an analysis on issues such as the convergence of $\mathbf{K}_i$ and the system performance in an explicit manner. Assuming that $(\mathbf{H}_0)_{12} = r_1$ and $(\mathbf{H}_1)_{12} = r_2$, then $|r_1| + |r_2| \le 1$. Since $\mathbf{M}_i = \mathbf{D}_i\mathbf{C}_i^{-1}$, by (3.20) the spectral radius of $\mathbf{M}_i$, denoted

as ρ_i, can be computed by using the recursive formula

$$\rho_i = \left| \frac{r_1 r_2}{x_i(1 - r_1^2/x_i)} \right| \tag{3.49}$$

where $x_{i+1} = 1 - r_2^2/(x_i - r_1^2)$ and $x_1 = 1$. This leads to

$$x = \lim_{i \to \infty} x_i = \frac{1 + r_1^2 - r_2^2 + \sqrt{(1 + r_1^2 - r_2^2)^2 - 4r_1^2}}{2} \tag{3.50}$$

Letting $i \to \infty$ in (3.49) and substituting (3.50) into (3.49) give

$$\rho = 2|r_1 r_2|/(\tau + \sqrt{\tau^2 - 2r_1^2 r_2^2}) \tag{3.51}$$

where $\tau = 1 - r_1^2 - r_2^2$. Note that $\rho = 1$ if $|r_1| + |r_2| = 1$, which corresponds to an unstable realization of the ideal decorrelating detector. The plot shown in Fig. 3.7 depicts ρ versus r_1 and r_2. It can be seen that ρ is usually quite small. Specifically, we have $\rho < 0.4$ if $|r_1| + |r_2| < 0.9$ whereas $\rho < 0.25$ if $|r_1| + |r_2| < 0.8$. The convergence rate of ρ_i, given by the smallest value of i such that $|\rho_i - \rho|/\rho < 0.01$, and the smallest window length given by (3.33) with $\epsilon = 0.01$ are given in Table 3.1. We see that even in the cases where the cross-correlation properties are much poorer than what is often encountered in practice, the convergence rate of ρ_i remains high and the window length required is moderate.

3.8.2 Multiple-User Systems

We now consider systems with multiple users. To demonstrate the performance of systems equipped with the proposed detector, extensive computer simulations were conducted. In all the simulations, signature codes were selected from a family of the 127-chip Gold code and a rectangular chip waveform was used.

To study the NF resistance of the OWD detector, both time-invariant and time-dependent systems were simulated, and the energy received from the desired user was assumed to be $e_{\min}$. The power-limited NF resistance achieved for time-invariant systems versus the number of users and the received power embalance are illustrated

Table 3.1. *Convergence Rate of ρ_i/Smallest Window Length Given by (3.33) with $\epsilon = 0.01$ in a Two-User System.*

$r_1 \backslash r_2$	0.1	0.2	0.3	0.4	0.5	0.6	0.7	0.8
0.1	2/5	2/5	2/5	2/5	2/5	2/5	3/5	3/7
0.2	2/5	2/5	2/5	2/7	2/7	3/7	3/11	
0.3	2/5	2/5	2/7	2/7	3/7	3/11		
0.4	2/5	2/7	2/7	3/9	3/11			
0.5	2/5	2/7	2/9	3/11				
0.6	2/5	2/7	3/11					
0.7	2/7	3/11						
0.8	2/9							

in Figs. 3.8 and Figs. 3.9, respectively. As expected, it can be seen that the loss in the NF resistance increases with the number of users and the received power imbalance. This phenomenon is particularly prominent for a window length of 3. However, as the window-length increases, the resultant NF-resistance curves quickly become more able to follow that of the ideal decorrelating detector. For a system with 20 users and a 20 dB power imbalance, the loss in the NF resistance is 0.12 for a window length of 3 and 0.01 for a window length of 5. For a system with 40 users and a 10 dB power imbalance, the loss in NF resistance is 0.2 for a window length of 3 and about 0.01 for a window length of 5. Hence, a window length of 5 is sufficient to yield an NF resistance close to that of the ideal decorrelating detector for a time-invariant system with a large number of users and moderate power imbalance. The power-limited NF resistance versus received power imbalance in a time-dependent system is demonstrated in Fig. 3.10. The time-dependent system was simulated by randomly selecting signature signals form the Gold code set for each information bit. Comparing the results in Figs. 3.9 and 3.10, we can see that for a fixed window length, the loss in the NF resistance in time-dependent systems is similar to or is slightly smaller

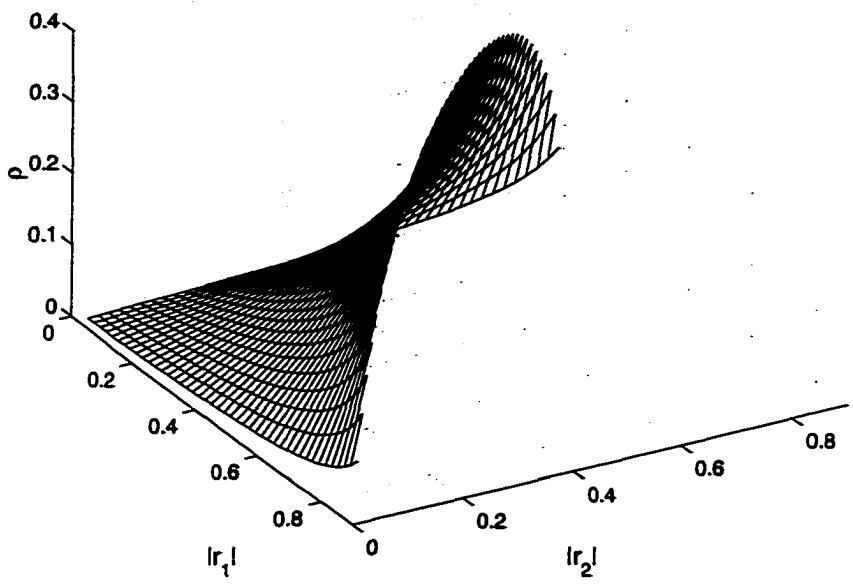

Figure 3.7. *Spectral radius of* $\mathbf{M}$ *in a two-user system.*

than that in time-invariant systems. This confirms that the impulse response of the detector decays slightly faster in time-dependent systems.

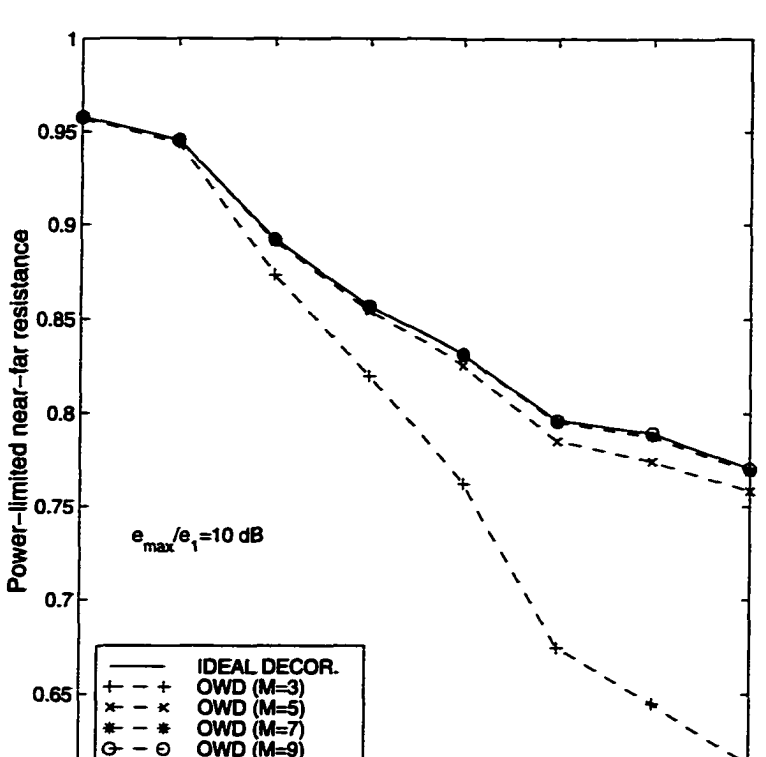

Figure 3.8. *Power-limited NF resistance as a function of the number of active users for user 1 in a time-invariant system.*

The average BER of all users as a function of signal-to-noise ratio (SNR) of the OWD detector for a time-invariant system with 20 users is plotted in Figs. 3.11 and 3.12. In Fig. 3.11, all users were assumed to have equal power. In Fig. 3.12, the user received energies per bit were uniformly distributed on interval $[e_{\min}, e_{\max}]$ and the power imbalance $e_{\max}/e_{\min}$ was assumed to be 10 dB. The performance of the detector under two conditions, i.e., using correct bits as feedback and using detected bits as feedback, is also compared in the figures. As is expected, no apparent differences in the performance under these two conditions are observed. This confirms our statements made in Sec. 3.3 and shows that the assumption made in Sec. 3.7 is reasonable. From the figures, we can also see that the performance of the OWD detector is close to

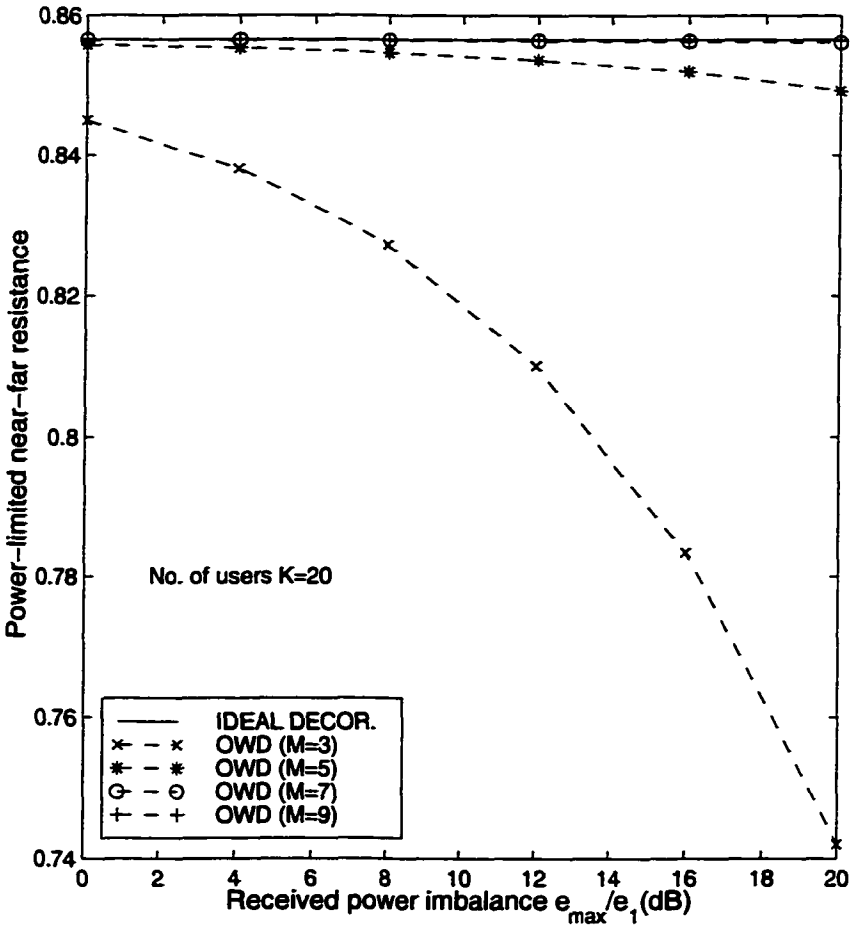

Figure 3.9. *Power-limited NF resistance as a function of the received power imbalancefor user 1 in a time-invariant system.*

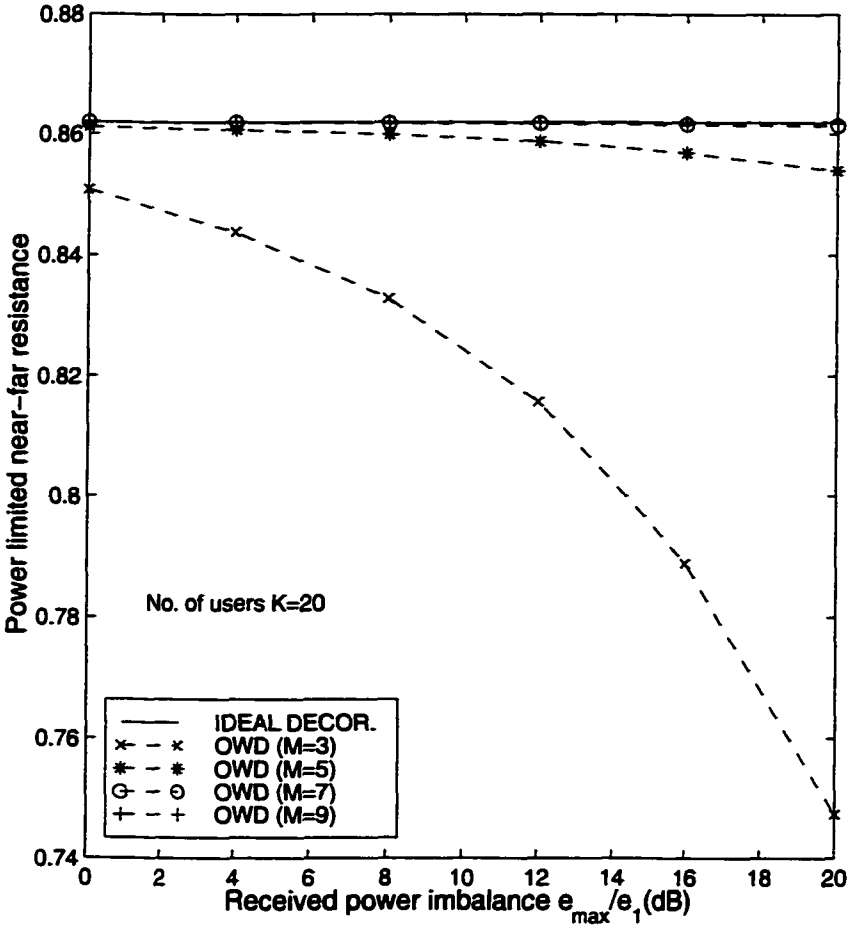

Figure 3.10. *Power-limited NF resistance for user 1 in a time-dependent system.*

that of the ideal decorrelating detector and sometimes it can even be slightly better. This is due to the fact that the OWD detector causes less noise enhancement.

The BER curves for a time-dependent system are illustrated in Figs. 3.13 and 3.14. A Raleigh fading channel with 6 resolvable paths was assumed and was simulated by using a method introduced in [42]. The path coefficients were assumed to be known and the RDD combination was adopted. The performance of the RDD using the ideal decorrelating detector is difficult to obtain in simulations. Instead, we used the average BER of the isolated RAKE receiver as a benchmark, where the term 'isolated' is taken to mean the absence of interfering users. Again, the BER curves obtained by using correct bits as feedback and using detected bits as feedback are almost indistinguishable. It can also be observed that in contrast to the NF resistance, the BER appears to be more insensitive to the window length used. The BER curve obtained with a window length of 3 is very close to that obtained with a window length of 7. This is because that the NF resistance is a worst-case performance measure; it does not necessarily relate to BER in a practical situation. For this time-dependent system, the OWD detector is sufficient to yield satisfactory BER with a window length of 3.

3.9 Conclusions

A comparison on the exact FIR decorrelator and the ideal decorrelating detector has been given. It has been shown that the ideal decorrelating detector consistently outperforms the exact FIR decorrelator. It has been also found that similar problems, such as computing and updating a large size matrix and window-length determination, exist in the two detectors.

The convergence of the ideal decorrelating detector to its limiting IIR filter and the decay of its impulse response have been studied. The results obtained show that the convergence rate of the ideal decorrelating detector to its limiting IIR filter as well as the decay rate of the decorrelating IR are related to the spectral radius of the Cholesky factors of the system's cross-correlation matrix. Based on these properties, an efficient window-based decorrelating detector and an algorithm for its updating have been proposed. The proposed OWD detector achieves a performance close to and sometimes even slightly better than that of the ideal decorrelating detector. The application of the proposed detector in multipath fading channels has also been investigated and the results obtained show that the proposed detector can be easily adopted in conjunction with conventional frequency-diversity techniques.

A signal-adapted criterion for the determination of the window length has been developed. This criterion enables the OWD detector to select the smallest window length, and hence the smallest processing delay, to achieve a prescribed NF resistance under a given NF situation. Theoretical analysis as well as simulation results have demonstrated that small to moderate window lengths are sufficient for various practical environments.

Because of the similarity of the decorrelating mapping and the MMSE mapping, the proposed detection scheme and the results obtained on the behavior of the ideal decorrelating detector can be easily extended to the case of the MMSE detector.

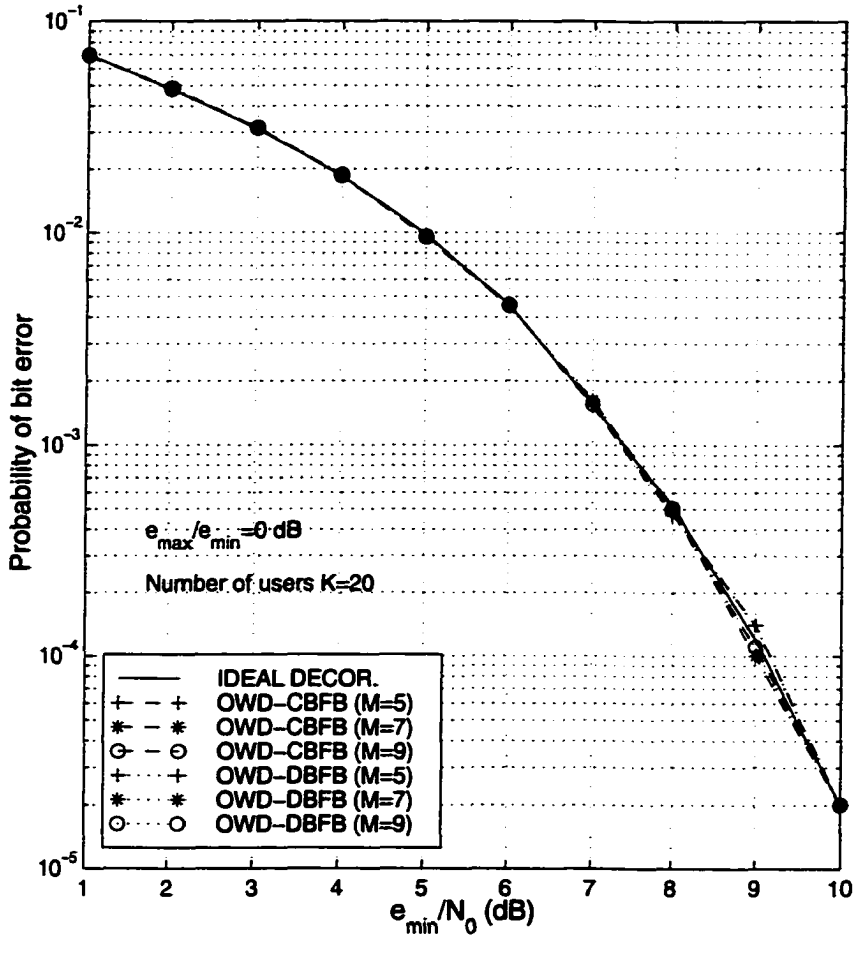

Figure 3.11. *Comparison of bit-error rate under the conditions of using correct bits as feedback (CBFB) and using detected bits as feedback (DBFB) over an AWGN channel with equal power users.*

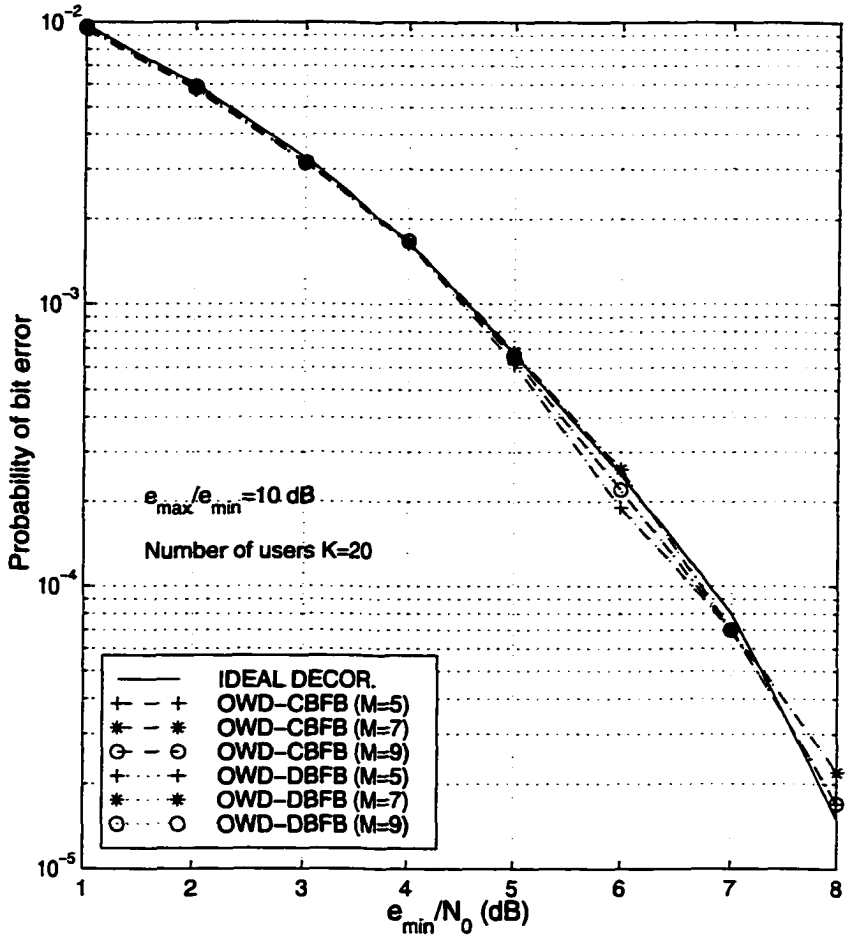

Figure 3.12. *Comparison of bit-error rate under the conditions of using correct bits as feedback (CBFB) and using detected bits as feedback (DBFB) over an AWGN channel with* 10 *dB received power imbalance.*

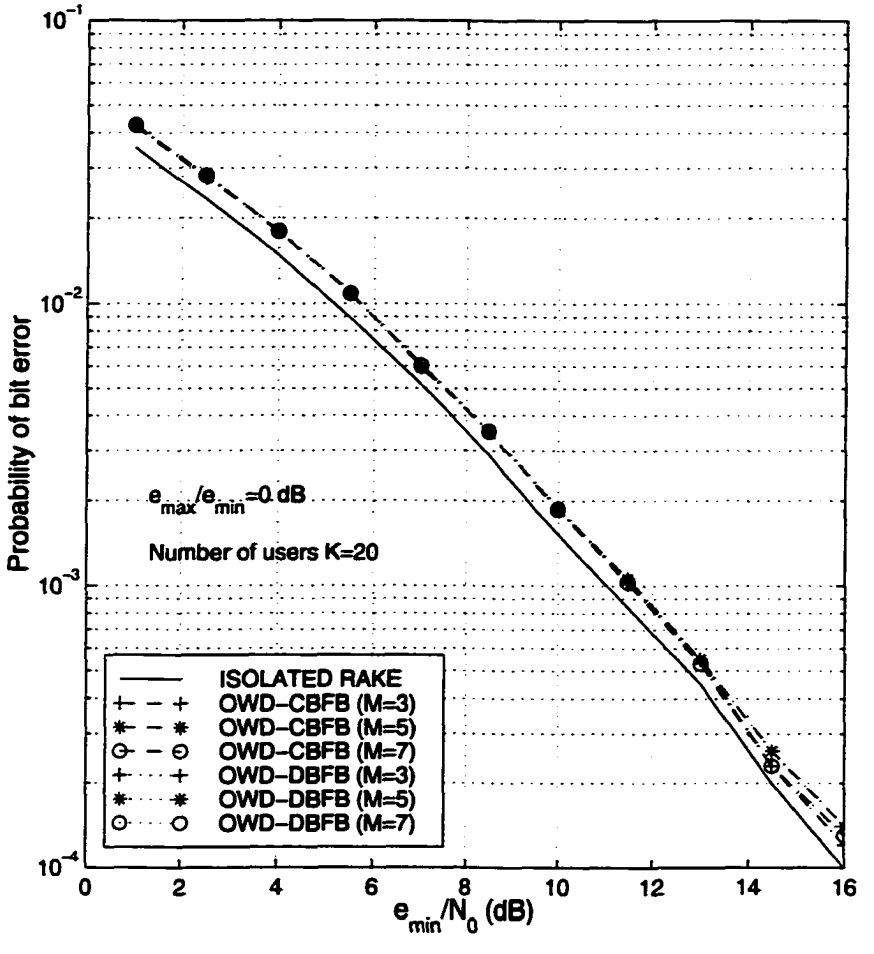

Figure 3.13. *Comparison of bit-error rate under the conditions of using correct bits as feedback (CBFB) and detected bits as feedback (DBFB) over a multipath Rayleigh fading channel with 6 resolvable paths with equal power users.*

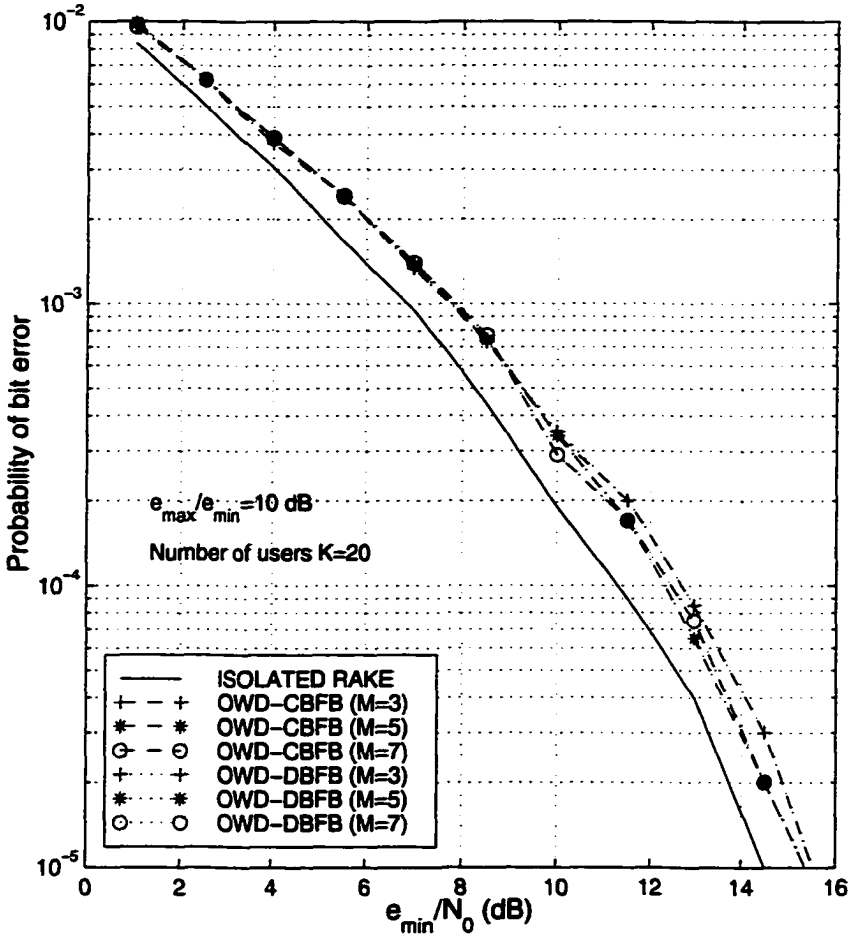

Figure 3.14. *Comparison of bit-error rate under the conditions of using correct bits as feedback (CBFB) and detected bits as feedback (DBFB) over a multipath Rayleigh fading channel with 6 resolvable paths with* 10 *dB received power imbalance.*

Chapter 4

Constrained Minimum-BER Multiuser Detection

4.1 Introduction

In the previous chapters, we have described linear multiuser detectors. As indicated by their names, the decorrelating detector and the minimum-mean squared error (MMSE) detector minimize the multiuser interference (MUI) and the mean-squared error (MSE), respectively. These detectors achieve optimal near-far resistance and hence both are worst-case optimal linear multiuser detectors [8]. However, there are situations in practice where the performance of the decorrelating and MMSE detectors is far from optimum. For example, when the properties of cross-correlations among signature signals are poor, the energy of the interferers is small relative to that of the desired signal and/or the number of simultaneous users is small in a micro-cell. In general, the decorrelating and MMSE detectors do not provide the lowest bit-error rate (BER) even among linear detectors. In fact, occasionally the conventional matched-filter receiver (MFR) outperforms the decorrelating and MMSE detectors. Since the ultimate performance index of a communication system is the BER, it is of interest to develop a new linear multiuser detector that minimizes the BER.

In [44], an *approximate* minimum BER criterion was proposed for combating inter-symbol interference (ISI) for single-user dispersive channels and it was shown to yield

significant performance gain over the conventional zero-forcing and MMSE criteria. In parallel with this development, the minimum BER criterion has also been considered for multiuser systems. In [45], an adaptive linear multiuser detector using an unconstrained stochastic gradient algorithm to minimize the BER was derived. However, the global convergence of this algorithm requires that the BER cost function be monotonic with respect to interference, fading, and noise statistics. This condition is very restrictive and difficult to verify. Very recently, another interesting linear minimum-BER multiuser detector has been developed in [46] based on a constrained recursive adaptation algorithm, which is directly applicable to channels with non-Gaussian noise. However, global convergence can be guaranteed only for the two-user case.

In this chapter, we study the minimum BER criterion as applied to linear multiuser detection for binary signaling and its biorthogonal extensions in DS-CDMA communication systems. Our attention is focused on base stations where information about the signature signals, timing, and received amplitudes of all active users is available or can be accurately estimated. Hence the linear multiuser detector that minimizes BER can be designed prior to its application. Note that the BER function is highly nonlinear for which several local minima may exist. In order to avoid unsatisfactory local minima, we propose a *constrained* minimum-BER (CMBER) multiuser detector that minimizes the BER cost function subject to a set of convex constraints. It is shown that if the decorrelating detector exists, then there exist an infinite number of detectors satisfying the constraints and that the constrained optimization problem has a unique minimizer.

To obtain the proposed detector, we convert the constrained optimization problem to an equivalent convex programming problem, and then develop a Newton barrier method that requires considerably less computation than that required by the method of sequential quadratic programming [47]. Even though the proposed detector cannot be shown to be always optimal because of the constraints imposed, our analysis

shows that it is optimal for many realistic situations. Simulations are carried out to demonstrate that the proposed detector yields the lowest BER among the results obtained from a large number of runs of an unconstrained optimization algorithm.

4.2 System Model

We consider binary-phase-shift-keying (BPSK) transmission over an additive white Gaussian noise (AWGN) channel in a DS-CDMA system. In this chapter, we will take a chip-rate approach. For a synchronous transmission, user detection can be performed symbol by symbol, i.e., the window length is 1. For an asynchronous transmission, an equivalent synchronous transmission can be obtained for an observation window and the detection can then be carried out window by window (see Sec. 3.2 and Fig. 3.1). Note that this modeling also applies to a single-user system over a dispersive channel where each transmitted information bit can also be deemed to be originating from a different user. If the single-user channel is time invariant, then all virtual users have identical signature signals, which are the impulse response (IR) of the channel, but delayed in time. Hence for the design of a linear receiver, it is sufficient to consider only synchronous multiuser systems.

To design a detector that minimizes BER, it is not convenient to work on the outputs of the matched filters. Hence we will start from the received signal, to which the linear mapping to be designed applies. Assume that there are K synchronous users and denote the information bit of the ith user and its amplitude as b_i and $\sqrt{e_i}$, respectively. Within the observation window, the critically sampled version of the received baseband signal $\mathbf{y}$ can be expressed as

$$\mathbf{y} = \mathbf{S}\mathbf{b} + \mathbf{n} \tag{4.1}$$

where

$$\mathbf{y} = [y_1 \; y_2 \; \cdots \; y_N]^T \tag{4.2}$$

$$\mathbf{b} = [b_1\ b_2\ \cdots\ b_K]^T \tag{4.3}$$

$$\mathbf{S} = [\sqrt{e_1}\mathbf{s}_1\ \sqrt{e_2}\mathbf{s}_2\ \cdots\ \sqrt{e_K}\mathbf{s}_K] \in R^{N\times K} \tag{4.4}$$

In (4.1), $\mathbf{n}$ is an AWGN signal with zero mean and variance $\sigma^2 = N_0/2$, and $\mathbf{s}_i \in R^{N\times 1}$ is the critically sampled signature signal of the ith synchronous user. For asynchronous systems, if the original discrete signature signal of the real user, who transmitted the ith information bit, is $\hat{\mathbf{s}}$, then from Fig. 3.1 $\mathbf{s}_i$ will be of the form $[0\ \cdots\ 0\ \hat{\mathbf{s}}^T\ 0\ \cdots\ 0]^T$.

4.3 Multiuser BER Cost Function

Consider the BER of a linear multiuser receiver with coefficient vector $\mathbf{c}$ for a multiuser channel. The BER of the kth user can be readily found as

$$P(\mathbf{c}) = \frac{1}{2^{K-1}}\sum_{i=1}^{2^{K-1}} Q\left(\frac{\mathbf{c}^T\mathbf{v}_i}{\|\mathbf{c}\|\sigma}\right) \tag{4.5}$$

where $\mathbf{v}_i = \mathbf{S}\hat{\mathbf{b}}_i$ and $\hat{\mathbf{b}}_i$ for $1 \le i \le 2^{K-1}$ is a possible information vector with its kth entry b_k equal to 1 and

$$Q(x) = \frac{1}{\sqrt{2\pi}}\int_x^\infty e^{-v^2/2}\,dv$$

Since the BER cost function with respect to $\mathbf{c}$ given in (4.5) depends only on the direction of $\mathbf{c}$, the existence of a global minimum of $P(\mathbf{c})$ is obvious. The detector whose coefficient vector $\mathbf{c}^*$ minimizes (4.5) is optimal among linear detectors and will be referred to as the *optimal linear detector*. If the gradient of $P(\mathbf{c})$ with respect to $\mathbf{c}$ is set to zero, we obtain

$$\mathbf{c} = c\sum_{i=1}^{2^{K-1}} \alpha_i\mathbf{v}_i \tag{4.6}$$

where c is an arbitrary constant and

$$\alpha_i = \exp\left[-\frac{(\mathbf{c}^T\mathbf{v}_i)^2}{2\|c\|^2\sigma^2}\right] \tag{4.7}$$

Hence, a $\mathbf{c}$ that satisfies (4.6) may be a local minimizer if $c > 0$ or a local maximizer if $c < 0$. It can also be seen that the optimal $\mathbf{c}^*$ is a weighted sum of all possible received noise-free signal, $\{\mathbf{v}_i\}$. Because the exponential function decreases fast as its argument increases, $\mathbf{c}^*$ is dominated by those received signals whose inner products with $\mathbf{c}$ are relatively small. This is natural since the optimal detector would achieve nearly equal signal-to-noise ratio (SNR) for all possible transmitted $\{\mathbf{b}_i\}$. Even though (4.6) provides some insights to the problem at hand, a closed-form expression for $\mathbf{c}^*$ is not available. Furthermore, since the BER function is highly nonlinear and there may exist more than one local minimum, convergence to $\mathbf{c}^*$ cannot generally be guaranteed by many nonlinear optimization algorithms.

The following proposition will be useful in the subsequent analysis.

Proposition 4.1: Any local minimizer of the BER cost function in (4.5) subject to

$$\mathbf{c}^T\mathbf{v}_i \geq 0 \quad \text{for } 1 \leq i \leq 2^{K-1} \tag{4.8}$$

is a global minimizer. Furthermore, with the constraint $\|\mathbf{c}\| = 1$, the global minimizer is unique.

Proof Since the BER cost function is independent of the length of $\mathbf{c}$, it is sufficient to consider minimizing $P(\mathbf{c})$ on the set

$$I = \{\mathbf{c} : \ \|\mathbf{c}\| = 1 \ \text{ and } \mathbf{c} \text{ satisfies (4.8)}\} \tag{4.9}$$

Let the global minimizer of the above constrained minimization problem be $\mathbf{c}_1 \in I$ and assume that there exists another local minimizer $\mathbf{c}_2 \in I$ such that

$$P(\mathbf{c}_1) < P(\mathbf{c}_2) \tag{4.10}$$

Let $\alpha < 1$ be a positive constant and assume that

$$\mathbf{c} = \frac{\alpha\mathbf{c}_1 + (1-\alpha)\mathbf{c}_2}{\|\alpha\mathbf{c}_1 + (1-\alpha)\mathbf{c}_2\|} \tag{4.11}$$

Since $\|\mathbf{c}\| = 1$ and $\mathbf{c}^T\mathbf{v}_i \geq 0$ for $1 \leq i \leq 2^{K-1}$, we conclude that $\mathbf{c} \in I$. Furthermore, because $\|\alpha\mathbf{c}_1 + (1-\alpha)\mathbf{c}_2\| \leq 1$, we have

$$\mathbf{c}^T\mathbf{v}_i \geq \alpha\mathbf{c}_1^T\mathbf{v}_i + (1-\alpha)\mathbf{c}_2^T\mathbf{v}_i \tag{4.12}$$

Hence

$$\begin{aligned} Q\left(\frac{\mathbf{c}^T\mathbf{v}_i}{\sigma}\right) &\leq Q\left[\frac{\alpha\mathbf{c}_1^T\mathbf{v}_i + (1-\alpha)\mathbf{c}_2^T\mathbf{v}_i}{\sigma}\right] \\ &\leq \alpha Q\left(\frac{\mathbf{c}_1^T\mathbf{v}_i}{\sigma}\right) + (1-\alpha)Q\left(\frac{\mathbf{c}_2^T\mathbf{v}_i}{\sigma}\right) \end{aligned} \tag{4.13}$$

where the second inequality follows from the fact that $Q(x)$ for $x \geq 0$ is a convex function. From (4.5) and (4.13), we have

$$\begin{aligned} P(\mathbf{c}) &= \frac{1}{2^{K-1}}\sum_{i=1}^{2^{K-1}} Q(\frac{\mathbf{c}^T\mathbf{v}_i}{\sigma}) \\ &\leq \frac{\alpha}{2^{K-1}}\sum_{i=1}^{2^{K-1}} Q\left(\frac{\mathbf{c}_1^T\mathbf{v}_i}{\sigma}\right) + \frac{1-\alpha}{2^{K-1}}\sum_{i=1}^{2^{K-1}} Q\left(\frac{\mathbf{c}_2^T\mathbf{v}_i}{\sigma}\right) \\ &= \alpha P(\mathbf{c}_1) + (1-\alpha)P(\mathbf{c}_2) \\ &< P(\mathbf{c}_2) \qquad \text{for all } \alpha \in (0,\, 1) \end{aligned} \tag{4.14}$$

Since $\mathbf{c} \to \mathbf{c}_2$ as $\alpha \to 0$, the inequality in (4.14) implies that in any arbitrary small neighborhood centered at $\mathbf{c}_2$, there always exists a vector $\mathbf{c}$ such that $P(\mathbf{c}) < P(\mathbf{c}_2)$. This contradicts the fact that $\mathbf{c}_2$ is a local minimizer and hence we have $P(\mathbf{c}_1) \geq P(\mathbf{c}_2)$. Since $\mathbf{c}_1$ is the global minimizer, we also have $P(\mathbf{c}_1) \leq P(\mathbf{c}_2)$. Therefore, $P(\mathbf{c}_1) = P(\mathbf{c}_2)$ and $\mathbf{c}_2$ is a global minimizer.

To show the uniqueness of the minimizer in set I, we note that any point in the set

$$I_0 = \{\mathbf{c} : \|\mathbf{c}\| = 1 \text{ and } \mathbf{c}^T\mathbf{v}_i = 0 \text{ for } 1 \leq i \leq 2^{K-1}\} \tag{4.15}$$

is a global maximizer. Hence it is sufficient to consider only those points in the convex set $I_1 = I - I_0$.

Since $Q(x)$ is strictly convex for $x > 0$, $P(\mathbf{c})$ in (4.5) is strictly convex on set I_1. Now assume that there are two distinct global minimizers $\mathbf{c}_1$ and $\mathbf{c}_2$ with $\mathbf{c}_1 \neq \mathbf{c}_2$. In such a case, any point

$$\mathbf{c} = \frac{\alpha\mathbf{c}_1 + (1-\alpha)\mathbf{c}_2}{\|\alpha\mathbf{c}_1 + (1-\alpha)\mathbf{c}_2\|} \tag{4.16}$$

with $0 < \alpha < 1$ would satisfy the inequality

$$P(\mathbf{c}) \geq P(\mathbf{c}_1) \tag{4.17}$$

Since $P(\mathbf{c})$ is strictly convex on I_1, we have

$$P(\mathbf{c}) < \alpha P(\mathbf{c}_1) + (1-\alpha)P(\mathbf{c}_2) = P(\mathbf{c}_1) \tag{4.18}$$

which contradicts (4.17). Therefore, the global minimizer is unique. ■

Note that in the above proposition, we have assumed that the set I defined by (4.9) is not empty. This assumption is true for most practical systems as shown in the following proposition.

Proposition 4.2: If the signature signals $\mathbf{s}_i$, $1 \leq i \leq K$, are linearly independent of each other, then there always exists an infinite number of elements in I.

Proof It is easy to show that if $\mathbf{s}_i$, $1 \leq i \leq K$, are linearly independent of each other, then the cross-correlation matrix $\mathbf{R} = \mathbf{S}^T\mathbf{S}$ is positive definite and the zero-forcing solution can be achieved. Denote the decorrelating linear mapping that applies to the received signal for user k as $\mathbf{c}_d$. Then, from (2.34), we have

$$\frac{\mathbf{c}_d^T\mathbf{v}_i}{\|\mathbf{c}_d\|} = \frac{\mathbf{e}_k^T\mathbf{R}^{-1}\mathbf{S}^T\mathbf{S}\hat{\mathbf{b}}_i}{\|\mathbf{c}_d\|} = \frac{\mathbf{e}_k^T\hat{\mathbf{b}}_i}{\|\ c\mathbf{c}_d\|} = \frac{1}{\|\mathbf{c}_d\|} > 0 \quad \text{for } 1 \leq i \leq 2^{K-1} \tag{4.19}$$

This means that $\mathbf{c}_d/\|\mathbf{c}_d\|$ is in set I. Now consider vector

$$\mathbf{c}_p = \frac{\mathbf{c}_d + \mathbf{p}}{\|\mathbf{c}_d + \mathbf{p}\|} \tag{4.20}$$

where $\mathbf{p}$ is a perturbation vector to be determined later. We have $\|\mathbf{c}_p\| = 1$ and

$$\begin{aligned} \mathbf{c}_p^T \mathbf{v}_i &= \frac{\mathbf{c}_d^T + \mathbf{p}^T \mathbf{v}_i}{\|\mathbf{c}_d + \mathbf{p}\|} = \frac{1 + \mathbf{p}^T \mathbf{v}_i}{\|\mathbf{c}_d + \mathbf{p}\|} \\ &\geq \frac{1 - \|\mathbf{p}\|\|\mathbf{v}_i\|}{\|\mathbf{c}_d + \mathbf{p}\|} \geq \frac{1 - \|\mathbf{p}\|(\max_i \|\mathbf{v}_i\|)}{\|\mathbf{c}_d + \mathbf{p}\|} \end{aligned} \tag{4.21}$$

It follows that if

$$\|\mathbf{p}\| \leq \frac{1}{\max\limits_{1 \leq i \leq 2^{K-1}} \|\mathbf{v}_i\|} \tag{4.22}$$

then (4.21) implies that $\mathbf{c}_p^T \mathbf{v}_i \geq 0$ for $1 \leq i \leq 2^{K-1}$. In other words, any vector $\mathbf{c}_p$ given by (4.20) with $\mathbf{p}$ satisfying (4.22) belongs to set I. ■

4.4 The Constrained Minimum-BER Detector

The CMBER multiuser detector is defined as the detector whose coefficient vector is the global minimizer of $P(\mathbf{c})$ in (4.5) subject to the constraints in (4.8). From Proposition 4.2, once the zero-forcing solution can be achieved, the CMBER detector exists and outperforms the decorrelating detector. However, the CMBER detector cannot be shown to be always optimal among linear detectors due to the constraints imposed.

Proposition 4.3: The CMBER detector achieves the optimal performance among linear multiuser detectors if

$$\mathbf{v}_i^T \mathbf{v}_j > 0 \quad \forall\, i, j \tag{4.23}$$

Proof Let $\mathbf{c}$ be a minimizer of the BER cost function in (4.5). Then, it follows from (4.6) and (4.23) that

$$\mathbf{c}^T \mathbf{v}_j = c \sum_{i=1}^{2^{K-1}} \alpha_i \mathbf{v}_i^T \mathbf{v}_j > 0 \tag{4.24}$$

This shows that under the conditions in (4.23), any local minimizer of $P(\mathbf{c})$ must satisfy the constraints in (4.8). Hence the CMBER detector is the global minimizer of $P(\mathbf{c})$. ■

The condition in (4.23) requires that the amplitude of the desired user is much larger than the amplitudes of other users. This condition is too restrictive and is often violated in practice. Even so, the CMBER detector still achieves the optimal performance for most realistic cases. An intuitive explanation is as follows: Since a detector with a coefficient vector $\mathbf{c}$ that does not satisfy (4.8) would usually yield a poorer BER than that of the decorrelating detector, the global minimizer most likely satisfies (4.8). Therefore, the constraints in (4.8) usually will not exclude the unconstrained global minimizer of $P(\mathbf{c})$ in (4.5), i.e., the CMBER detector will in most realistic cases represent the same unconstrained global minimizer. The following proposition will be useful to further clarify the above idea.

Proposition 4.4: For a linear receiver with a coefficient vector $\mathbf{c}$ that does not satisfy the constraints in (4.8), the corresponding BER is bounded as

$$P(\mathbf{c}) \geq \frac{1}{2^{K-1}} \left[0.5 + \sum_{i=1}^{K-1} \binom{K-1}{i} Q\left(\frac{2id}{K-1} \right) \right] \tag{4.25}$$

regardless of the user signature signals, where $d = \sqrt{e_k}/\sigma$, K is the number of users, and $\binom{k}{n}$ is the binominal coefficient $n!/[k!(n-k)!]$.

Proof Since there is no constraint on user signature signals, smaller inner products of $\mathbf{c}$ and $\mathbf{v}_i$ will result in a larger BER bound. Hence, we consider the case where the smallest inner product is 0. Without loss of generality, we assume that the possible received signal corresponding to the smallest inner product be $\mathbf{v}_1$, i.e., $\mathbf{c}^T\mathbf{v}_1 = 0$ and $\mathbf{c}^T\mathbf{v}_i \geq$ for $i > 1$. Consider those possible information vectors that differ from $\mathbf{b}_1$ in exactly n bits. Clearly, there are $M = \binom{K-1}{n}$ such bit sequences,

which we denote as $\mathbf{v}_2$, ..., $\mathbf{v}_{M+1}$. Then, we have

$$\begin{aligned}\sum_{i=2}^{M+1}\mathbf{c}^T\mathbf{v}_i &= \sum_{i=2}^{M+1}\mathbf{c}^T\mathbf{S}(\mathbf{b}_I - \mathbf{b}_1)\\ &= \frac{2nM}{K-1}\mathbf{c}^T\mathbf{S}\mathbf{b}_1^-\end{aligned} \tag{4.26}$$

where $\mathbf{b}_1^-$ is a vector of length K whose kth entry is zero and its other entries are the corresponding entries of $\mathbf{b}_1$ with opposite signs. By the definition of $\mathbf{b}_1^-$, we have

$$\mathbf{c}^T\mathbf{S}(\mathbf{b}_1 + \mathbf{b}_1^-) = \sqrt{e_k}\mathbf{c}^T\mathbf{s}_k \tag{4.27}$$

If $\mathbf{c}$ has unit energy, then from (4.27) we have

$$\mathbf{c}^T\mathbf{S}\mathbf{b}_1^- \le \sqrt{e_k} \tag{4.28}$$

Substituting (4.28) into (4.26), we obtain

$$\sum_{i=2}^{M+1}\mathbf{c}^T\mathbf{v}_i \le \frac{2nM}{K-1}\sqrt{e_k} \tag{4.29}$$

By the fact that $Q(c)$ is convex for $x \ge 0$, the lowest BER will be achieved when

$$\begin{aligned}\mathbf{c}^T\mathbf{v}_j &= \frac{1}{M}\sum_{i=2}^{M+1}\mathbf{c}^T\mathbf{v}_i\\ &\le \frac{2n}{K-1}\sqrt{e_k} \quad \text{for } 2 \le j \le M+1\end{aligned} \tag{4.30}$$

From the above equation and (4.5), the overall BER contributed by possible transmission of $\{\mathbf{b}_j, 2 \le j \le M\}$ is given by

$$P_n = \frac{M}{2^{K-1}}Q\left(\frac{2nd}{K-1}\right) \tag{4.31}$$

By summing $\{P_n\}$ for $n = 0, 1, \ldots, K-1$, we obtain (4.25). ■

The above BER bound is useful for examining whether the CMBER detector is optimal among linear detectors for realistic cases. If the BER bound in (4.25) is larger than the BER of a detector whose coefficient vector satisfies the constraints in (4.8)

(e.g., the decorrelating detector), then the coefficient vector of the CMBER detector is the global minimizer of the BER cost function. In Fig. 4.1, the smallest SNR, defined by e_k/N_0, required by the decorrelating detector to achieve smaller BER than the bound given by (4.25) is illustrated as a function of the angle between $\mathbf{s}_k$ and the interference subspace. From the figure, we can see that if the SNR is 6 dB or larger, then the required angle of $\mathbf{s}_k$ relative to its interference subspace is $\pi/3$ for a system of 20 users. In other words, if the angle of $\mathbf{s}_k$ relative to the interference subspace is $\pi/3$ and the SNR is 6 dB or larger, then the CMBER detector achieves the optimal performance among linear detectors. As the angle increases to $5\pi/12$, the required SNR becomes 1 dB. Since pseudo-random sequences are usually used in practice, the angle of a signature signal relative to its interference subspace is usually large, say greater than $\pi/3$. This implies that for practical systems where the SNR is around 10 dB or more, the CMBER detector is optimal. It is worthy to note that the above bound is not tight and the CMBER detector can be optimal for much worse cases as indicated above. In our simulations, it was found that for systems where the SNR at the output of the decorrelating detector is not very low (e.g., the SNR is greater than 0 dB), the CMBER multiuser detector is identical with the linear minimum-BER detector whose coefficient vector minimizes the BER cost function (4.5) without any constraints.

The above result applies directly to the case of channel equalization for single-user communication systems. Even though an exact zero-forcing solution is not always achievable with a finite-length linear equalizer, the channel is still *equalizable* for most cases. In other words, set I is most likely not empty and a constrained minimum-BER equalizer exists.

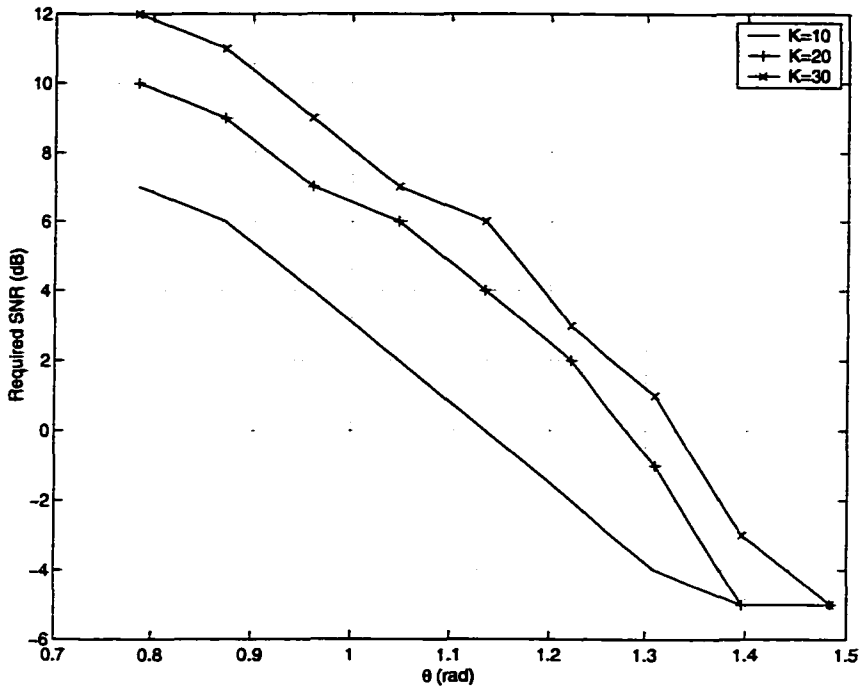

Figure 4.1. *The smallest SNR required by the decorrelating detector to achieve smaller BER than the bound given by (4.25) as a function of the angle of* $\mathbf{s}_k$ *relative to the interference subspace.*

4.5 A Newton Barrier Method for the CMBER Problem

We now discuss the computation of the coefficient vector of the CMBER detector. The problem of minimizing the BER in (4.5) subject to constraints in (4.8) is equivalent to the optimization problem

$$\begin{aligned} \text{minimize} \quad & \hat{P}(\mathbf{c}) && && (4.32a) \\ \text{subject to} \quad & \mathbf{c}^T \hat{\mathbf{v}}_i \geq 0 && \text{for } 1 \leq i \leq 2^{K-1} && (4.32b) \\ & \|\mathbf{c}\| = 1 && && (4.32c) \end{aligned}$$

where

$$\hat{P}(\mathbf{c}) = \frac{1}{2^{K-1}} \sum_{i=1}^{2^{K-1}} Q(\mathbf{c}^T \hat{\mathbf{v}}_i)$$

and

$$\hat{\mathbf{v}}_i = \frac{\mathbf{v}_i}{\sigma} \quad \text{for } 1 \leq i \leq 2^{K-1}$$

Note that the problem in (4.32a-4.32c) is *not* a convex programming problem because the feasible region characterized by (4.32b) and (4.32c) is not convex. However, it can be readily verified that the solution of (4.32a-4.32c) coincides with the solution of the constrained optimization problem

$$\begin{aligned} \text{minimize} \quad & \hat{P}(\mathbf{c}) && \text{(4.33a)} \\ \text{subject to} \quad & \mathbf{c}^T \hat{\mathbf{v}}_i \geq 0 \quad \text{for } 1 \leq i \leq 2^{K-1} && \text{(4.33b)} \\ & \|\mathbf{c}\| \leq 1 && \text{(4.33c)} \end{aligned}$$

This is because for any $\mathbf{c}$ with $\|\mathbf{c}\| < 1$, one always has $\hat{P}(\hat{\mathbf{c}}) \leq \hat{P}(\mathbf{c})$ where $\hat{\mathbf{c}} = \mathbf{c}/\|\mathbf{c}\|$. In other words, the minimizer $\mathbf{c}^*$ of the problem in (4.33a-4.33c) always satisfies $\|\mathbf{c}^*\| = 1$. A key distinction between the problems in (4.32a-4.32c) and (4.33a-4.33c) is that the latter one is a convex programming problem for which a number of efficient algorithms are available. The optimization algorithm described below fits into the class of barrier function methods [48][49] but it has several additional features that are uniquely associated with the present problem. These include a closed-form formula for evaluating the Newton direction and an efficient line search.

By taking a barrier function approach, we can in addition drop the nonlinear constraint in (4.33c) and convert the problem in (4.33a-4.33c) into

$$\begin{aligned} \text{minimize} \quad & F_\mu(\mathbf{c}) = \hat{P}(\mathbf{c}) - \mu \log(1 - \mathbf{c}^T \mathbf{c}) && \text{(4.34a)} \\ \text{subject to} \quad & \mathbf{c}^T \hat{\mathbf{v}}_i \geq 0 \quad \text{for } 1 \leq i \leq 2^{K-1} && \text{(4.34b)} \end{aligned}$$

where $\mu > 0$ is the barrier parameter. With a strictly feasible initial point $\mathbf{c}_0$, which strictly satisfies the constraints in (4.33b) and (4.33c), the logarithmic term in (4.34a)

is well defined. It is also evident that regardless of the value of μ, the minimum of (4.34a-4.34b) is the global minimum of the problem of minimizing (4.5) subject to the constraints in (4.8). The gradient and Hessian matrix of $F_\mu(\mathbf{c})$ are given by

$$\nabla F_\mu(\mathbf{c}) = -\sum_{i=1}^{M} \frac{1}{M} e^{-\beta_i^2/2} \hat{\mathbf{v}}_i + \frac{2\mu \mathbf{c}}{1 - \|\mathbf{c}\|^2} \tag{4.35}$$

$$\nabla^2 F_\mu(\mathbf{c}) = \sum_{i=1}^{M} \frac{1}{M} e^{-\beta_i^2/2} \beta_i \hat{\mathbf{v}}_i \hat{\mathbf{v}}_i^T + \frac{2\mu}{1 - \|\mathbf{c}\|^2} \mathbf{I} + \frac{4\mu}{(1 - \|\mathbf{c}\|)^2} \mathbf{c}\mathbf{c}^T \tag{4.36}$$

where $M = 2^{K-1}$ and $\beta_i = \mathbf{c}^T \hat{\mathbf{v}}_i$ for $1 \leq i \leq M$. Note that the Hessian matrix in the interior of the feasible region, i.e., $\mathbf{c}$ with $\beta_i = \mathbf{c}^T \hat{\mathbf{v}}_i > 0$ and $\|\mathbf{c}\| < 1$, is positive definite. This suggests that at the $(k+1)$th iteration, $\mathbf{c}_{k+1}$ can be obtained as

$$\mathbf{c}_{k+1} = \mathbf{c}_k + \alpha_k \mathbf{d}_k \tag{4.37}$$

where the search direction $\mathbf{d}_k$ is computed using

$$\mathbf{d}_k = -[\nabla^2 F_\mu(\mathbf{c}_k)]^{-1} \nabla F_\mu(\mathbf{c}_k) \tag{4.38}$$

The positive scalar α_k in (4.37) is determined by a line search step as follows. First, note that the one-variable function $F_\mu(\mathbf{c}_k + \alpha \mathbf{d}_k)$ is strictly convex on the interval $[0, \bar{\alpha}]$ where $\bar{\alpha}$ is the largest positive scalar such that $\mathbf{c}_k + \alpha \mathbf{d}_k$ remains feasible for $0 \leq \alpha \leq \bar{\alpha}$. Once $\bar{\alpha}$ is determined, $F_\mu(\mathbf{c}_k + \alpha \mathbf{d}_k)$ is a unimodal function on $[0, \bar{\alpha}]$ and the search for the minimizer of the function can be carried out using one of the well-known line search methods such as quadratic or cubic interpolation, the Golden-section method, or some direct search method [47][50][49]. To find $\bar{\alpha}$, we note that a point $\mathbf{c}_k + \alpha \mathbf{d}_k$ satisfies the constraints in (4.33b) if

$$(\mathbf{c}_k + \alpha \mathbf{d}_k)^T \hat{\mathbf{v}}_i \geq 0 \quad \text{for } 1 \leq i \leq M \tag{4.39}$$

Since $\mathbf{c}_k$ is feasible, we have $\mathbf{c}_k^T \hat{\mathbf{v}}_i \geq 0$ for $1 \leq i \leq M$. Hence for those indices i such that $\mathbf{d}_k^T \hat{\mathbf{v}}_i \geq 0$, any nonegative α will satisfy (4.39). In other words, only those constraints in (4.33b) whose indices are in the set

$$\mathcal{I}_k = \{i : \mathbf{d}_k^T \hat{\mathbf{v}}_i < 0\} \tag{4.40}$$

will affect the largest value of α that satisfies (4.39), and the largest value of α can be computed as

$$\bar{\alpha}_1 = \min_{i \in \mathcal{I}_k} \left(\frac{\mathbf{c}_k^T \mathbf{v}_i}{-\mathbf{d}_k^T \mathbf{v}_i} \right) \tag{4.41}$$

In order to satisfy the constraint in (4.33c), we solve $\|\mathbf{c}_k + \alpha \mathbf{d}_k\|^2 = 1$ for α and the solution is given by $\alpha = \bar{\alpha}_2$ with

$$\bar{\alpha}_2 = \frac{[(\mathbf{c}_k^T \mathbf{d}_k)^2 - \|\mathbf{d}_k\|^2(\|\mathbf{c}_k\|^2 - 1)]^{1/2} - \mathbf{c}_k^T \mathbf{d}_k}{\|\mathbf{d}_k\|^2} \tag{4.42}$$

The value of $\bar{\alpha}$ can now be taken as $\min(\bar{\alpha}_1, \bar{\alpha}_2)$. In practice, one must keep the next iterate strictly inside the feasible region to ensure that the barrier function in (4.36) is well defined. To this end we use

$$\bar{\alpha} = 0.99 \min(\bar{\alpha}_1, \bar{\alpha}_1) \tag{4.43}$$

This iterative optimization procedure continues until the difference between two successive solutions is less than a prescribed tolerance. Even though with a strictly feasible initial point, the barrier Newton method described above always converges to the global minimizer for an arbitrary positive μ, the value of μ does affect the behavior of the algorithm. A small μ would lead to an ill-conditioned Hessian matrix, while a large μ would lead to slow convergence. Considering that the probability of error is always less than 1, it is then reasonable to set the upper bound of μ to 0.1 to ensure that the second term in the right-hand side of (4.34a) does not dominate over the first term. Hence, a μ in the interval $[0.001, 0.1]$, which would guarantee a well-conditioned Hessian matrix and allow a fast convergence, is desirable. Note that the selection of μ does not involve specific signal models and other system parameters.

4.6 Numerical Examples

4.6.1 Example 1

As a first example, we consider a two-user system. The simplicity of the system leads to a deeper understanding of the optimal linear multiuser detector, especially when the optimal linear detector considerably outperforms the decorrelating and MMSE detectors. Assume that the signature signals multiplied by the corresponding amplitudes are $\hat{\mathbf{s}}_0$ and $\hat{\mathbf{s}}_1$ as depicted in Fig. 4.2 and the desired user is user 0. The corresponding coefficient vector $\mathbf{c}_d$ of the decorrelating detector must be orthogonal to $\hat{\mathbf{s}}_1$ as illustrated in Fig. 4.2. Clearly, in this case, the CMBER detector is equivalent to the optimal linear detector since the energy of the desired signal is stronger than the energy of the interferer. Hence, the CMBER detector will not be mentioned further in this example. If a linear detector is used and the angle between its coefficient vector and $\hat{\mathbf{s}}_0$ is θ, the BER for this example can be obtained as

$$P(\theta) = \frac{1}{2}\left[Q\left(\frac{1.25\cos\theta + 0.125\sin\theta}{\sigma}\right) + Q\left(\frac{0.75\cos\theta - 0.125\sin\theta}{\sigma}\right)\right] \tag{4.44}$$

Hence, the BER of the decorrelating detector is

$$P(\mathbf{c}_d) = Q\left(\frac{1}{\sqrt{5}\,\sigma}\right) \tag{4.45}$$

and the BER of the MFR with coefficient vector $\mathbf{s}_0$ is

$$P(\mathbf{s}_0) = \frac{1}{2}\left[Q\left(\frac{5}{4\sigma}\right) + Q\left(\frac{3}{4\sigma}\right)\right] \tag{4.46}$$

Comparing (4.45) with (4.46), we can see that the MFR in this case outperforms the decorrelating detector regardless of the SNR because the cross-correlation of the two signature signals is large while the MUI is sufficiently small relative to the desired signal energy. Under these circumstances, the loss of signal energy inherent in the decorrelating detection is always larger than the loss of signal energy due to signal cancellation when the MFR is employed. Even though the MMSE detector can to

some extent balance the effects of MUI and AWGN, its performance is still close to that of the decorrelating detector since it treats the residual MUI and AWGN as equally harmful. On the other hand, the optimal linear detector can better balance the effects of MUI and AWGN and, as a result, its performance is always better than that of the MFR. For an SNR of 15 dB ($\sigma = 0.126$), the coefficient vector of the MMSE detector, $\mathbf{c}_m$, and the coefficient vector of the optimal linear detector, $\mathbf{c}_c$, are illustrated in Fig. 4.2. The BER's of the decorrelating detector, MMSE, MFR, and optimal linear detectors are given in Table 4.1. As can be observed from the table, the optimal linear detector and even the MFR significantly outperform the decorrelating and MMSE detectors.

Table 4.1. *BER's for a Two-User System (SNR=15 dB).*

Detectors	Decorrelating	MMSE	MFR	Minimum-BER
BER	1.91×10^{-4}	2.09×10^{-7}	6.40×10^{-10}	3.86×10^{-10}

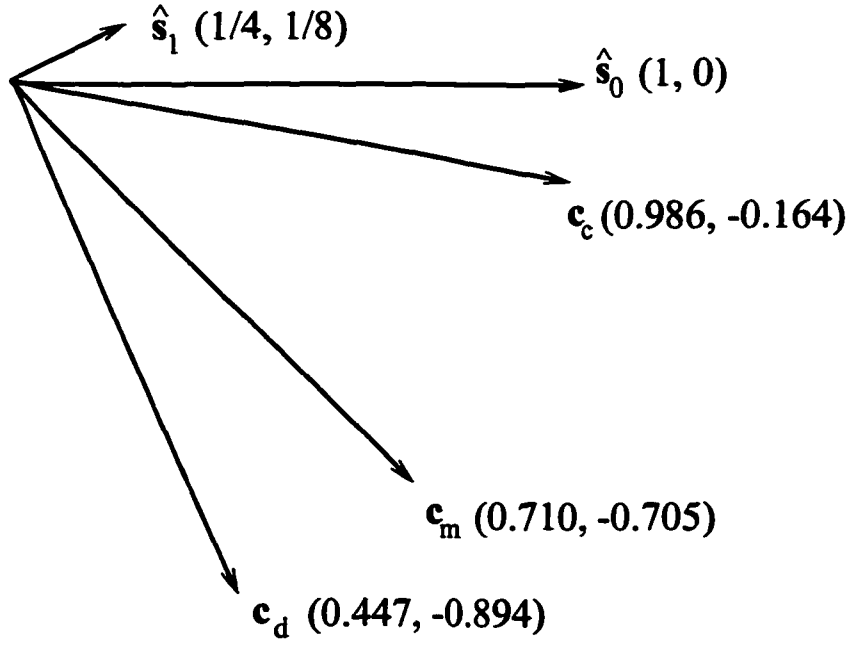

Figure 4.2. *Singnature signals and multiuser detectors for a two-user system.*

4.6.2 Example 2

As a second example, we compare the performance of the CMBER with that of the optimal linear detector. Shown in Fig. 4.3 are the BER curves of different detectors for a system with 10 equal-power users. The optimal linear detector was taken as the best solution of 40 runs of a quasi-Newton optimization algorithm. In order to simulate a case in which the CMBER detector differs from the optimal linear multiuser detector, the user signature signals were randomly selected and the SNR was chosen to be unrealistically small. As can be seen in Fig. 4.3, the BER curve of the CMBER detector and that of the optimal linear detector are indistinguishable. In fact, these two detectors have the same coefficient vector when the SNR is larger than -3 dB. From the figure, it is also evident that the MMSE detector achieves very similar performance as that of the optimal linear detector while the decorrelating detector yields a considerably poorer performance.

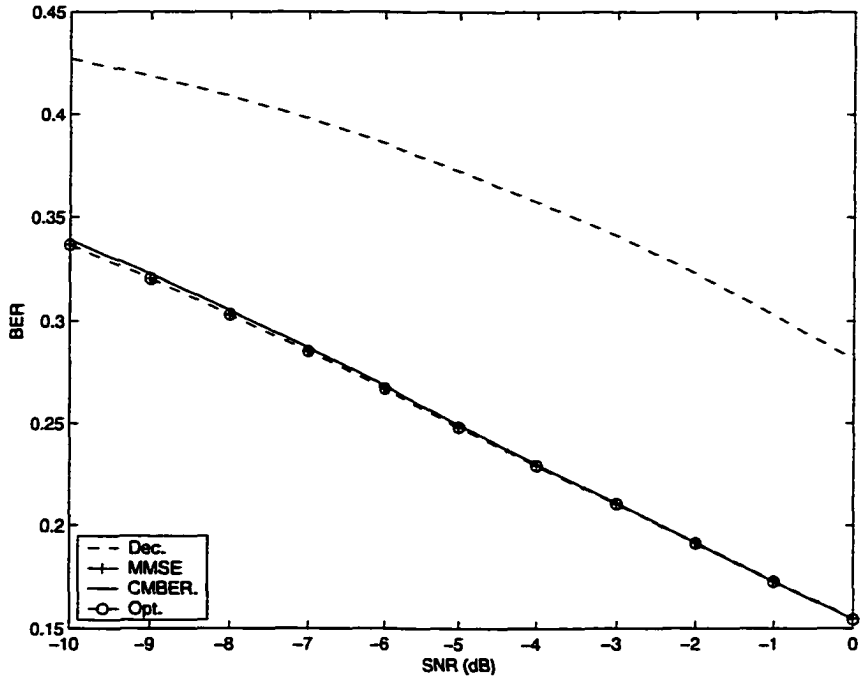

Figure 4.3. *Performance comparison of linear multiuser detectors:* 10 *equal-power users.*

We now consider more practical situations where the SNR is larger than 0 dB. Figs. 4.4 and 4.5 show the BER curves for a 10-user single-path and a multipath system, respectively. In both systems, the power of the desired user was set to 0 dB and the power of the interfering users was randomly generated in the range -10 dB to 0 dB. The number of resolvable paths was assumed to be 6 for Fig. 4.5. For the multipath system, the SNR for a particular user is defined as the ratio of the total received signal energy of the user to the energy of the Gaussian noise. We also assumed a slowly fading enviroment where the path gains can be accurately estimated. Hence all previous equations hold for the decorrelating, MMSE, and CMBER multiuser detectors if the signature signal of a particular user is replaced by its composite signature signal, which is the sum of the delayed versions of the original signature signal multiplied by the path gains that correspond to the delays. As can be observed, in both cases, the CMBER detector outperforms the decorrelating and MMSE detectors. For the single-path system, the cross-correlation among signature signals is small and the three BER curves are close to each other. On the other hand, for the multipath system, where the cross-correlation properties are relatively poorer, the performance gain of the CMBER detector over those of the decorrelating and the MMSE detectors is quite significant. Note that the coefficient vector of the CMBER detector was equal to that of the optimal linear detector whose performance curve is not shown in the figures.

4.6.3 Example 3

As a last example, we used the proposed CMBER detector, the zero-forcing equalizer, and the MMSE equalizer to a single user system over a dispersive channel with impulse response $h = \{0.7317, 0.6707, -0.1219\}$. The detector and equalizers were assumed to be of 3 taps and the detection delay was assumed to be 2. The BER curves of the zero-forcing equalizer, the MMSE equalizer, and the CMBER detector are illustrated in Fig. 4.6. As can be seen in the figure, the performance of the zero-

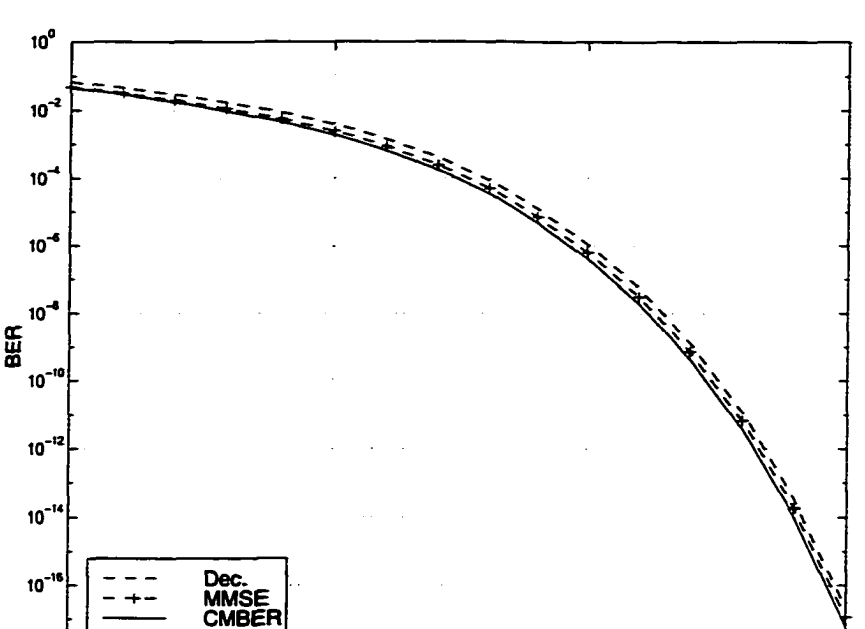

Figure 4.4. *Performance comparison of linear multiuser detectors:* 31*-chip Gold codes and sigle path.*

forcing equalizer is similar to that of the MMSE equalizer while the CMBER detector offers a performance gain as large as 5 dB over the MMSE equalizer.

4.6.4 Use of MATLAB

We have also compared the proposed barrier Newton method with the constrained optimization method provided by MATLAB routine *constr* in terms of computational complexity. This MATLAB routine was based on a sequential quadratic programming algorithm [47]. It was found that for a system with ten users and signature signals of length 31 chips, the MATLAB routine required 40 to 100 times more flops than the barrier Newton method. As the number of users and the length of signature signals increase, the barrier Newton method becomes even more efficient in terms of computation than the MATLAB routine.

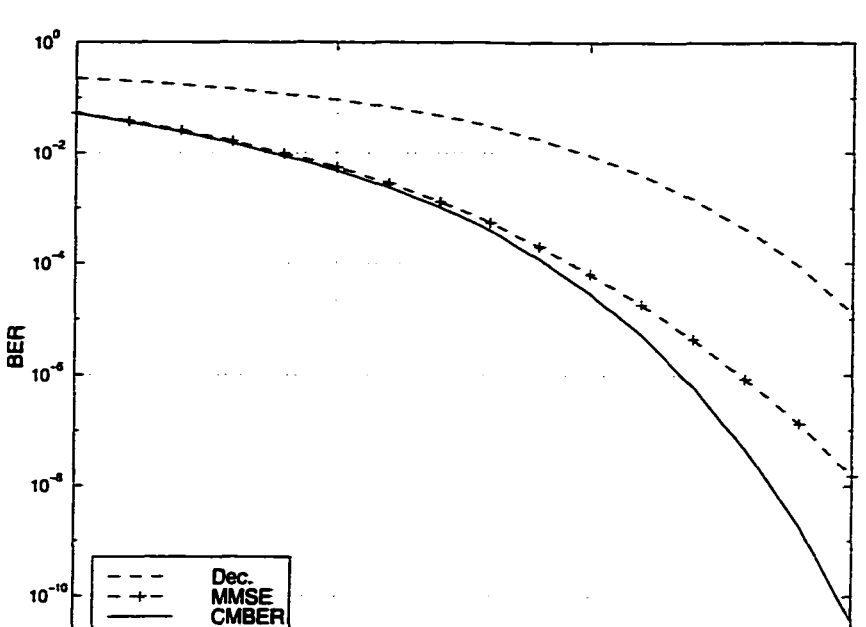

Figure 4.5. *Performance comparison of linear multiuser detectors:* 31*-chip Gold codes and multipaths.*

4.7 Conclusions

We have studied the minimum BER criterion as applied to multiuser detection as well as channel equalization for single-user systems and proposed a constrained minimum-BER multiuser detector. The proposed detector minimizes the BER cost function subject to the constraint that the corresponding eye pattern is open no matter what information bits are transmitted by interferers. We have shown that under this constraint, the BER cost function has a unique minimizer. Consequently, we were able to use a Newton barrier method to find the coefficients of the proposed detector that requires only a very small amount of computation relative to the popular method of sequential quadratic programming. Even though the proposed detector requires information about timing, amplitudes, and signature signals of all users, the idea is enlightening for an adaptive implementation where information about interferers

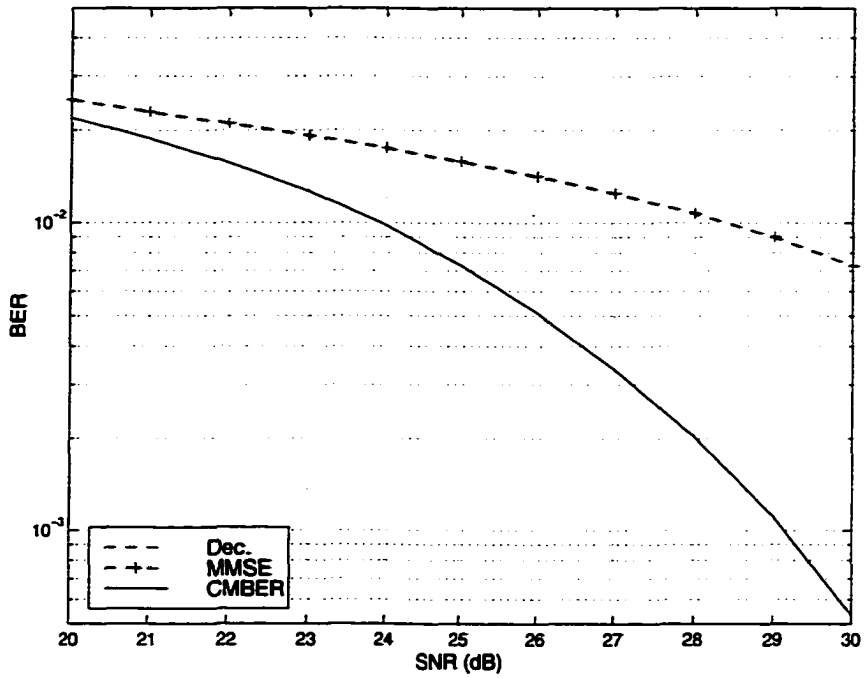

Figure 4.6. *Performance comparison of linear equalizers for a dispersive channel.*

is unavailable. Analysis and numerical examples have demonstrated that the performance gain of the proposed detector over those of the decorrelating and MMSE detectors can be quite significant in many cases.

It is worthy to point out that the analysis and results presented in this dissertation, especially the identification of the convergence region defined by the set of convex constraints, are also useful for possible adaptive implementations of the proposed algorithm. Even though identifying the proposed convergence region exactly would need information about the interferers, it is possible to identify, without the knowledge of the interferers, a convergence region that is approximately equal to or is included in the proposed region. For example, a constraint on the angle of the coefficient vector to be optimized relative to the coefficient vector of the decorrelator can be used to define such a region.

Chapter 5

Blind Multiuser Detection for Frequency-Selective Fading CDMA Channels

5.1 Introduction

So far focused on we have the design of multiuser detectors for mobile base stations. These centralized detectors demodulate all user signals simultaneously by utilizing information about the signature signals, timing, and sometimes received amplitudes of all users. For mobile stations, however, only the desired signal needs to be demodulated and the information of interfering users is not available. This precludes the use of centralized multiuser detectors. Consequently, decentralized detectors that can implicitly exploit information about interferers must be used. Note that even in a base station, the receiver may not have information about some interferers, e.g., interferers from adjacent cells. A centralized detector then has to treat this unknown interference as additive white Gaussian noise (AWGN). On the other hand, a decentralized detector indiscriminately suppresses interference from all users.

Recently, attempts have been made to develop adaptive multiuser detectors to eliminate the need for information about interfering users. An adaptive decorrelating detector was developed to integrate newly activated users for base stations in [19][20].

Since this detector can adaptively augment an existing decorrelator to take into account new users, it can also be extended to deal with mobile stations. A more popular adaptive multiuser detector is the minimum mean-squared error (MMSE) detector which minimizes the mean-squared error (MSE) between the outputs of the detector and the transmitted information bits [21][22]. Along this line, a notable progress was made in [23] based on the observation that minimizing the output energy of a linear detector under the constraint that the energy of the desired user is maintained is equivalent to minimizing the MSE. A blind adaptive detector, namely, the minimum mean output energy (MOE) detector, was then derived to further eliminate the need for training sequences. This blind adaptation mechanism is of particular importance for fading channels where frequent retraining is required by an adaptive detector. Following the MOE detector, other blind adaptive multiuser detectors were proposed from Wiener's reconstruction-filter point of view [51].

The aforementioned adaptive multiuser detectors are all aimed at AWGN channels. In comparison, relatively less progress has been made in the development of adaptive multiuser detection for fading channels. In [52], the MMSE multiuser detector was considered in a flat fading channel. Since the signal bandwidth in mobile radio and indoor DS-CDMA channels is often larger than the coherent bandwidth of the channels, transmitted signals often undergo frequency-selective fading. However, like the MFR for AWGN channels, the RAKE receiver used in conventional DS-CDMA systems for frequency-selective channels suffers from near-far (NF) effects in the presence of multiuser interference (MUI). Hence it is highly desirable to design adaptive multiuser detectors that achieve diversity gain in frequency-selective fading channels with NF resistance capability.

Apparently, a possible way to obtain a NF-resistant diversity receiver for multipath channels is to employ a RAKE structure where each finger is an MMSE adaptive filter instead of a matched filter. Furthermore, by applying the minimum MOE criterion, each MMSE detector may be adapted blindly. However, as will be demonstrated,

the minimum MOE criterion is not readily applicable for multipath channels. This observation motivates us to develop a new blind multiuser detector for frequency-selective fading channels. The proposed detector consists of a bank of blind adaptive filters, each one corresponding to a resolvable path and requiring only information about the signature signal and timing of the desired user. The coefficient vector of each filter consists of two mutually orthogonal components: one is fixed as the decorrelating linear mapping for the corresponding path as if there were no interferers, and the other is constrained to be orthogonal to the desired signal subspace but is otherwise free to be adapted according to the MMSE criterion. The resulting detector is a constrained MMSE detector or a partially decorrelating partially MMSE detector. The analysis presented below shows that as the background noise vanishes, the new detector is equivalent to the diversity decorrelating detector. Furthermore, the output error variance of the proposed detector is between those of the decorrelating detector and the MMSE detector. Note, however, that neither the diversity decorrelating detector nor the MMSE detector can be adaptively implemented without the need for training.

To examine the effect of fading rate on the performance of the proposed detector, the detector is interpreted from a bit-rate approach point of view for two extreme cases. Results show that the proposed detector may perform differently depending on the coherence time of the channel relative to the symbol interval. In general, by neglecting the performance loss due to imperfect adaptation, the proposed detector offers better performance for slowly fading channels.

The output error of each proposed adaptive filter is shown to be nearly Gaussian. As a result, a channel estimator, which essentially resembles the carrier recovery technique for single-user systems [53], can be used to estimate the channel coefficients. Having estimated the channel coefficients, a coherent diversity combiner can be employed to demodulate the data bits and hence achieves the largest diversity gain. Based on the fact that the output error is nearly Gaussian, a study on the error

probability and AME of the proposed detector is also given.

For the adaptation of the proposed detector, a stochastic algorithm is developed. The convergence as well as the output MSE of the algorithm is also studied. The results obtained allow us to compare the proposed blind adaptation algorithm with the conventional decision-directed least-mean square (LMS) algorithm [54] and clarify some issues pertaining to the algorithm's practical implementations. Simulation results show that the proposed detector provides significant performance gain with respect to the conventional RAKE receiver, even though the latter assumes perfect knowledge of the channel coefficients of the desired user.

5.2 System Model

Since a phase ambiguity always exists for a blind adaptive receiver, we consider differential phase-shift-keying (DPSK) modulation with antipodal signaling [11]. That is, if information bit n is the same as bit $n-1$, a $+1$ is transmitted at time n; otherwise, a -1 is transmitted. Because of the lack of information about interferers, matched filters for interferers cannot be constructed and the bit-rate approach is inapplicable. Hence, we will take the chip-rate approach. In this case, it is sufficient to consider only synchronous transmission as described before. The channel is assumed to be a wide-sense stationary uncorrelated scattering (WSSUS) channel with L resolvable paths [30]. Assuming that the channel coefficients are constant during one transmission interval, a channel coefficient vector for the kth user at the nth transmission interval can be defined as $\mathbf{c}_k(n) = [c_{k,1}(n)\ c_{k,2}(n)\ \cdots\ c_{k,L}(n)]^T$. For the WSSUS model, $\{c_{k,l}(n)\}$ are mutually uncorrelated random process and their absolute values are either Ricean or Rayleigh distributed depending on whether there exists an LOS or specular path. The received baseband signal observed at the nth symbol interval can be obtained by letting $\tau_k = 0$ for all k in (2.12) as

$$y_n(t) = \sum_{k=1}^{K} \sqrt{e_k} b_k(n) \sum_{l=1}^{L} c_{k,l}(n) s_k[t - (l-1)/W] + z(t) \tag{5.1}$$

where e_k, $b_k(n)$, $s_k(t)$ denote the energy per bit, the nth bit, and the normalized signature signal of user k, respectively, and $z(t)$ is a complex AWGN of zero mean and power spectral density $N_0/2$. In the rest of the chapter, we will assume that $\sqrt{e_k} = 1$ for $1 \leq k \leq K$ since if this is not the case, the amplitudes can always be incorporated into channel coefficients. Without loss of generality, we assume that the desired user is user 1. If we denote the critically sampled versions of $s_k(t)$, $y_n(t)$, and $n(t)$ by N-dimensional column vectors $\mathbf{s}_k$, $\mathbf{y}(n)$, and $\mathbf{n}$, respectively, then (5.1) can be expressed as

$$\mathbf{y}(n) = b_1(n)\mathbf{S}_1\mathbf{c}_1(n) + \mathbf{S}_I(n)\mathbf{b}_I(n) + \mathbf{n} \tag{5.2}$$

where

$$\mathbf{S}_I(n) = [\mathbf{S}_2\mathbf{c}_2(n)\ \mathbf{S}_2\mathbf{c}_2(n)\ \cdots\ \mathbf{S}_K\mathbf{c}_K(n)] \tag{5.3}$$

$$\mathbf{b}_I(n) = [b_2(n)\ b_3(n)\ \cdots\ b_K(n)]^T \tag{5.4}$$

$\mathbf{S}_k$ is an $N \times L$ Toeplitz matrix whose first column is $\mathbf{s}_k$ and first row is $[s_k(1)\ 0\ \cdots 0]$, and $\mathbf{n}$ is a complex AWGN vector of zero mean and covariance matrix $\sigma^2\mathbf{I}$ with $\sigma^2 = N_0/2$.

5.3 Linear Detection for Multipath Channels

To facilitate subsequent explanation, we first examine linear multiuser detection from a linear filtering point of view. A linear multiuser detector can be viewed as a linear time-dependent filter followed by a sampler which samples the output of the filter at $t = nT$. For multipath channels, there are two approaches to derive a linear detector as described below.

(a) A linear filter is employed to directly detect $b_1(n)$.

(b) Each path signal, $c_{1,l}(n)b_1(n)$, is treated as a random source and estimated by an individual filter. Following the filtering, a diversity combiner is used to obtain the decision statistics for $b_1(n)$.

Since the system model of interest can also be viewed as a CDMA system where each user signal, with signature signal $\mathbf{S}_k\mathbf{c}_k(n)$ instead of $\mathbf{s}_k$, is transmitted through a single-path channel, approach (a) leads to the same linear detectors as those for single-path channels [8]-[10]. The linear detectors thus obtained require information about the signature signals and the channel coefficients, hence they are difficult to implement at a mobile station. For this reason, only Approach (b) will be considered.

For systems of interest, the filters are finite-duration impulse response (FIR) filters of length N and are operated symbol-by-symbol. Consequently, we can drop time index n in the rest of the chapter wherever no confusion will be caused. Assuming that a linear filter with coefficient vector $\mathbf{w}_l$ is used for the lth path, then the sampled output of the filter is given by

$$\mathbf{w}_l^H\mathbf{y} = \mathbf{w}_l^H\mathbf{S}_1\mathbf{c}_1 b_1 + \mathbf{w}_l^H\mathbf{S}_I\mathbf{b}_I + \mathbf{w}_l^H\mathbf{n} \tag{5.5}$$

5.3.1 Decorrelating Detection

A decorrelating detector seeks to completely eliminate MAI regardless of the presence of background noise. Recalling that the lth decorrelating filter is designated to the detection of $c_{1,l}b_1$, from (5.5), this zero-forcing solution can be achieved if

$$\mathbf{S}^H\mathbf{w}_l = \mathbf{e}_l \tag{5.6}$$

where $\mathbf{S} = [\mathbf{S}_1\ \mathbf{S}_I]$ and $\mathbf{e}_l$ stands for the lth coordinate vector with an appropriate dimension. If $N > K+L-1$, (5.6) has an infinite number of solutions. Among them, the minimum norm solution provides the highest SNR and can be found as

$$\mathbf{w}_{d,l} = (\mathbf{S}^H)^\dagger\mathbf{e}_l = \mathbf{S}\mathbf{R}^{-1}\mathbf{e}_l \tag{5.7}$$

where $\dagger$ indicates the Moore-Penrose psuedo-inverse and $\mathbf{R} = \mathbf{S}^H\mathbf{S}$ is the cross-correlation matrix and is assumed to be positive definite as is the usual case. Denoting $\mathbf{S}_1^H\mathbf{S}_1$, $\mathbf{S}_1^H\mathbf{S}_I$, and $\mathbf{S}_I^H\mathbf{S}_I$ by $\mathbf{R}_1$, $\mathbf{R}_{12}$, and $\mathbf{R}_2$, respectively, then matrix $\mathbf{R}$ can be

expressed as

$$\mathbf{R} = \begin{bmatrix} \mathbf{R}_1 & \mathbf{R}_{12} \\ \mathbf{R}_{12}^H & \mathbf{R}_2 \end{bmatrix} \tag{5.8}$$

If $z_{d,l} = \mathbf{w}_l^H \mathbf{y}$ is the output of the lth filter and $\mathbf{z}_d = [z_{d,1} \cdots z_{d,L}]^T$ is the collection of the L outputs, it then follows from (5.5) and (5.7) that

$$\mathbf{z}_d = \mathbf{c}_1 b_1 + \mathbf{n}_d \tag{5.9}$$

In (5.9), $\mathbf{n}_d$ is a Gaussian noise vector with zero mean and covariance matrix

$$E[n_d n_d^H] = \sigma^2 \mathbf{F}_d = \sigma^2 (\mathbf{R}_1 - \mathbf{R}_{12}\mathbf{R}_2\mathbf{R}_{12}^H)^{-1} \tag{5.10}$$

This means that the zero-forcing solution is obtained at the cost of an increase in noise power.

Since the noise components in $\mathbf{n}_d$ are correlated, a noise whitening operator, which is the inverse of the Cholesky factor of $\mathbf{F}_d$, is first applied to $\mathbf{z}_d$. Following the noise whitening operator, MRC can then be performed and the output is given by

$$v_d = \mathbf{c}_1^H \mathbf{F}_d^{-1} \mathbf{z}_d \tag{5.11}$$

Notice that the channel coefficients of the desired user can be estimated from the outputs of the decorrelating filters, hence they need not be known a priory. The need for the channel coefficients of the interfering users can be further eliminated by using an alternative solution of (5.6), which is given by

$$\hat{\mathbf{w}}_{d,l} = (\hat{\mathbf{S}}^H)^\dagger \mathbf{e}_l = \hat{\mathbf{S}}\hat{\mathbf{R}}^{-1}\mathbf{e}_l \tag{5.12}$$

where

$$\hat{\mathbf{S}} = [\mathbf{S}_1\ \mathbf{S}_2\ \cdots\ \mathbf{S}_L] \tag{5.13}$$

$$\hat{\mathbf{R}} = \hat{\mathbf{S}}^T\hat{\mathbf{S}} \tag{5.14}$$

This solution leads to the multipath decorrelating detector (MDD) described in Chapter 3. However, both solutions given by (5.6) and (5.12) need information about the signature signals of all users and hence the corresponding decorrelating detectors are difficult to implement at a mobile receiver.

5.3.2 MMSE Detection

In contrast to the decorrelating detector, the MMSE detector seeks to maximize the signal-to-interference plus noise ratio (SINR). For the lth path, this is achieved by minimizing the MSE given by

$$E[|c_{1,l}b_1 - \mathbf{w}_l^H\mathbf{y}|^2] = E[|c_{1,l}|^2] - 2\mathrm{Re}\{E[c_{1,l}^* b_1 \mathbf{w}_l^H\mathbf{y}]\} + E[|\mathbf{w}_l^H\mathbf{y}|^2] \tag{5.15}$$

where E is the expectation operation. The minimizer of the above equation is found to be

$$\mathbf{w}_{m,l} = \mathbf{\Gamma}^{-1}\mathbf{d} \tag{5.16}$$

where $\mathbf{\Gamma} = E[\mathbf{y}\mathbf{y}^H]$ and $\mathbf{d} = E[c_{1,l}^* b_1 \mathbf{y}]$. This MMSE detector can be implemented in an adaptive way with only knowledge about the timing and signature signal of the desired user. However, this implementation has two immediate disadvantages: (a) The channel coefficients of the desired user has to be estimated to adapt the detector. The inaccuracy of the estimates, which is of particularly significant during the training period, will make the convergence of the detector difficult. As a result, a long training period is usually required. (b) The adaptive detector may require frequent retraining in a Rayleigh fading channel [52], which is obviously undesirable.

It can be shown that the maximum SINR can be achieved by minimizing the MSE in (5.15) subject to

$$\mathbf{w}_l^H\mathbf{S}_1\mathbf{e}_l = c \tag{5.17}$$

for any constant c. Recall that the channel coefficients are assumed to be mutually uncorrelated and thus the constraint in (5.17) implies that the second term in the right-hand side of (5.15) is constant. Hence, minimizing MOE subject to the constraint in (5.17) is equivalent to maximizing SINR. However, unlike the case of single-path channels, the MOE criterion is not readily applicable to multipath channels. In an adaptive implementation, the ensemble average, E, in (5.15) is replaced by time average. For a realistic fading channel where detector coefficients may be

virtually constant over a large number of symbol intervals, the time average of the second term at the right-hand side of (5.15) will depend on the projection of $\mathbf{w}_l$ in the desired signal subspace (the space spanned by the columns of $\mathbf{S}_1$). In this case, minimizing the MOE is no longer equivalent to minimizing the MSE.

5.4 A Blind Multipath Receiver

5.4.1 Constrained MMSE Detection

As demonstrated in the preceding section, in order to apply the minimum MOE criterion, the projection of the filter coefficient vector, $\mathbf{w}_l$, on the desired signal space has to be known and fixed in advance. Recalling that the decorrelating detector is NF resistant and its coefficient vector is independent of $\mathbf{c}_1$, it is, therefore, reasonable to fix the projection of $\mathbf{w}_l$ on the desired signal subspace as that of $\mathbf{w}_{d,l}$. If we introduce the projection operator as

$$\mathbf{P} = \mathbf{S}_1\mathbf{R}_1^{-1}\mathbf{S}_1^T \tag{5.18}$$

which projects a vector onto the space spanned by the columns of $\mathbf{S}_1^T$, then, from (5.7), we have

$$\mathbf{P}\mathbf{w}_{d,l} = \mathbf{S}_1\mathbf{R}_1^{-1}\mathbf{e}_l \tag{5.19}$$

Hence, instead of minimizing MSE over all possible $\mathbf{w}_l$, we impose a constraint that $\mathbf{w}_l$ be of the form

$$\mathbf{w}_l = \mathbf{S}_1\mathbf{R}_1^{-1}\mathbf{e}_l + \mathbf{x}_l \tag{5.20}$$

where $\mathbf{x}_l$ satisfies the equation

$$\mathbf{x}_l^H\mathbf{S}_1 = \mathbf{0} \tag{5.21}$$

and is a steering vector to be optimized. The minimizer of (5.15) subject to the constraint in (5.20) and (5.21) constitutes a new detector, which will be referred to

as the *constrained MMSE* (CMMSE) detector. Substituting (5.20) and (5.21) into (5.5), we have

$$E[c_{1,l}^* b_1 \mathbf{w}_l^H \mathbf{y}] = 2E[|c_{1,l}|^2] \tag{5.22}$$

Note that the above equation holds for both ensemble average and time average. Hence, minimizing (5.15) subject to (5.20) and (5.21) is equivalent to minimizing

$$E[|\mathbf{w}_l^H \mathbf{y}|^2] = E[|(\mathbf{S}_1 \mathbf{R}_1^{-1} \mathbf{e}_l + \mathbf{x}_l)^H \mathbf{y}|^2] \tag{5.23}$$

This shows that under the constraints in (5.20) and(5.21), minimizing MOE is equivalent to minimizing MSE. As a consequence, the CMMSE detector can be adapted without the need for training. By using the Lagrange multipliers, the minimizer $\bar{\mathbf{w}}_l$ of (5.23) can be found as

$$\bar{\mathbf{w}}_l = \mathbf{\Gamma}^{-1} \mathbf{S}_1 (\mathbf{S}_1^T \mathbf{\Gamma}^{-1} \mathbf{S}_1)^{-1} \mathbf{e}_l \tag{5.24}$$

It follows that the MOE of the adaptive filter is given by

$$M_l = E[|\bar{\mathbf{w}}_l^H \mathbf{r}|^2] = \mathbf{e}_l^T (\mathbf{S}_1^T \mathbf{\Gamma}^{-1} \mathbf{S}_1)^{-1} \mathbf{e}_l \tag{5.25}$$

Evidently, the CMMSE detector completely eliminates self-interference due to multiple paths and minimizes background noise plus MUI from interferers. Hence the proposed detector is a combined decorrelating and MMSE detector. As a matter of fact, the following proposition applies:

Proposition 5.1: Both the MMSE detector and the CMMSE detector converge to the decorrelating detector as the background noise vanishes ($\sigma^2 \to 0$).

Proof As the background noise vanishes, the only impairment is MUI. Consequently, minimizing SINR is equivalent to minimizing MUI. This implies that the MMSE detector and the decorrelating detector tend to be identical as $\sigma^2 \to 0$. Since the projections of $\bar{\mathbf{w}}_l$ and $\mathbf{w}_{d,l}$ on the signal subspace are equal and $\mathbf{x}_l(n)$ minimizes SINR, the CMMSE detector also converges to the decorrelating detector as the background noise vanishes. ■

As in the case of the decorrelating and MMSE multiuser detectors, Proposition 5.1 implies that the CMMSE detector is NF resistant. On comparing the CMMSE detector with the decorrelating and the MMSE detectors when background noise exists, we have the following proposition:

Proposition 5.2: The output SINR of the CMMSE detector is lower than or equal to the output SINR of the MMSE, but is higher than the output SNR of the decorrelating detector.

Proof The CMMSE detector is obtained as a suboptimal solution of (5.15) and hence its output SINR cannot be higher than that of the MMSE. At the output of the decorrelating detector, only the variance of AWGN needs to be considered since there is no MUI, which can be found from (5.10) and (5.8) as

$$V_l^d = \sigma^2 \mathbf{e}_l^T [\mathbf{R}_1 - \mathbf{R}_{12}\mathbf{R}_2^{-1}\mathbf{R}_{12}^H]^{-1}\mathbf{e}_l \tag{5.26}$$

Substituting (5.22) and (5.25) into (5.15), we obtain the MSE at the output of the CMMSE detector as

$$J_l^{\min} = \sigma^2 \mathbf{e}_l^T \{\mathbf{R}_1 - \mathbf{R}_{12}[\mathbf{R}_2 + \sigma^2\mathbf{I}]^{-1}\mathbf{R}_{12}^H\}^{-1}\mathbf{e}_l \tag{5.27}$$

Comparing (5.26) with (5.27), we can see that the MSE at the output of the BM detector is smaller than the average energy of the output noise of the decorrelating detector. This proves the proposition. ■

It is worthwhile to note that in parallel with the work reported here, another blind multiuser detector named *orthogonally anchored MMSE (OAMMSE) detector* was developed by Huang and Verdú [55]. In the OAMMSE detector, the L adaptive filters were used with each anchored on a coordinate of an orthonormal basis of the signal subspace, i.e., $\mathbf{x}_l(n) = \mathbf{d}_l$ with $\mathbf{d}_l$ as a coordinate. Because of the orthogonality among coordinates, minimizing MMSE is equivalent to minimizing MOE and the adaptive filters can be adapted blindly. However, the projection of the received signal

on each coordinate will contain the contributions from all paths. As a consequence, the outputs of the adaptive filters will no longer be uncorrelated thereby resulting in difficulties in diversity combining. For instance, selective combining, which is simple but quite effective whenever the channel coefficients can be constantly monitored, and maximum-ratio combining, which is the optimal combining scheme, cannot be employed in OAMMSE in a direct manner [30].

5.4.2 Effect of Fading

Since the ensemble average, E, must be approximated by the time average, the resulting coefficient vector will depend on the varying rate of $\{c_{k,l}(n)\}$ with respect to n. Stated in another way, depending on the coherence time of the channel relative to the symbol interval, the adaptive detector can perform differently. To examine the effect of channel fading on the performance of the detector, an alternative interpretation of the detector will be useful. The proposed detector was developed from a chip-rate approach. This approach is convenient for developing an adaptive detector that will directly work on the received signal. On the other hand, an interpretation of a detector in terms of a linear mapping applied to the outputs of matched filters provides us more insight to the performance of the detector. In this subsection, we will interpret the proposed detector from a bit-rate point of view and examine the effect of time varying rate of the channel on performance.

Note that, in practice, the coefficient vector of an adaptive detector is a random process due to adaptation. In what follows, we will refer the coefficient vector as the expectation of the coefficient vector. We consider two extreme cases:

- The channel fading is essentially static within a large number of symbol intervals such that the detector can perfectly track the channel variation and achieve the best performance for each set of instantaneous channel coefficients, and
- the channel fading is sufficiently fast such that the detector cannot track the channel variation but the long-term average behavior of the channel.

A practical situation always lies in between of the above two extreme cases.

For the first case, the coefficient vector of the CMMSE detector is given by (5.24) with

$$\mathbf{\Gamma} = \mathbf{S}_1\mathbf{c}_1\mathbf{c}_1^H\mathbf{S}_1 + \mathbf{S}_I\mathbf{S}_I^H + \sigma^2\mathbf{I} \tag{5.28}$$

Note that matrix $\mathbf{\Gamma}$ in this case is time-dependent even though it varies slowly. In order to interpret the detector from a bit-rate point of view, we need to represent the coefficient vector by cross-correlations among signature signals. In Appendix E, it is shown that (5.24) with $\mathbf{\Gamma}$ given by (5.28) can be expressed as

$$\bar{\mathbf{w}}_l = \mathbf{S}(\mathbf{R} + \sigma^2\mathbf{D}_1)^{-1}\mathbf{e}_l \tag{5.29}$$

where $\mathbf{D}_1$ is a $(L+K-1)\times(L+K-1)$ diagonal matrix whose first L diagonal entries are zeros and the remaining diagonal entries are ones. Similarly, (5.16) can be rewritten as

$$\mathbf{w}_{m,l} = \mathbf{S}(\mathbf{R} + \sigma^2\mathbf{I})^{-1}\mathbf{e}_l \tag{5.30}$$

Comparing (5.7), (5.29), and (5.30), we can see that the three coefficient vectors differ from each other only in the associated inverse matrices. If the information about the interferers is available, then the detection can be carried out through the bit-rate approach with two steps: First the matrix $\mathbf{S}$ is applied and then the corresponding inverse matrix is applied. By (5.4), each column of matrix $\mathbf{S}_I$ is a composite signature signal weighted by the amplitude associated with an interferer. Hence, the first step can be accomplished by a set of RAKE receivers with each dedicated to an interferer. The detector implemented through the bit-rate approach with the coefficient vector given by (5.29) will be referred to as the *Rake Constrained MMSE* (R-CMMSE) detector. The block diagram of the R-CMMSE detector is shown in Fig. 5.1.

For the second extreme case, since the channel is assumed to be wide-sense stationary, the correlation matrix of the received signal in (5.25) is a constant and is

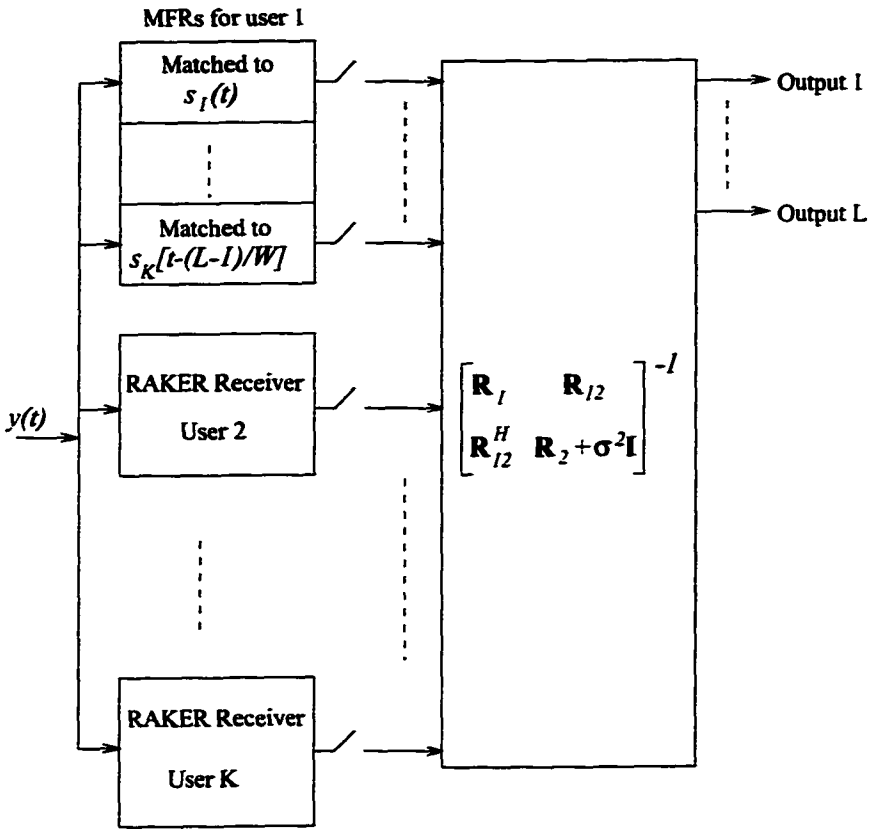

Figure 5.1. *A block diagram of the R-CMMSE detector.*

given by

$$\mathbf{\Gamma}(n) \equiv \mathbf{\Gamma} = \mathbf{S}_1\mathbf{W}_1\mathbf{S}_1^H + \hat{\mathbf{S}}_I\mathbf{W}_I\mathbf{S}_I + \sigma^2\mathbf{I} \tag{5.31}$$

where

$$\hat{\mathbf{S}}_I = [\mathbf{S}_2\ \mathbf{S}_3\ \cdots\ \mathbf{S}_K] \tag{5.32}$$

$$\mathbf{W}_I = \text{diag}\{\mathbf{W}_2\ \mathbf{W}_3\ \cdots\ \mathbf{W}_K\} \tag{5.33}$$

$$\mathbf{W}_k = \text{diag}\{E[|c_{k,1}(n)|^2\ E[|c_{k,2}(n)|^2]\ \cdots\ E[|c_{k,L}(n)|^2]\} \tag{5.34}$$

As for the proof given in Appendix E, it can be shown that (5.24) with $\mathbf{\Gamma}$ given by (5.31) becomes

$$\bar{\mathbf{w}}_l \equiv \bar{\mathbf{w}}_l(n) = \hat{\mathbf{S}}(\hat{\mathbf{R}} + \sigma^2\mathbf{D}_2)^{-1}\mathbf{e}_l \tag{5.35}$$

where $\hat{\mathbf{R}}$ is given by (5.14) and $\mathbf{D}_2$ is a $KL \times KL$ diagonal matrix whose first L diagonal entries are zeros and the remaining diagonal entries are ones. In this case, (5.16) becomes

$$\mathbf{w}_{m,l} = \hat{\mathbf{S}}(\hat{\mathbf{R}} + \sigma^2\mathbf{I})^{-1}\mathbf{e}_l \tag{5.36}$$

Comparing (5.12), (5.35), and (5.36), we can see again that the three coefficient vectors differ from each other only in the corresponding linear mappings applied to the matched-filter outputs. The detector implemented through the bit-rate approach with the coefficient vector given by (5.35) will be referred to as the *multipath constrained MMSE* (M-CMMSE) detector; its block diagram is illustrated in Fig. 5.2.

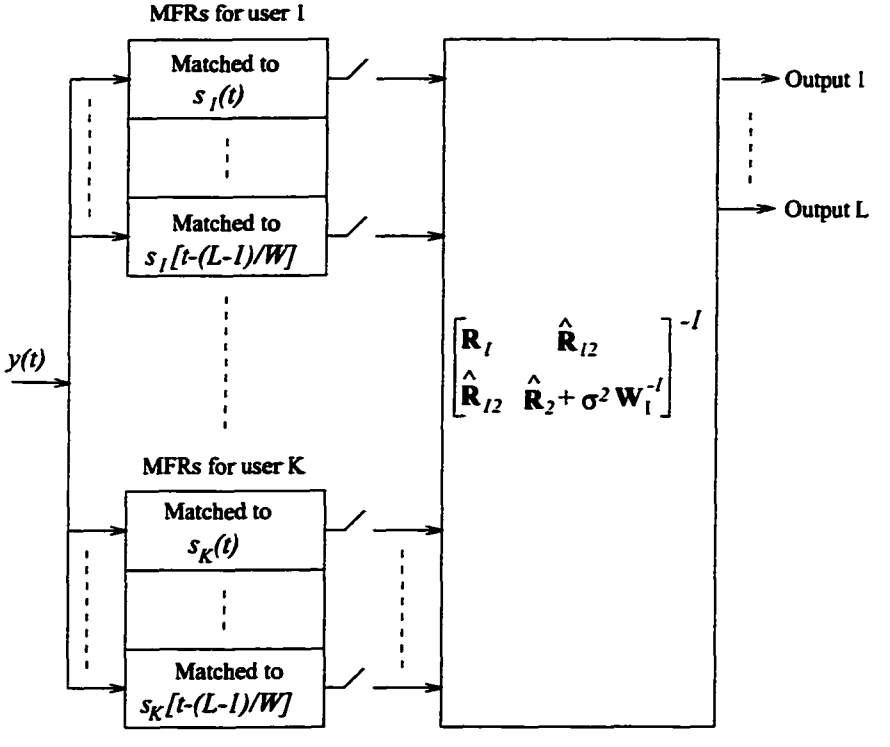

Figure 5.2. *A block diagram of the M-CMMSE detector.*

In the two extreme cases, an adaptively implemented CMMSE detector will converge to either the R-CMMSE detector or the M-CMMSE detector. On comparing the performance of the two detectors, the following proposition can be stated:

Proposition 5.3: The output SINR of the R-CMMSE detector is greater than or equal to that of the M-CMMSE.

Proof The proof is omitted since it is similar to that in the comparison of the RAKE decorrelating detector (RDD) and MDD in Appendix D. ■

Proposition 5.3 shows that the CMMSE detector yields better performance when the channel fading is slow. Neglecting the performance loss due to imperfect adaptation, the performance of the proposed detector will decrease from that of the R-CMMSE detector to that of the M-CMMSE detector as the channel varying rate increases.

An alternative way to examine the effect of fading on performance is to consider the steady-state excess MSE of an adaptation algorithm in a nonstationary environment [56]. From this point of view, the performance loss due to fading is regarded as caused by the imperfect adaptation. Hence, we will only consider the first extreme case before we discuss the blind adaptation. The performance index thus obtained will serve as an upper bound for the performance of the proposed detector in practice.

5.5 Diversity Combining and Channel Estimation

5.5.1 Maximal Ratio Combining

Having obtained the outputs of the L adaptive filters, the decision statistics can then be evaluated by using one of existing diversity combining schemes [30]. For the problem at hand, we will only consider maximal-ratio combining (MRC). In order for the application of MRC, channel coefficients must be accurately estimated. Since the MUI at the outputs of the CMMSE adaptive filters is largely suppressed, estimating the channel coefficients becomes much easier than directly estimating from the received signal. As will be shown, a simple channel estimator can provide fairly accurate estimation when channel fading is relatively slow. MRC is optimal only when the output

noise of the L adaptive filters are Gaussian. As a matter of fact, in this case MRC results in a maximum-likelihood receiver [30]. In order to show that MRC is nearly optimal when used in conjunction with the proposed detector, we first examine the output of the CMMSE detector.

The statistic properties of the MMSE output were intensively studied in [43]. It was found that when the user number is large, the output of the MMSE detector is fairly Gaussian. Since the CMMSE detector is partially a decorrelating detector and partially an MMSE detector, the amount of MUI at the CMMSE output can be shown to be less than that at the MMSE output while the Gaussian noise at the CMMSE output is more than that at the MMSE output. Consequently, the output of the CMMSE detector is also close to Gaussian when the number of users is large. In what follows, we take another approach to show that the CMMSE outputs are nearly Gaussian regardless of the number of users.

By (5.5) and (5.29), the output of the lth adaptive filter can be expressed as

$$z_l = c_{1,l} b_1 + n_l + I_l \tag{5.37}$$

where n_l is a Gaussian noise term and I_l is the residual MUI. Denoting the variance or average energy of the Gaussian noise as $V_{n,l}$ (i.e., $V_{n,l} = E[|n_{b,l}|^2]$) and the average energy of the residual MUI as $V_{I,l}$ (i.e., $V_{I,l} = E[|I_l|^2]$). Comparing $V_{n,l}$ and $V_{I,l}$, we have the following proposition:

Proposition 5.4: If θ_l be the angle of $\mathbf{S}_1\mathbf{e}_l$ relative to the interference subspace spanned by $\mathbf{S}_1\mathbf{e}_i$ for $i \neq l$ and columns of $\mathbf{S}_I$, then we have

$$\frac{V_{n,l}}{V_{I,l}} > \tan^2 \theta_l \tag{5.38}$$

Proof In Proposition 5.2, we have shown that

$$V_{n,l} + V_{I,l} = J_l^{\min} < V_l^d \tag{5.39}$$

From (5.7) and (5.26), V_l^d can be rewritten as

$$V_l^d = \frac{\sigma^2}{1 - s_l^T \tilde{\mathbf{S}}_I (\tilde{\mathbf{S}}_I^H \tilde{\mathbf{S}}_I)^{-1} \tilde{\mathbf{S}}_I^H s_l} \tag{5.40}$$

where

$$\tilde{\mathbf{S}}_I = [\mathbf{S}_1 \mathbf{e}_2 \ \cdots \ \mathbf{S}_1 \mathbf{e}_{l-1} \ \mathbf{S}_1 \mathbf{e}_{l+1} \ \cdots \ \mathbf{S}_1 \mathbf{e}_L \ \mathbf{S}_I] \tag{5.41}$$

Since $\tilde{\mathbf{S}}_I (\tilde{\mathbf{S}}_I^H \tilde{\mathbf{S}}_I)^{-1} \tilde{\mathbf{S}}_I^H$ is the operation that projects a vector onto the interference subspace spanned by coulmns of $\tilde{\mathbf{S}}_I$, (5.38) and (5.40) imply that

$$V_{n,l} + V_{I,l} < \frac{\sigma^2}{1 - \cos^2 \theta_l} = \frac{\sigma^2}{\sin^2 \theta_l} \tag{5.42}$$

It can be readily verified that

$$V_{n,l} \geq \sigma^2 \tag{5.43}$$

Combining (5.42) and (5.43), we have (5.38). ■

Proposition 5.4 shows that once $\theta_l > \pi/4$, Gaussian noise dominates the MUI at the output of CMMSE detector. This proposition also holds for the MMSE detector. Note that θ_l serves as an indicator of the cross-correlation properties among signature signals. If the cross-correlations among signature signals are small or, equivalently, θ_l is large, then $V_{n,l}/V_{I,l}$ will be large. In cases where Gold codes of length 127 are used, θ_l for any l is usually close to $\pi/2$ and the resulting lower bound for $V_{n,l}/V_{I,l}$ is greater than 5. Hence, even if the number of users is small and the central limit theorem does not apply to the output MUI, the output error is still approximately Gaussian.

If $\mathbf{z} = [z_1 \ z_2 \ \cdots \ z_L]^T$, then the foregoing analysis implies that $\mathbf{z}$ can be expressed as

$$\mathbf{z} = \mathbf{c}_1 b_1 + \hat{\mathbf{n}} \tag{5.44}$$

where $\hat{\mathbf{n}}$ is approximately a Gaussian noise term with zero mean and covariance matrix

$$\begin{aligned} E[\hat{\mathbf{n}}\hat{\mathbf{n}}^H] &= \sigma^2 \mathbf{F} \\ &= \sigma^2 [\mathbf{R}_1 - \mathbf{R}_{12} (\mathbf{R}_2 + \sigma^2 \mathbf{I})^{-1} \mathbf{R}_{12}^H]^{-1} \end{aligned} \tag{5.45}$$

Since $\hat{\mathbf{n}}$ is not white, a noise whitening operator needs to be applied to $\mathbf{z}$ before MRC. The noise whitening operator, $\mathbf{T}^{-H}$ is obtained by performing the Cholesky decomposition $\mathbf{F} = \mathbf{T}^H\mathbf{T}$. After the noise whitening operation, we have

$$\hat{\mathbf{z}} = \mathbf{T}^{-H}\mathbf{c}_1 b_1 + \mathbf{T}^{-H}\hat{\mathbf{n}} \tag{5.46}$$

MRC can then be performed and the output is given by

$$v = \mathbf{c}_1^H\mathbf{T}^{-1}\hat{\mathbf{z}} = \mathbf{c}_1^H\mathbf{F}^{-1}\mathbf{z} \tag{5.47}$$

From (5.47), knowledge of $\mathbf{c}_1$ and $\mathbf{F}$ is required before MRC can be performed. Since $\mathbf{F}$ can be easily estimated from previous desicion outputs or simply approximated as $\text{diag}[J_1^{\min} \cdots J_L^{\min}]$ when cross-correlations among signature signals are small, we only discuss the estimation of channel coefficients in the sequel.

5.5.2 Channel Estimation

The use of a channel estimator is motivated by the potential performance improvement of coherent combining as compared to noncoherent combining. Since the output of the adaptive filter can be well approximated as Gaussian, the techniques used for channel estimation in single user systems can also be used here. When the fading processes are Markov processes, the optimal channel estimator is a Kalman filter. Under the assumption that the fading process is wide-sense stationary, an MMSE estimator, which is asymptotically equivalent to the Kalman filter, can be used for each path independently. Let the autocorrelation function of the lth fading process be $R_c(\tau)$. The coefficients of a pth-order MMSE estimator can be derived as

$$\mathbf{a} = (\mathbf{R}_c + J_l^{\min}\mathbf{I})^{-1}\mathbf{v} \tag{5.48}$$

where $\mathbf{R}_c$ is a $p \times p$ matrix with the (i,j)th entry as

$$\mathbf{R}_c(i,j) = R_c(iT - jT) \tag{5.49}$$

and $\mathbf{v}$ is a vector of length p whose ith entry is $v_i = R_c(-iT)$. The channel coefficients at time n can then be estimated as

$$\hat{c}_{1,l}(n) = \sum_{i=1}^{p} \mathbf{a}_i \tilde{c}_{1,l}(n-p) \tag{5.50}$$

where $\tilde{c}_{1,l}(n) = \hat{b}_1(n) z_l(n)$. The MSE of this estimator is given by

$$P_l = R_c(0) - \mathbf{v}^H \mathbf{a} \tag{5.51}$$

For the WSSUS model, the autocorrelation function of the fading process is given by

$$R_c(\tau) = \frac{1}{2} E[|c_{1,l}|^2] J_0(2\pi f_d \tau) \tag{5.52}$$

where f_d is the Doppler shift and J_0 is the zeroth-order Bessel function of the first kind. The order of the estimator can be determined by examining the singular values of the corresponding $\mathbf{R}_c$. It was found that an order of 2 or 3 is usually sufficient.

After MRC, the information bit at time n is estimated as

$$\hat{b}_1(n) = \text{sign}[\hat{b}_1(n-1) v(n)] \tag{5.53}$$

Note that this decision scheme is different from the conventional noncoherent decision scheme for DPSK modulated signal. If we assume that there is only one resolvable path (i.e., $L = 1$) and the channel estimator is of order 1, then (5.53) becomes

$$\hat{b}_1(n) = \text{sign}[v^H(n-1) v(n)] \tag{5.54}$$

which is the conventional decision scheme for DPSK. For frequency-nonselective channels, this noncoherent DPSK modulation-demodulation results in about a 3-dB performance loss as compared with BPSK modulation-demodulation. The performance loss can be larger for frequency-selective channels because MRC is not applicable. Evidently, performance gain can be achieved by using the channel estimator with an order higher than 1. In fact, if we assume that the channel coefficients and $b_1(n-1)$ are estimated without error, then the decision scheme given by (5.53) yields a BER as if BPSK modulation and optimal combining were used.

In summary, the CMMSE detector can be implemented using the structure illustrated in Fig. 5.3.

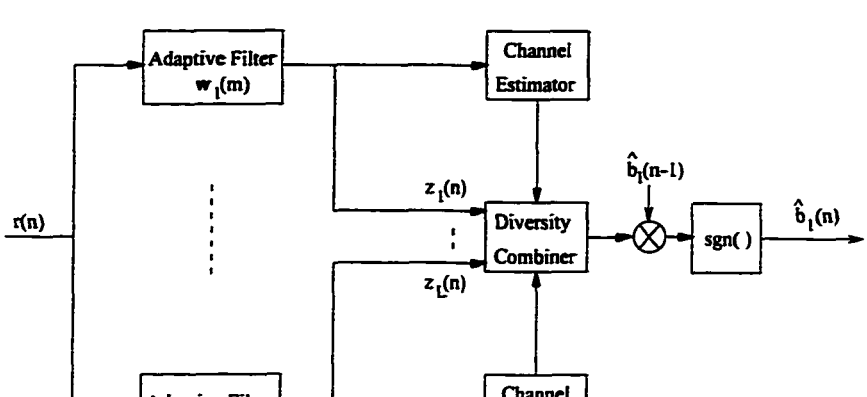

Figure 5.3. *Block diagram of the proposed blind multipath receiver.*

5.6 Error Probability and Asymptotic Multiuser Efficiency

In this section, we study the error probability and AME of the proposed CMMSE under the assumption that channel coefficients are estimated without error. In this case, the conditional error probability of the proposed detector can be found from (5.44), (5.47), and (5.53) as

$$P(\mathbf{c}_1) = Q\left(\sqrt{\frac{\mathbf{c}_1^H \mathbf{F}^{-1} \mathbf{c}_1}{\sigma^2}}\right) \tag{5.55}$$

The uncoditional probability can then be obtained by averaging the conditional error probability over the probability density function of $\mathbf{c}_1^H \mathbf{F}^{-1} \mathbf{c}_1$. Note that

$$E[\mathbf{c}_1^H \mathbf{F}^{-1} \mathbf{c}_1] = \mathrm{tr}[\mathbf{F}^{-1} \boldsymbol{\Sigma}_c] = \sum_{l=1}^{L} \lambda_l \tag{5.56}$$

where λ_l is a distinct eigenvalue of $\mathbf{F}^{-1}\boldsymbol{\Sigma}_c$ and $\boldsymbol{\Sigma}_c = E[\mathbf{c}_1 \mathbf{c}_1^H]$. We now define L statistically independent random processes, $\{\gamma_l,\ 1 \leq L\}$, that are chi-squared distributed with two degrees of freedom. That is

$$p(\gamma_l) = \frac{1}{\bar{\gamma}_l} e^{-\gamma_l / \bar{\gamma}_l} \tag{5.57}$$

where $\bar{\gamma}_l = \lambda_l/\sigma^2$. Hence the probability density function of $\mathbf{c}_1^H\mathbf{F}^{-1}\mathbf{c}_1/\sigma^2$ can be found as [11]

$$p(\mathbf{c}_1^H\mathbf{F}^{-1}\mathbf{c}_1/\sigma^2) = \sum_{l=1}^{L}\frac{\pi_l}{\bar{\gamma}_l}e^{-\gamma_l/\bar{\gamma}_l} \tag{5.58}$$

where

$$\pi_l = \prod_{i=1,i\neq l}^{L}\frac{\bar{\gamma}_l}{\bar{\gamma}_l - \bar{\gamma}_i} \tag{5.59}$$

Averaging the conditional error probability in (5.55) over the density function in (5.58), we obtain

$$P = \sum_{l=1}^{L}\frac{\pi_l}{2}\left[1 - \sqrt{\frac{\bar{\gamma}_l}{1+\bar{\gamma}_l}}\right] \tag{5.60}$$

In practice where $\bar{\gamma}_l \gg 1$, the error probability can be approximated as [11]

$$P \approx \binom{2L-1}{L}\prod_{l=1}^{L}\frac{1}{2\gamma_k} \tag{5.61}$$

Denoting λ_l^c as an distinct eigenvalue of $\mathbf{\Sigma}_c/\sigma^2$, an input geometric mean SNR can be defined as

$$\gamma_e \equiv \left(\prod_{l=1}^{L}\lambda_l^c\right)^{1/L} \tag{5.62}$$

Since

$$\prod_{l=1}^{L}\bar{\gamma}_l = \det(\mathbf{F}^{-1})\gamma_e^L \tag{5.63}$$

Eq. (5.61) can be expressed as

$$P \approx \prod_{l=1}^{L}\frac{f_L}{\det(\mathbf{F}^{-1})\gamma_e^L} \tag{5.64}$$

where

$$f_L = \binom{2L-1}{L}\frac{1}{2^{L+1}} \tag{5.65}$$

As another important indicator of performance, the AME characterizes performance loss of a detector caused by MUI in a vanishing noise case relative to the optimal detector in the absence of MUI. For frequency-selective channels, the AME of a detector is defined as [26]

$$\eta = \lim_{\sigma \to 0} \frac{\gamma_e}{\gamma_o} \tag{5.66}$$

where γ_o is the input geometric mean SNR required by the optimal detector in the absence of MUI to achieve the same performance as that of the detector of interest. For a single-user frequency-selective channel, the optimal receiver is the RAKE receiver and the resulting decision statistic can be found as

$$d_r = \mathbf{c}_1^H \mathbf{R}_1 \mathbf{c}_1 b_1 + n_r \tag{5.67}$$

where n_r is a Gaussian noise term with zero-mean and variance $\mathbf{c}_1^H \mathbf{R} \mathbf{c}_1$. Following the same procedure as above, the unconditional error probability of the RAKE receiver can be deduced as

$$P_r \approx \prod_{l=1}^{L} \frac{f_L}{\det(\mathbf{R}_1)\gamma_o^L} \tag{5.68}$$

where γ_o is also given by (5.62) with $\mathbf{c}_1$ replaced by the coefficient vector of the sigle-user multipath channel. Letting $P = P_r$, then (5.64), (5.66), and (5.68) lead to

$$\eta = \left[\frac{\det(\mathbf{R}_1 - \mathbf{R}_{12}\mathbf{R}_2^{-1}\mathbf{R}_{12}^H)}{\det(\mathbf{R}_1)} \right]^{1/L} \tag{5.69}$$

5.7 Blind Adaptation

In order to obtain an adaptation rule, we extend the stochastic gradient algorithm proposed in [23] to the problem at hand. For the lth path, the adaptation rule can be obtained from (5.5), (5.20), and (5.21) as

$$z_l(n) = \mathbf{w}_l^H(n-1)\mathbf{y}(n) \tag{5.70}$$

$$\mathbf{w}_l(n) = \mathbf{w}_l(n-1) - \mu \mathbf{P}^{\perp}\mathbf{y}(n) z_l^*(n) \tag{5.71}$$

where μ is the step-size parameter controlling the adaptation speed and stability of the adaptive filter, and $\mathbf{P}^{\perp} = \mathbf{I} - \mathbf{P}$ is the projection operator that projects a vector onto the null space of $\mathbf{S}_1$. Since $\mathbf{w}_l(n)$ is not equal to $\bar{\mathbf{w}}_l(n)$ in general, the MSE of the adaptive filter is no longer given by (5.24).

In what follows, we examine the behavior of this blind adaptive filter. To simplify the analysis, we assume that the channel is time invariant. Thus, $\mathbf{\Gamma}(n)$ and $\bar{\mathbf{w}}_l(n)$ are independent of n so that we can drop the time index n. Defining the coefficient error as

$$\boldsymbol{\varepsilon}_l(n) = \mathbf{w}_l(n) - \bar{\mathbf{w}}_l \tag{5.72}$$

the MSE of the blind adaptive filter can be expressed as

$$J_l(n) = J_l^{\min} + J_l^{ex}(n) \tag{5.73}$$

where

$$J_l^{ex}(n) = \boldsymbol{\varepsilon}_l(n)^H \mathbf{\Gamma} \boldsymbol{\varepsilon}_l(n) \tag{5.74}$$

Since $\mathbf{P}^{\perp}\boldsymbol{\varepsilon}_l(n) = \boldsymbol{\varepsilon}_l(n)$, (5.74) leads to

$$\begin{aligned} E[J_l^{ex}(n)] &= E[\boldsymbol{\varepsilon}_l(n)^H \mathbf{P}^{\perp} \mathbf{\Gamma} \mathbf{P}^{\perp} \varepsilon_l(n)] \\ &= \mathrm{tr}\{\mathbf{P}^{\perp} \mathbf{\Gamma} \mathbf{P}^{\perp} E[\boldsymbol{\varepsilon}_l^H(n) \varepsilon_l(n)]\} \end{aligned} \tag{5.75}$$

Now a coordinate rotation operator $\mathbf{Q}^H$ can be defined by means of the singular value decomposition of $\mathbf{P}^{\perp}\mathbf{\Gamma}\mathbf{P}^{\perp}$, i.e,

$$\mathbf{P}^{\perp} \mathbf{\Gamma} \mathbf{P}^{\perp} = \mathbf{Q} \mathbf{\Lambda} \mathbf{Q}^H \tag{5.76}$$

where $\mathbf{Q}$ is unitary and $\mathbf{\Lambda}$ is a diagonal matrix whose diagonal entries are the eigenvalues of $\mathbf{P}^{\perp}\mathbf{\Gamma}\mathbf{P}^{\perp}$. Defining the covariance matrix of the rotated coefficient error as

$$\mathbf{K}_l(n) = E[\mathbf{Q}^H \boldsymbol{\varepsilon}_l^H(n) \boldsymbol{\varepsilon}_l(n) \mathbf{Q}] \tag{5.77}$$

we obtain

$$E[J_l^{ex}(n)] = \mathrm{tr}[\mathbf{\Lambda} \mathbf{K}_l(n)] \tag{5.78}$$

In Appendix F, it is shown that

$$\mathbf{K}_l(n+1) \approx \mathbf{K}_l(n) + \mu^2 \mathbf{\Lambda} \mathrm{tr}[\mathbf{\Lambda}\mathbf{K}_l(n)] - \mu \mathbf{K}_l(n)\mathbf{\Lambda} - \mu \mathbf{\Lambda}\mathbf{K}_l(n) + \mu^2 M_l \mathbf{\Lambda} \tag{5.79}$$

If $d_i(n)$ is the ith diagonal entry of $\mathbf{K}_l(n)$ and

$$\mathbf{d}(n) = [d_1(n) \ \cdots \ d_N(n)]^T \tag{5.80}$$

then (5.79) implies that

$$\mathbf{d}(n+1) = \mathbf{B}\mathbf{d}(n) + \mu^2 M_l \boldsymbol{\lambda} \tag{5.81}$$

where

$$\mathbf{B} = \mathbf{I} + \mu^2 \boldsymbol{\lambda}\boldsymbol{\lambda}^T - 2\mu\mathbf{\Lambda} \tag{5.82}$$

$$\boldsymbol{\lambda} = \mathrm{diag}\ \mathbf{\Lambda} \tag{5.83}$$

Since the difference equation (5.81) is exactly the same as that for the conventional least-mean-square (LMS) algorithm, it follows from [54] that the adaptive filter described in (5.71) and (5.71) is convergent in the mean square if and only if

$$0 < \mu < \frac{2}{\mathrm{tr}(\mathbf{\Lambda})} \tag{5.84}$$

Notice that $\mathrm{tr}(\mathbf{\Lambda})$ is equal to $\mathrm{tr}(\mathbf{P}^{\perp}\mathbf{\Gamma}\mathbf{P}^{\perp})$, which is the total energy of the input signal in the null space of $\mathbf{S}_1^T$. The steady-state excess MSE can be derived as

$$J_l^{ex}(\infty) = \frac{\mu M_l}{2 - \mu \mathrm{tr}(\mathbf{\Lambda})} \tag{5.85}$$

where M_l is given by (5.25).

Let us now compare this blind adaptation algorithm with the conventional decision-directed LMS algorithm for the adaptation of the MMSE detector. The steady-state MSE of the LMS algorithm is given by [54]

$$\xi_l = \xi_l^{\min} + \xi_l^{ex} \tag{5.86}$$

where ξ_l^{ex} is the steady-state excess MSE of the LMS algorithm given by

$$\xi_l^{ex} = \frac{\mu \xi_l^{\min}}{2 - \mu \mathrm{tr}(\mathbf{\Gamma})} \tag{5.87}$$

When the user signature signals are nearly orthogonal, as is often encountered in practice, the minimum output MSE of the MMSE detector, $\xi_l^{\min}$, can be accurately approximated by $J_l^{\min}$. Since M_l is usually much larger than $J_l^{\min}$, by (5.85) and (5.87), the blind adaptation algorithm is noisier as compared with the LMS algorithm. However, if μ is small, the values of ξ_l and J_l will be dominated by the first terms in the right-hand sides of (5.73) and (5.86), respectively, and their difference will be small. Notice that the results stated in (5.86) and (5.87) for the LMS algorithm were obtained under the assumption of perfect decision feedback. In practice, the performance of the LMS algorithm can be even worse than that of the blind adaptation algorithm due to the possibility of incorrect decision feedback. In summary, if the fading is slow such that a small μ is preferred, the blind adaptation algorithm can be used throughout the data transmission; on the other hand, if a large μ has to be used, the adaptive filter should switch from blind mode to decision-directed mode once the filter is close to its steady state.

5.8 Numerical Examples

Extensive simulations have been conducted to study the behavior of the blind adaptation algorithm and evaluate the performance of the proposed detector. In all simulations, there were 9 interfering users, each had an energy 10 dB higher than the energy of the desired user; the signature signals with a rectangular chip waveform were selected from a family of 127-chip Gold code, and the Rayleigh fading channel was simulated by using the method proposed in [42].

We first compare the blind adaptation algorithm with the conventional LMS algorithm for time-invariant channels. Illustrated in Fig. 5.4 are learning curves for these two algorithms. The learning curves for the LMS algorithm were obtained under the

assumption of perfect decision feedback. As is expected, the MSE of the LMS algorithm is always smaller than that of the blind adaptation algorithm; the difference in their MSE's is quite small when μ is small (i.e., $\mu/tr(\mathbf{\Gamma}) < 0.1$), and becomes significant when a large μ is used.

We now examine the performance of the proposed detector. The bit-error rate versus SNR of the proposed detector under two fading environments is shown in Fig. 5.5. In the first fading environment, all users were assumed to be moving at a speed of 96 km/hour which corresponds to a Doppler shift of $f_d = 80$ Hz; in the second fading environments, a speed of 20 km/hour ($f_d = 16$ Hz) was assumed. In order to clarify the effect of imperfect channel estimation, the performance of the proposed detector under the assumption of perfect channel estimation is also presented. As expected, the BER of the proposed detector is reduced as the user speed is reduced. The effect of imperfect channel estimation is also clear from the figure: Since the normalized variance of the channel estimation error will converge to the variance of the excitation noise of the Markov channel model as SNR increases, an error floor is imposed on the performance of the detector. For comparison, the performance of the RAKE receiver is also illustrated in the figure. As can be seen from the figure, even though the channel coefficients were assumed to be known to the RAKE receiver, its performance is still poor and does not show significant improvement as the SNR increases since the performance of the RAKE receiver is MUI limited.

5.9 Conclusions

The linear multiuser detector was examined from a linear filtering point of view. It has been shown that for frequency-selective fading channels, both the decorrelating detector and the MMSE detector require information that may not be available at the mobile receiver. Motivated by this observation, we have developed a new linear multiuser detector. The proposed detector is a constrained MMSE detector that allows a blind adaptation. Consequently, only information about the signature and timing of the desired user is required. It has been shown that the proposed detector has comparable performance as that of the decorrelating and MMSE detectors. As a matter of fact, the proposed detector, the decorrelating detector, and the MMSE detector tend to be identical as the noise vanishes.

The proposed detector was also interpreted from a bit-rate approach point of view. Based on this interpretation, the effect of fading on performance has been examined for two extreme cases. The output error of the proposed detector has been shown to be nearly Gaussian regardless of the number of users. This observation motivated us to develop a channel estimator. The estimates of channel coefficients enable the use of an MFR thereby resulting a coherent diversity combining and decision. A study on the error probability and the AME of the proposed detector have been conducted.

For the adaptation of the proposed detector, a stochastic gradient algorithm has been proposed. A study of the output MSE and the stability condition of the blind adaptation rule has been conducted to clarify several implementation issues. Simulations have been carried out to examine the performance of the proposed detector and the learning characteristics of the proposed blind adaptation algorithm as compared to the characteristics of the conventional LMS algorithm for trained MMSE multiuser detector.

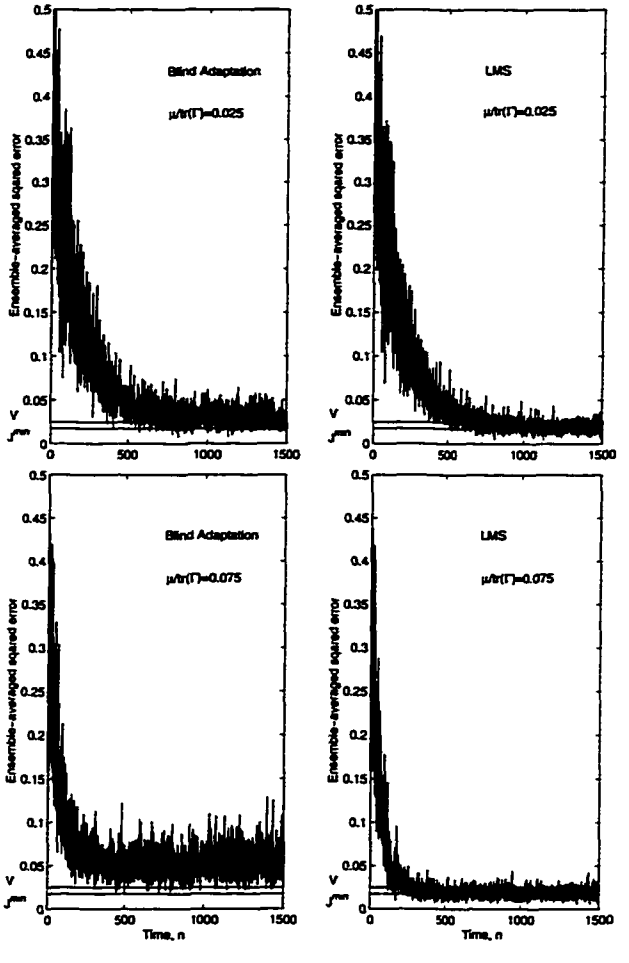

Figure 5.4. *Learning curves for the blind adaptation algorithm and the LMS algorithm for multiuser detection in static frequency-selective fading channels, where* $J^{min} = \sum_{l=1}^{L} J_l^{\min}$ *and* $V = \sum_{l=1}^{L} V_l^d$.

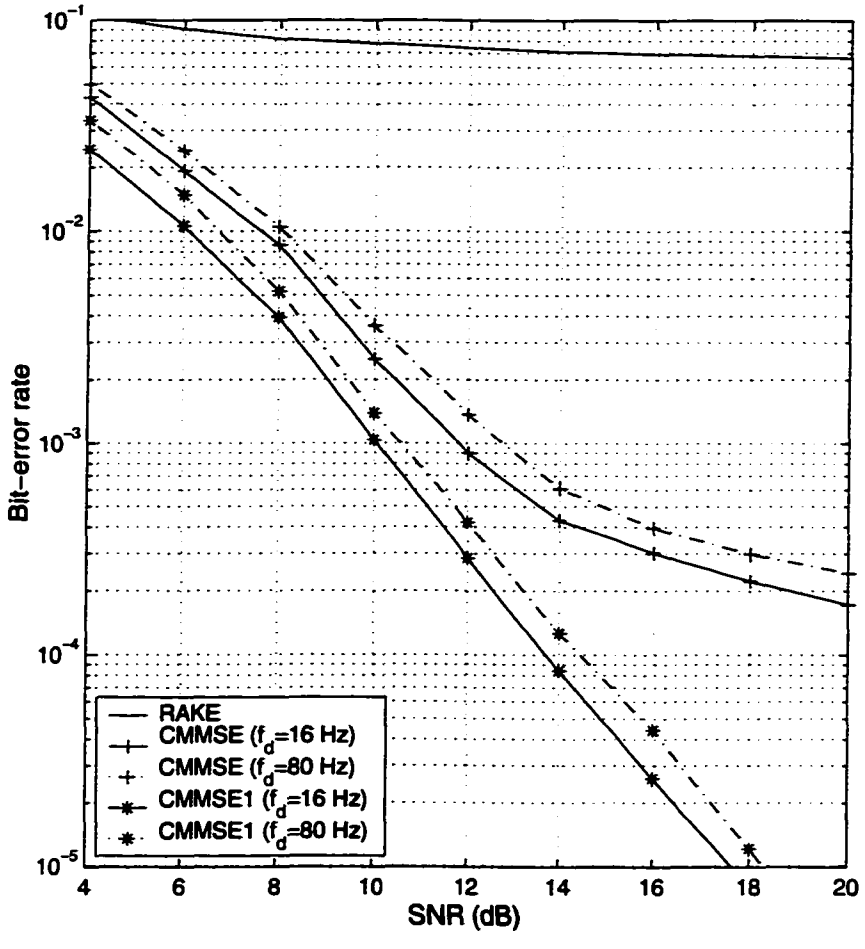

Figure 5.5. *BER of user* 1 *versus SNR in frequency-selective Rayleigh fading channels, where CMMSE1 stands for the proposed detector with perfect channel estimation, and the SNR is defined as* $\mathrm{tr}(E[\mathbf{c}_1(n)\mathbf{c}_1^H(n)])/N_0$ *($f_D = 80$ Hz).*

Chapter 6

Conclusions and Future Work

6.1 Conclusions

We have developed three multiuser detectors for different application scenarios. The overlapping window decorrelating (OWD) and constrained minimum-BER (CMBER) detectors are designed to jointly detect all user signals in a system and, therefore, are suitable for base stations. On the other hand, the CMMSE detector is aimed at mobile stations where only one user is of interest.

6.1.1 OWD Detector

In Chapter 3, our attention was focused on mobile stations where information about signature signals and the timing of all active users is available. We first compared two design approaches for multiuser detection at mobile stations where user signals usually arrive asynchronously. One approach is to employ a bank of matched filter-receivers (MFRs) followed by a linear mapping performed at symbol rate. The other approach is to apply a linear mapping directly to the received signal at chip rate. Although both approaches lead to exact decorrelating solutions, it has been shown that the ideal infinite-duration impulse response (IIR) decorrelating detector based on the bit-rate approach always outperforms an exact finite-duration impulse response (FIR) decorrelating detector obtained using the chip-rate approach. It has also been shown that the bit-rate approach can lead to a simpler implementation although

the algorithms derived from both approaches involve the same problems of window-length determination and inversion of a matrix of large size. Next, we have proposed the OWD detector based on the bit-rate approach, where the multiuser interference (MUI) at the left edge of a working window is eliminated by decision feedback and the MUI at the right edge is treated as Gaussian noise. By exploiting the block tri-diagonal structure of the cross-correlation matrix of the signature signals, algorithms for updating and user detection with much reduced computational complexity have been developed.

In order to control the right-edge MUI, a study on the ideal decorrelating detector was presented. The results obtained include a necessary and sufficient condition for the stability of the detector and the decay rate of its impulse response (IR), which were both given in terms of the Cholesky factors of the system cross-correlation matrix. These results constitute an important contribution of the dissertation, not only because they facilitate window-length determination for the OWD detector but also because they shed light on linear multiuser detection for asynchronous transmission as a whole. For instance, the decay rate of the decorrelating IR can be used to determine the window length of an FIR decorrelating detector to trade off complexity with performance. Due to the similarity of the MMSE and decorrelating linear mappings, the decay rate obtained can also be used to guide the implementation of the MMSE detector. Based on these results, an algorithm for window-length determination for an OWD detector with a given NF situation has been developed. The proposed OWD detector was further extended to Rayleigh fading channels and two methods for combining multiuser detection and diversity reception were examined.

6.1.2 CMBER Detector

In Chapter 4, we have developed the CMBER detector which is linear and minimizes the BER function subject to a set of convex constraints. It has been shown that (a) if the set defined by the imposed constraints is not empty, the BER function has a

unique minimizer; and (b) once the decorrelating detector exists, the set defined by the constraints is not empty and the resulting detector outperforms the decorrelating detector. Because of the constraints added, the proposed detector cannot be shown to be always optimal among linear detectors. However, analysis and computer simulations have demonstrated that the proposed detector achieves the optimal linear solution for most realistic cases. Taking advantage of the uniqueness of the solution, we developed a Newton barrier method to solve the constrained optimization problem. For the optimization problem at hand, the proposed method is much more efficient than the popular sequential quadratic programming method. Numerical examples have demonstrated that the performance gain of the proposed detector over those of the decorrelating and minimum mean-squared error (MMSE) detectors can be quite significant.

Even though the CMBER detector needs information about timing, amplitudes, and signature signals of all users, the idea and results described in Chapter 4 are useful for an adaptive implementation that requires no knowledge of the interferers.

6.1.3 CMMSE Detector

In Chapter 5, we focused our attention on the detector design of multiuser detectors for mobile stations. Since the information about interferers is unknown at mobile stations, an adaptive implementation is preferable. For frequency-selective multipath channels, we proposed to employ a bank of filters with each filter resolving one path signal. We also proposed to decompose the coefficient vector of each filter into two orthogonal components: One is in the signal space and orthogonal to all other delayed versions of the signature signal of the desired user, and the other is orthogonal to the signal space and free to be adapted based on the mean-squared error (MSE) criterion. The outputs of the filters have been shown to be nearly Gaussian. This, along with a proposed channel estimator, allows us to directly employ a maximal-ratio combiner (MRC) to obtain the decision statistics. It has also been shown that because of the

decomposition of the filter coefficient vector, minimizing the MSE is equivalent to minimizing the output energy. Consequently, we were able to develop a stochastic algorithm for blind adaptation of the filters. The convergence as well as the output MSE of the algorithm were studied. The results obtained were compared with the characteristics of the well-known least-mean square (LMS) algorithm.

The effects of the fading rate on the performance of the proposed CMMSE detector was examined by interpreting the detector from a bit-rate approach point of view. This interpretation allows one to directly compare the proposed CMMSE detector with the RDD and MDD described in Chapter 3. It is evident from this interpretation that the proposed detector outperforms the RDD detector in a sufficiently slowly varying channel and the MDD in a fast varying channel. The unconditional error probability as well as the AME of the proposed detector were also given, showing that the proposed detector is NF resistant.

6.1.4 Comparisons of Proposed Detectors

All the three proposed detectors are worst-case optimal linear detectors that significantly outperform the conventional MFR or RAKE. Their computational complexity is linear with the number of users. Both the OWD and CMBER detectors need information about all the active users in a system. On the other hand, the CMMSE detector does not need information about interferers. Hence, the OWD and CMBER detectors are targeted for base stations while the CMMSE detector is aimed at mobile stations.

One might ask whether one should chose the OWD detector or the CMBER detector for a base station. The answer depends on the complexity and performance tradeoff of the two detectors. If the coefficients of the detectors are known, the computations required by user detection in the OWD and CMBER detectors are comparable. However, for a system with a large number of users, the computational complexity of obtaining the CMBER detector coefficients is much higher. Furthermore, the per-

formance gain of the CMBER detector with respect to that of the OWD detector becomes insignificant as the number of users increases. These factors clearly make the OWD detector the preferred choice for a system with a large number of users. On the other hand, it is preferable to use the CMBER detector for a system with a small number of users. For example, for the TDD mode of the wideband-CDMA proposal [58] where at most 16 users exist in one time-slot, the CMBER detector becomes a sensible choice.

6.2 Future Work

Two future research topics can be immediately identified as a continuation of the work in this thesis:

- One can attempt to improve the CMBER detector. In the proposed CMBER criterion, the number of constraints grows exponentially with the number of active users. For a system with a large number of users, the amount of computation required in checking all the constraints is large. A promising approach to solve this problem is to reduce the number of constraints by utilizing the properties of the BER cost function. Based on our preliminary studies, it was found that, given a good initial point, most of the constraints remain inactive. Therefore, it is reasonable to expect that the same solution can be reached by solving an equivalent minimization problem with a much reduced number of constraints. As mentioned before, it is also possible to derive an adaptive multiuser detector based on the results obtained for CMBER detector. Even though identifying the convergence region defined by the constraints in (4.8) needs information about interferers, yet it is possible to find a convergence region that is approximately the same as or is included in the proposed region without knowledge of interferers.
- With the advent of multimedia communications, future CDMA systems will be

multirate with multiple spreading factors, e.g., the wideband-CDMA system [58]. In such a system, the proposed OWD and CMBER detectors work equally well as in a single-rate system, except that each high-rate user must be treated as several virtual users as described in Sec. 3.3.1. However, the extension of existing adaptive detectors into multirate systems is not trivial. This is because the period of the second-order statistics of the signal is no longer the symbol rate. Instead, it is the lowest symbol rate allowed in the system. If the symbol rate of the desired user is M times the lowest symbol rate in the system, then an immediate solution is to use M adaptive filters for AWGN channels with each adapted for every M symbols in a round-robin fashion. Several questions may arise in such a scenario: (a) Is there a way to jointly adapt these filters? (b) Is there an efficient way to combine adaptation with coding? (c) Is there a more computationally efficient approach? These questions need to be addressed in the development of adaptive multiuser detectors for multirate CDMA systems.

Bibliography

[1] W. C. Y. Lee, "Overview of cellular CDMA," *IEEE Trans. Vehic. Tech.*, vol. 40, May 1991, pp. 291-302.

[2] K. S. Gilhousen et al., "On the capacity of a cellular CDMA system," *IEEE Trans. Vehic. Tech.*, vol. 40, May 1991, pp. 303-312.

[3] R. L. Pikholtz, L. B. Milstein, and D. L. Schilling, "Spread spectrum for mobile communications," *IEEE Trans. Vehic. Tech.*, vol. 40, May 1991, pp. 303-312.

[4] A. J. Viterbi, "The Orthogonal-random waveform dichotomy for digital mobile personal communications," *IEEE Pers. Commun.*, 1st qtr., 1994, pp. 18-24.

[5] S. Verdú, "Minimum probability of error for asynchronous Gaussian multiple-access channels," *IEEE Trans. Inform. Theory*, vol. 32, pp. 85-96, Jan. 1986.

[6] S. Verdú, "Demodulation in the presence of multiuser Interference: progress and misconceptions," *Intelligence Methods in Signal Processing and Communications*, D. Docampo, A. Figueriras-Vidal and F. Perez-Gonzalez, Eds., pp. 15-44, Birkhauser, Boston, 1997.

[7] S. Moshavi, "Multi-user detection for DS-CDMA communications," *IEEE Commun. Mag.*, vol. 34, pp. 124-136, Oct. 1996.

[8] R. Lupas and S. Verdú, "Linear multiuser detectors for synchronous code-division multiple-access channels," *IEEE Trans. Inform. Theory*, vol. 35, pp. 123-136, Jan. 1989.

[9] R. Lupas and S. Verdú, "Near-far resistance of multiuser detectors in asynchronous channels," *IEEE Trans. Commun.*, vol. 38, pp. 725-736, April 1990.

[10] Z. Xie, R. T. Short, and C. K. Rushforth, "A family of suboptimum muti-user detectors," *IEEE JSAC*, vol. 8, pp. 683-90, May 1990.

[11] J. G. Proakis, *Digital Communications*, 3rd ed., New York: McGraw-Hill, 1995.

[12] A. J. Viterbi, "Very low rate convolutional codes for maximum theoretical performance of spread-spectrum multiple-access channels, " *IEEE JSAC*, vol. 8, no. 4, pp. 641-649, May 1990.

[13] R. Kohno et al., "Combination of an adaptive array antenna and a canceller of interference for direct-sequence multiple-access system," *IEEE JSAC*, vol. 8, no. 4, pp. 675-682, May 1990.

[14] M. Varanasi and B. Aazhang, "Near-optimum detectors in synchronous code-division multiple-access systems," *IEEE Trans. Commun.*, vol. 39, pp. 725-736, May 1991.

[15] M. Varanasi and B. Aazhang, "Multi-stage detection in asychronous code-division multiple-access communications," *IEEE Trans. Commun.*, vol. 38, pp. 509-519, Apr. 1990.

[16] A. Duel-Hallen, "Decorrelating decision-feedback multi-user receiver for synchronous for code-division multiple access channel," *IEEE Trans. Commun.*, vol. 41, pp. 285-290, Feb. 1993.

[17] A. Duel-Hallen, "A family of multi-user decision-feedback detectors for asynchronous code-division multiple access channels," *IEEE Trans. Commun.*, vol. 43, pp. 421-434, Feb./Mar./Apr., 1995.

[18] A. Klein, G. K. Kaleh, and P. W. Baier, "Zero-forcing and minimum mean-squared-error equalization for multi-user detection in code-division multiple-access channels," *IEEE Trans. Vehic. Tech.*, vol. 45, pp. 276-287, May. 1996.

[19] U. Mitra and H. Poor, "Adaptive receiver algorithms for near-far resistant CDMA," *IEEE Tran. Commun.*, vol. 43, pp. 1713-1724, Feb. 1995.

[20] U. Mitra and H. Poor, "Analysis of an adaptive decorrelating detector for synchronous CDMA channels," *IEEE Tran. Commun.*, vol. 44, pp. 257-268, Feb. 1996.

[21] U. Madhow and M. Honig, "MMSE interference suppression for direct-sequence spread spectrum CDMA, " *IEEE Trans, Commun.*, vol. 42, pp. 3178-3188, Dec. 1994.

[22] S. L. Miller, "An adaptive direct-sequence code-division multiple-access receiver for multiuser interference rejection," *IEEE Trans, Commun.*, vol. 43, pp. 1746-1754, Feb./March/April. 1995.

[23] M. Honig, U. Madhow, and S. Verdú, "Blind adaptive multiuser detection," *IEEE Trans. Inform. Theory.*, vol. 41, pp. 944-960, July, 1995.

[24] X. Wang and H. V. Poor, "Blind equalization and multiuser detection for CDMA communication in dispersive channels," *IEEE Trans, Commun.*, vol. 46, pp. 91-103, Jan. 1998.

[25] A. Klein and P. W. Baier, "Linear unbiased data estimation in mobile radio systems applying CDMA," *IEEE JSAC*, vol. 11, pp. 1058-1066, Sept. 1993.

[26] Z. Zvonar, "Combined multiuser detection and diversity reception for wireless CDMA systems," *IEEE Trans. Veh. Technol.*, vol. 45, pp. 205-211, 1996.

[27] H. Wu and A. Duel-Hallen, "A comparative analysis of linear multiuser detectors for fading multipath channels," *Proc. Globcom'94.*, pp. 11-15, 1994.

[28] P. D. Alexander et al., "Iterative multiuser interference reduction: Turbo CDMA," *IEEE Trans. Commun.*, vol. 47. pp. 1008-1014, July 1999.

[29] X. Wang and H. V. Poor, "Iterative (Turbo) soft interference cancellation and decoding for coded CDMA," *IEEE Trans. Commun.*, vol. 47. pp. 1046-1061, July 1999.

[30] G. L. Stüber, *Principle of Mobile Communications*, Boston: Kluwer Academic Publishers, 1996.

[31] A. N. Barbosa and S. L. Miller, "Adaptive Detection of DS/CDMA signals in Fading Channels," *IEEE Trans. Commun.*, vol. 46. pp. 115-124, Jan. 1998.

[32] T. S. Rappaport, *Wireless Communications: Principles and Practice*, Prentice Hall PTR, 1996.

[33] Y. Steinberg and H. Poor, "Sequential amplitude estimation in multiuser communications," *IEEE Trans. Information Theory*, vol. 38, pp. 11-20, Jan. 1994.

[34] S. Verdú, "Computational complexity of optimum multiuser detection," *Algorithmica*, no. 4, pp. 303-312, 1989.

[35] R. A. Horn and C. R. Johanson, *Matrix Analysis*, Cambridge: Cambridge University Press, 1990.

[36] F. Zheng and S. K. Barton, "Near far resistant detection of CDMA signals via isolation bit insertion," *IEEE Trans. Commun.*, vol. 43, pp. 1313-1317, Feb./Mar./Apr. 1995.

[37] S. S. H. Wijayasuria, G. H. Norton, and J. P. McGeehan, "A sliding window decorrelating receiver for multiuser DS-CDMA mobile radio networks", *IEEE Trans. Veh. Technol.*, vol. 45, pp. 503-521, Aug. 1996.

[38] M. J. Juntti and B. Aazhang, "Finite memory-length linear multiuser detection for asynchronous CDMA communications," *IEEE Trans. Commun.*, vol. 45, pp. 611-622, May. 1997.

[39] M. K. Tsatsanis and G. B. Giannakis, "Optimal decorrelating receivers for DS-CDMA systems: a signal processing framework," *IEEE Trans. Signal Processing*, vol. 44, pp. 3044-3055, Dec. 1996.

[40] L. Wei and K. Rasmussen, "A near ideal noise whitening filter for an asynchronous time-varying CDMA system," *IEEE Trans. Commun.*, vol. 43, pp. 1313-1317, Feb./Mar./Apr. 1995.

[41] R. E. Crochiere and L R. Rabiner, *Multirate Digital Signal Processing*, Englewood Cliffs, NJ: Prentice-Hall, 1983.

[42] *JTC(AIR)/94.09.23-065R6.*

[43] H. V. Poor and S. Verdú, "Probability of error in MMSE multiuser detection," *IEEE Trans. Info.*, vol. 43, pp. 858-871, May 1997.

[44] C.-C. Yeh and J. R. Barry, "Approximate minimum-bit error rate equalization for binary signaling," *Proc. IEEE Int. Conf. Commun.*, pp. 1095-1099, 1997.

[45] N. B. Mandayam and B. Aazhang, "Gradient Estimation for sensitivity analysis and adaptive multiuser interference rejection in code-division multiple-access systems," *IEEE Tran. Commun.*, vol. 45, pp. 848-858, July 1997.

[46] I. N. Psaromiligkos, S. N. Batalama, and D. A. Pados, "On adaptive minimum probability of error linear filter receiver for DS-CDMA channels," *IEEE Tran. Commun.*, vol. 47, pp. 1092-1102, July 1999.

[47] R. Fletcher, *Practical Methods of Optimization*, 2nd ed., Wiley, New York, 1987.

[48] J. A. Nelder and R. Mead, "A simplex method for function minimization," *Computer J.*, vol. 7, pp. 308-313, 1965.

[49] V. Torczon, "On the convergence of pattern search algorithm," *SIAM J. Optim.*, vol. 7, pp. 1-25, 1997.

[50] M. H. Wright, "Interior methods for constrained optimization," *Acta Numerica*, vol. 1, pp. 341-407, Cambridge Univ. Press, 1992.

[51] D. A. Pados and S. N. Batlama, "Low-Complexity Blind Detection of DS-CDMA signals: auxiliary-vector receiver," *Int.*, vol. 45, pp. 1586-1594, Dec. 1997.

[52] A. N. Barbosa and S. Miller, "Adaptive Detection of DS/CDMA signals in Fading Channels ," *IEEE. Trans. Commun.*, vol. 46. pp. 115-124, Jan. 1998.

[53] C. Kchao and G. Stúber, "Performance analysis of a single cell direct sequence mobile radio system," *IEEE Trans. Commun.*, vol. 41, pp. 1507-1516, Oct. 1993.

[54] S. Haykin, *Adaptive Filter Theory,* Prentice-Hall, 1986.

[55] H. C. Huang and S. Verdú, "Linear differentially coherent multiuser detection for multipath channels," *Intl. J. Wireless Personal Communications*, vol. 6, pp. 113-136, Jan. 1998.

[56] Widrow, B., et al., "Stationary and nonstationary learning characteristics of the LMS adaptive filters," *Proc. IEEE*, vol. 64, pp. 1152-1162, 1976.

[57] V. K. Garg, K. Smolik, and J. E. Wilkes, *Application of Code-Division Multiple Access (CDMA) in Wireless/Personal Communications,* Upper Saddle River, NJ: Prentice Hall,1996.

[58] *Technical Specification Group: Radio Access Network*, 3rd Generation Partnership Project, ver. 3.1.0, Dec. 1999.

[59] A. J. Paulraj and C. B. Papadias, "Space-time processing for wireless communications," *IEEE Signal Processing Mag.*, vol. 14, pp. 49-83, Nov. 1997.

[60] T. Kailath, *Linear Systems*, Englewood Cliffs, NJ: Prentice-Hall, 1980.

Appendix A

Proof of Proposition 3.1

Assume that there exists an exact zero-forcing solution for a window length n, then the associated cross-correlation matrix $\mathbf{R}_n$ is positive definite. Denote the cross-correlation matrix associated with a window length $n+1$ as $\mathbf{R}_{n+1}$, then it follows from (3.1)that

$$\mathbf{R}_{n+1} = \begin{bmatrix} \mathbf{R}_n & \mathbf{0} \\ \mathbf{0} & \mathbf{0} \end{bmatrix} + \begin{bmatrix} \mathbf{0} & \mathbf{0} & \mathbf{0} \\ \mathbf{0} & \mathbf{X}_1 & \mathbf{Y}^T \\ \mathbf{0} & \mathbf{Y} & \mathbf{X}_2 \end{bmatrix} \tag{A.1}$$

For an arbitrary column vector $\mathbf{a}$ of length $K(n+2)-1$, we partition it into

$$\mathbf{a} = [\mathbf{a}_1^T \ \mathbf{a}_2^T]^T \tag{A.2}$$

where $\mathbf{a}_1$ and $\mathbf{a}_2$ are of length $K(n+1)-1$ and K, respectively. It then follows from (A.1) that

$$\begin{aligned} \mathbf{a}^T\mathbf{R}_{n+1}\mathbf{a} &= \mathbf{a}_1^T\mathbf{R}_n\mathbf{a}_1 + [\mathbf{a}_{12}^T \ \mathbf{a}_2^T]\mathbf{R}_1[\mathbf{a}_{12}^T \ \mathbf{a}_2^T]^T \\ &= \mathbf{a}_1^T\mathbf{R}_n\mathbf{a}_1 + \mathbf{a}_{12}^T\mathbf{X}_1\mathbf{a}_{12} + 2\mathbf{a}_2^T\mathbf{Y}\mathbf{a}_{12} + \mathbf{a}_2^T\mathbf{X}_2\mathbf{a}_2 \end{aligned} \tag{A.3}$$

where $\mathbf{a}_{12}$ is the vector consisting of the last $K-1$ entries of $\mathbf{a}_1$. Using the fact that $\mathbf{R}_n$ is positive definite and $\mathbf{R}_1$ is positive semidefinite, it can be verified from (A.3) that $\mathbf{a}^T\mathbf{R}_{n+1}\mathbf{a} > 0$ for any given nonzero $\mathbf{a}$. Therefore, $\mathbf{R}_{n+1}$ is positive definite and there exists an exact zero-forcing solution for a window length $n+1$. It can be readily deduced that if an exact zero-forcing solution exists for a window length n, then it

exists for any other window length $M > n$. This in conjunction with the fact that $\mathbf{R}_1$ in (3.6) is the cross-correlation matrix associated with a window length 1 completes the proof.

Appendix B

Proof of The Fact Used in Proposition 3.2

Remember we need to prove that if the matrix obtained by replacing a principle matrix of a positive matrix $\mathbf{A}$ by the difference between the principle matrix and another positive definite matrix $\mathbf{B}$ is positive (semi)definite, then subtracting the corresponding principle matrix of $\mathbf{A}^{-1}$ from $\mathbf{B}^{-1}$ results in a positive (semi)definite matrix.

In the sequel, we will use the notation $\mathbf{A} \succ \mathbf{B}$ or $\mathbf{A} \succeq \mathbf{B}$ to indicate that $\mathbf{A} - \mathbf{B}$ is positive definite or positive semidefinite.

Since the set of positive definite matrices is closed under permutation congruence [35], we may assume that

$$\mathbf{A} = \begin{bmatrix} \mathbf{A}_{11} & \mathbf{A}_{12} \\ \mathbf{A}_{12}^H & \mathbf{A}_{22} \end{bmatrix} \tag{B.1}$$

and the principle submatrix of concern is $\mathbf{A}_{11}$. Since

$$\hat{\mathbf{A}} = \begin{bmatrix} \mathbf{A}_{11} - \mathbf{B} & \mathbf{A}_{12} \\ \mathbf{A}_{12}^H & \mathbf{A}_{22} \end{bmatrix} \tag{B.2}$$

is positive (semi)definite, we have [35]

$$\mathbf{A}_{11} - \mathbf{B} \overset{(\succeq)}{\succ} \mathbf{A}_{12}\mathbf{A}_{22}^{-1}\mathbf{A}_{12}^H \tag{B.3}$$

or, equivalently,

$$\mathbf{A}_{11} - \mathbf{A}_{12}\mathbf{A}_{22}^{-1}\mathbf{A}_{12}^{H} \overset{(\succeq)}{\succ} \mathbf{B} \tag{B.4}$$

Since the left-hand side of (B.4) is the inverse of the principle submatrix of $\mathbf{A}^{-1}$ corresponding to $\mathbf{A}_{11}$, the principle submatrix of $\mathbf{A}^{-1}$ is smaller than or equal to $\mathbf{B}^{-1}$ [35].

Appendix C

Convergence of $\mathbf{K}_i$

For systems with time-invariant correlations, (3.22) implies that

$$\mathbf{K}_{i+1} = \mathbf{H}_0 - \mathbf{H}_1\mathbf{K}_i^{-1}\mathbf{H}_1^T \text{ for } 1 \leq i \leq N-1 \tag{C.1}$$

where $\mathbf{K}_1 = \mathbf{H}_0$ and $\mathbf{K}_i$ are positive definite. It follows that

$$\mathbf{K}_{i+1} - \mathbf{K}_i = \mathbf{H}_1\mathbf{K}_i^{-1}(\mathbf{K}_i - \mathbf{K}_{i-1})\mathbf{K}_{i-1}^{-1}\mathbf{H}_1^T \tag{C.2}$$

By repeating (C.2) in conjunction with (3.20c), we obtain

$$\mathbf{K}_{i+1} - \mathbf{K}_i = \prod_{j=0}^{p-1}\mathbf{M}_{i-j} \cdot (\mathbf{K}_{i+1-p} - \mathbf{K}_{i-p}) \cdot \prod_{n=i-p}^{i-1}\mathbf{M}_n \tag{C.3}$$

Hence

$$\frac{\|\mathbf{K}_{i+1} - \mathbf{K}_i\|}{\|\mathbf{K}_{i+1-p} - \mathbf{K}_{i-p}\|} \leq \|\prod_{j=0}^{p-1}\mathbf{M}_{i-j}\| \, \|\prod_{n=i-p}^{i-1}\mathbf{M}_n\| \tag{C.4}$$

Now if $i-p$ is sufficiently large such that $\mathbf{K}_{i-p} \approx \mathbf{K}$ and $\mathbf{M}_{i-p} \approx \mathbf{M}$, then we have

$$\|\prod_{j=0}^{p-1}\mathbf{M}_{i-j}\|\|\prod_{n=i-p}^{i-1}\mathbf{M}_n\| \approx \|\mathbf{M}^p\|^2 \tag{C.5}$$

It can be shown that there exists a constant c such that $\|\mathbf{M}^p\| \leq c[\rho^p(\mathbf{M}) + \epsilon]$ for a given $\epsilon > 0$ [35], which, in conjunction with (C.4) and (C.5), gives

$$\frac{\|\mathbf{K} - \mathbf{K}_{i+1}\|}{\|\mathbf{K} - \mathbf{K}_i\|} \leq c_1[\rho(M) + \epsilon]^2 \tag{C.6}$$

This implies that $\mathbf{K}_i$ converges linearly with $\rho^2(\mathbf{M})$ when $\mathbf{K}_i$ is close to $\mathbf{K}$.

Appendix D

Performance Comparison of RDD and MDD

From (3.40) and (3.41), the SNR's of the decision variable for the ith bit of the kth user are $2e_k(i)/N_0(\mathbf{R}_N^{-1})_{ll}$ and $2e_k(i)\mathbf{c}_k(i)^H\mathbf{A}(l,l)^{-1}\mathbf{c}_k(i)/N_0$, respectively, where $l=(i-1)K+k$. Hence the performance of the RDD will be uniformly better than that of the MDD if and only if

$$\frac{1}{(\mathbf{R}_N^{-1})_{ll}} \geq \mathbf{c}_k(i)^H\mathbf{A}(l,l)^{-1}\mathbf{c}_k(i) \qquad \text{for } 1\leq k\leq K \text{ and } 1\leq i\leq N \tag{D.1}$$

The condition in (D.1) holds if and only if

$$\begin{bmatrix} 1/(\mathbf{R}_N^{-1})_{ll} & \mathbf{c}_k(i)^H \\ \mathbf{c}_k(i) & \mathbf{A}(l,l)^{-1} \end{bmatrix} \succeq 0$$

or, equivalently, if

$$\mathbf{A}(l,l)-\mathbf{c}_k(i)(\mathbf{R}_N^{-1})_{ll}\mathbf{c}_k(i)^H \succeq 0 \tag{D.2}$$

where $\mathbf{X}\succeq 0$ denotes that matrix $\mathbf{X}$ is positive semidefinite. Since $\mathbf{R}_N=\mathbf{W}^H\tilde{\mathbf{R}}_N\mathbf{W}$, then (D.2) holds if and only if

$$\mathbf{X}=\tilde{\mathbf{R}}_N^{-1}-\mathbf{W}(\mathbf{W}^H\tilde{\mathbf{R}}_N\mathbf{W})^{-1}\mathbf{W}^H\succeq 0 \tag{D.3}$$

whereas $\mathbf{X}\succeq 0$ if and only if $\rho(\mathbf{Y})\leq 1$, where

$$\mathbf{Y}=\mathbf{W}(\mathbf{W}^H\tilde{\mathbf{R}}_N\mathbf{W})^{-1}\mathbf{W}^H\tilde{\mathbf{R}}_N \tag{D.4}$$

From (D.4), it is clear that $\mathbf{Y} = \mathbf{YY}$. Hence, its eigenvalues must be zeros or ones. This shows that (D.1) holds for $1 \leq k \leq K$ and $1 \leq i \leq N$ and hence the performance of the RDD is uniformly better than that of the MDD.

Appendix E

Derivation of (5.29)

Define

$$\mathbf{\Delta} = \mathbf{S}_I \mathbf{S}_I^H + \sigma^2 \mathbf{I} \tag{E.1}$$

Then (5.28) can be rewritten as

$$\mathbf{\Gamma} = \mathbf{S}_1 \mathbf{c}_1 \mathbf{c}_1^H \mathbf{S}_1^H + \mathbf{\Delta} \tag{E.2}$$

Using the well-known *Sherman-Morrison* matrix inversion formula [60], we have

$$\mathbf{\Gamma}^{-1} = \mathbf{\Delta}^{-1} - \mathbf{\Sigma}^{-1} \mathbf{c}_1 (\mathbf{c}_1^H \mathbf{S}_1^T \mathbf{\Delta}^{-1} \mathbf{c}_1 + 1)^{-1} \mathbf{c}_1^H \mathbf{S}_1^T \mathbf{\Delta}^{-1} \tag{E.3}$$

where $\mathbf{\Sigma} = \mathbf{S}_1^T \mathbf{\Delta}^{-1} \mathbf{S}_1$. It follows from (E.3) that

$$\begin{aligned} \mathbf{S}_1^T \mathbf{\Gamma}^{-1} \mathbf{S}_1 &= \mathbf{\Sigma} - \mathbf{\Sigma} \mathbf{c}_1 (\mathbf{c}_1^H \mathbf{\Sigma} \mathbf{c}_1 + 1)^{-1} \mathbf{c}_1^H \mathbf{\Sigma} \\ &= (\mathbf{\Sigma}^{-1} + \mathbf{c}_1 \mathbf{c}_1^H)^{-1} \end{aligned} \tag{E.4}$$

From (E.4), we have

$$(\mathbf{S}_1^T \mathbf{\Gamma}^{-1} \mathbf{S}_1)^{-1} = \mathbf{\Sigma}^{-1} + \mathbf{c}_1 \mathbf{c}_1^H \tag{E.5}$$

It can then be readily verified that

$$\mathbf{\Gamma}^{-1} \mathbf{S}_1 (\mathbf{S}_1^T \mathbf{\Gamma}^{-1} \mathbf{S}_1)^{-1} = \mathbf{\Delta}^{-1} \mathbf{S}_1 \mathbf{\Sigma}^{-1} \tag{E.6}$$

Using the matrix inversion formula again, we have

$$\mathbf{\Delta}^{-1} \mathbf{S}_1 = 1/\sigma^2 [\mathbf{S}_1 - \mathbf{S}_I (\mathbf{R}_2 + \sigma^2 \mathbf{I})^{-1} \mathbf{R}_{12}^H] \tag{E.7}$$

$$\mathbf{\Sigma}^{-1} = \sigma^2 [\mathbf{R}_1 - \mathbf{R}_{12} (\mathbf{R}_2 + \sigma^2 \mathbf{I})^{-1} \mathbf{R}_{12}^H]^{-1} \tag{E.8}$$

Afetr some caculations, (E.8) and (E.8) lead to

$$\mathbf{\Delta}^{-1}\mathbf{S}_{\mathrm{I}}\mathbf{\Sigma}^{-1} = \mathbf{S}\begin{bmatrix} \mathbf{R}_{\mathrm{I}} & \mathbf{R}_{12} \\ \mathbf{R}_{12}^{H} & \mathbf{R}_2 + \sigma^2\mathbf{I}^{-1} \end{bmatrix}^{-1} [\mathbf{I}_L \ \mathbf{0}]^T \tag{E.9}$$

where $\mathbf{I}_L$ is the $L \times L$ idtentity matrix. Combining (E.6), (E.9), and (5.24) gives (5.29).

Appendix F

Derivation of (5.79)

From (5.71), (5.71), and (5.72), we have

$$\boldsymbol{\varepsilon}_l(n+1) = (\mathbf{I} - \mu\mathbf{P}\mathbf{y}(n)\mathbf{y}^H(n)\mathbf{P})\boldsymbol{\varepsilon}_l(n) - \mu\mathbf{P}\mathbf{y}(n)\mathbf{y}^H(n)\bar{\mathbf{w}}_l \tag{F.1}$$

Define

$$\tilde{\boldsymbol{\varepsilon}}_l(n) = \mathbf{Q}^H\boldsymbol{\varepsilon}_l(n) \tag{F.2}$$

$$\mathbf{Y}(n) = \mathbf{Q}^H\mathbf{P}\mathbf{y}(n)\mathbf{y}^H(n)\mathbf{P}\mathbf{Q} \tag{F.3}$$

$$\mathbf{X} = \mathbf{Q}^H\mathbf{P} \tag{F.4}$$

Then, from (F.1), we have

$$\begin{aligned} & E\left[\,\tilde{\boldsymbol{\varepsilon}}_l(n+1)\tilde{\boldsymbol{\varepsilon}}_l^H(n+1)\right] \\ &= E[\tilde{\boldsymbol{\varepsilon}}_l(n)\tilde{\boldsymbol{\varepsilon}}_l^H(n)] - \mu\tilde{\boldsymbol{\varepsilon}}_l(n)\tilde{\boldsymbol{\varepsilon}}_l^H(n)\mathbf{Y}(n) \\ &\quad -\mu\mathbf{Y}(n)\tilde{\boldsymbol{\varepsilon}}_l(n)\tilde{\boldsymbol{\varepsilon}}_l^H(n) + E[T1] + E[T2] - E[T3] - E[T4] \\ &= \mathbf{K}_l(n) - \mu\mathbf{K}_l(n)\Lambda - \mu\Lambda\mathbf{K}_l(n) + E[T1] + E[T2] - E[T3] - E[T4] \end{aligned} \tag{F.5}$$

where

$$T1 = \mu^2\mathbf{Y}(n)\tilde{\boldsymbol{\varepsilon}}_l(n)\tilde{\boldsymbol{\varepsilon}}_l^H(n)\mathbf{Y}(n) \tag{F.6}$$

$$T2 = \mu^2\mathbf{X}\mathbf{y}(n)\mathbf{y}^H(n)\bar{\mathbf{w}}_l\bar{\mathbf{w}}_l^H\mathbf{y}(n)\mathbf{y}^H(n)\mathbf{X}^H \tag{F.7}$$

$$\begin{aligned} T3 = {} & \mu\tilde{\boldsymbol{\varepsilon}}_l(n)\bar{\mathbf{w}}_l^H\mathbf{y}(n)\mathbf{y}^H(n)\mathbf{X}^H \\ & -\mu^2\mathbf{X}\mathbf{y}(n)\mathbf{y}^H(n)\mathbf{P}\boldsymbol{\varepsilon}_l(n)\bar{\mathbf{w}}_l^H\mathbf{y}(n)\mathbf{y}^H(n)\mathbf{X}^H \end{aligned} \tag{F.8}$$

$$T4 = T3^H \tag{F.9}$$

In the following derivation, a fourth-order moment expression of the higher-order term [54] will be useful. For evaluating $E[T1]$, this expression leads to

$$E[\mathbf{Y}(n)\tilde{\boldsymbol{\varepsilon}}_l(n)\tilde{\boldsymbol{\varepsilon}}_l^H(n)\mathbf{Y}(n)] \approx E[\mathbf{Y}(n)]\mathrm{tr}(E[\mathbf{Y}(n)]\mathbf{K}_l(n)) \tag{F.10}$$

By (5.76) and (F.4), we have

$$E[\mathbf{Y}(n)] = \Lambda \tag{F.11}$$

and hence

$$E[T1] = \mu^2\Lambda\mathrm{tr}(\Lambda\mathbf{K}(n)) \tag{F.12}$$

With the same approximation as in (F.10), we have

$$\begin{aligned} E[T2] &\approx \mu^2\mathbf{X}\boldsymbol{\Gamma}\mathrm{tr}(\boldsymbol{\Gamma}\bar{\mathbf{w}}_l\bar{\mathbf{w}}_l^H)\mathbf{X}^H \\ &= u^2\mathbf{X}\boldsymbol{\Gamma}\bar{\mathbf{w}}_l\boldsymbol{\Gamma}\bar{\mathbf{w}}_l^H\mathbf{X}^h \\ &= \mu^2\mathbf{M}_l\mathbf{X}\boldsymbol{\Gamma}\mathbf{X}^H \\ &= \mu^2 M_l\Lambda \end{aligned} \tag{F.13}$$

In order to evaluate $E[T3]$, the following equation will be useful

$$\bar{\mathbf{w}}_l^H\boldsymbol{\Gamma}\mathbf{P}\mathbf{Q} = 0 \tag{F.14}$$

The expectation of the first term in $T3$ is given by

$$E[\mu\tilde{\boldsymbol{\varepsilon}}_l(n)\bar{\mathbf{w}}_l^H\mathbf{y}(n)\mathbf{y}^H(n)\mathbf{X}^H] = \mu E[\tilde{\boldsymbol{\varepsilon}}_l(n)]\bar{\mathbf{w}}_l^H\boldsymbol{\Gamma}\mathbf{P}\mathbf{Q} = 0 \tag{F.15}$$

Using the same approximation as in (F.10), the expectation of the second term in $T3$ can be found as

$$-\mu^2\mathbf{X}\boldsymbol{\Gamma}\mathrm{tr}(\boldsymbol{\Gamma}\mathbf{P}E[\boldsymbol{\varepsilon}_l(n)]\bar{\mathbf{w}}_l^H)\mathbf{X}^H = -\mu^2\mathbf{X}\boldsymbol{\Gamma}\bar{\mathbf{w}}_l^H\boldsymbol{\Gamma}\mathbf{P}E[\boldsymbol{\varepsilon}_l(n)]\mathbf{X}^H = 0 \tag{F.16}$$

Combining (F.15) and (F.16), we have

$$E[T3] = E[T4] = 0 \tag{F.17}$$

Substituting (F.12), (F.13), and (F.17) into (F.5) gives (5.79).